Rosa Estela Abreu do Nascimento

Bachelor Degree in Biochemistry

Development of Polymeric Matrices Based on Banana Plant Extracts for Biomedical Applications

Dissertation to obtain the Master Degree in Biochemistry

Supervisor: Dr. Luísa Alexandra Graça Neves, Auxiliary Researcher

Faculdade de Ciências e Tecnologia da Universidade Nova de Lisboa (FCT NOVA)

Jury:

President: Dr. Teresa Sacadura Santos-Silva, Assistant Professor, FCT NOVA

Examiner: Dr. Cristiana Andreia Vieira Torres, Researcher, FCT NOVA

Supervisor: Dr. Luísa Alexandra Graça Neves, Auxiliary Researcher, FCT NOVA

November 2019

FACULDADE DE CIÊNCIAS E TECNOLOGIA
UNIVERSIDADE NOVA DE LISBOA

Rosa Estela Abreu do Nascimento

Bachelor Degree in Biochemistry

Development of Polymeric Matrices Based on Banana Plant Extracts for Biomedical Applications

Dissertation to obtain the Master Degree in Biochemistry

Supervisor: Dr. Luísa Alexandra Graça Neves, Auxiliary Researcher

Faculdade de Ciências e Tecnologia da Universidade Nova de Lisboa (FCT NOVA)

November 2019

Copyright

Development of Polymeric Matrices Based on Banana Plant Extracts for Biomedical Applications

Agradecimentos

Agradeço à minha orientadora Dra. Luísa Neves, por me ter aceite de braços abertos e por toda a confiança depositada em mim, possibilitando-me desenvolver o projeto que lhe propus; por toda a preocupação, disponibilidade e carinho transmitidos; e pelos horizontes que me abriu para as escolhas futuras que se avizinham.

Obrigada ao Professor Auxiliar Dr. Vítor Alves e aos técnicos Dra. Carla Rodrigues, Dra. Isabel Nogueira, Dra. Luz Fernandes, Dr. Nuno Costa e Dr. Rodrigo Duarte, por terem contribuído para esta tese com a análise das minhas amostras nas suas respetivas técnicas e por toda a disponibilidade em esclarecem as dúvidas que lhes apresentei. Às auxiliares dos laboratórios de aulas do 4º e 5º pisos do edifício departamental da FCT NOVA, obrigada por disponibilizarem prontamente todo o material que necessitei.

Um obrigada às alunas e investigadoras com quem contactei do *Laboratory of Membrane Processes* (FCT NOVA): *PhD* Joana Monte, Mafalda Cadima, *MSc* Maria Sampaio, *PhD* Paloma Ortiz, *PhD* Rita Nabais e *PhD* Rita Valério; e do grupo BIOENG (FCT NOVA): Professora Auxiliar Dra. Filomena Freitas, *MSc* Marta Ramos e *PhD* Virgínia Carvalho, pela disponibilidade que demostraram em me ajudar sempre que necessitei e por todos os momentos divertidos partilhados.

Agradeço a todos os docentes, investigadores e alunos com os quais contactei ao logo destes cinco anos, pelo conhecimento, experiência e momentos partilhados.

Um especial agradecimento aos meus pais, Benvinda e José, e à minha irmã Glória, por me terem proporcionado tudo aquilo que me permitiu chegar a onde estou hoje, por me apoiarem nas minhas decisões, por me fazerem ver qual o caminho mais indicado a seguir e por estarem sempre a meu lado. Obrigada aos meus familiares pela preocupação constante, por estarem sempre à espera do meu próximo regresso a casa e por me demonstrarem que com empenho e dedicação conseguimos sempre alcançar os nossos objetivos.

Aos meus amigos de cá: Andreia Fernandes, Beatriz Batista, Bruno Fernandes, João Alves, Mariana Simões, Pedro Rosado, Rita Baptista e Stefan do Ó; e de lá: Bruna Oliveira, Diogo Fernandes, Luís Pestana, Matilde Gonçalves e Margarida Constantino, obrigada por me acompanharem, ajudando-me a ultrapassar os obstáculos e a celebrar as conquistas.

Esta dissertação foi fruto de um trabalho conjunto. Estamos todos de parabéns! A nós!

“Para ser grande, sê inteiro: nada
Teu exagera ou exclui.
Sê todo em cada coisa. Põe quanto és
No mínimo que fazes.”

Ricardo Reis

Resumo

O objetivo desta tese foi o desenvolvimento e caraterização de matrizes poliméricas, sob a forma de filme ou gel, utilizando compostos extraídos da folha e do pseudocaule da bananeira, de forma a avaliar o seu potencial para aplicações biomédicas e eventualmente para aplicações na área alimentar, de acordo com as caraterísticas das matrizes obtidas.

Diferentes extratos foram obtidos através de extração *Batch* Sólido-Líquido e *Soxhlet*, com diferentes períodos de extração e diferentes temperaturas de secagem das amostras. Após a determinação do teor total em compostos fenólicos (TPC) e da atividade antioxidante, pelos métodos *Folin Ciocalteau* e 2,2-difenil-1-picrilhidrazilo (DPPH), respetivamente, os extratos foram caraterizados por Cromatografia Líquida de Alta Pressão (HPLC) e Cromatografia Líquida-Espectroscopia de Massa (LC-MS).

As matrizes poliméricas foram preparadas usando celulose extraída do pseudocaule da bananeira (PS) ou celulose comercial (hidroxietil celulose – HEC), glucose (G) e/ou ureia (U), e compostos fenólicos extraídos das folhas da bananeira (L) como compostos bioativos.

As matrizes preparadas foram caraterizadas por Microscopia Eletrónica de Varrimento (SEM), Difração de Raios-X (XRD), Calorimetria de Varredura Diferencial (DSC), Análise Termogravimétrica (TGA), Espectroscopia de Infravermelho (FTIR), ângulo de contacto, *swelling*, propriedades mecânicas, reologia e estudos de permeação de gases.

Os resultados obtidos mostraram que as folhas de bananeira apresentam um TPC superior ao obtido para a pele e polpa da banana, e para o pseudocaule da bananeira, sendo a extração *Batch* Sólido-Líquido por 3 dias com folhas secas a 40 °C (BSL_3_40) que permitiu um teor em compostos fenólicos mais elevado. Foi ainda possível extrair celulose do pseudocaule da bananeira. Em geral, as matrizes preparadas são hidrofílicas e apenas as matrizes HEC expostas a 84% a_w apresentam uma estrutura densa. A presença de plastificantes e a atividade da água demonstraram influenciar as propriedades mecânicas, que podem ser manipuladas de acordo com a aplicação desejada.

Palavras-chave: bananeira, celulose, compostos fenólicos, estruturas poliméricas, folha e pseudocaule.

Abstract

The aim of this thesis was the development and characterization of polymeric matrices, in the form of film or gels, using compounds extracted from banana plant leaves and pseudostem, in order to evaluate their potential for biomedical applications and eventually for food applications, accordingly to the features of the obtained matrices.

Different extracts were obtained through Batch-Solid Liquid and Soxhlet extraction, with different extraction periods and different drying temperatures of the samples. After determination of Total Phenolic Content (TPC) and antioxidant activity, by Folin-Ciocalteau and 2,2-difenil-1-picrilhidrazilo (DPPH) methods, respectively, the extracts were characterized by High Pressure Liquid Chromatography (HPLC) and Liquid Chromatography-Mass Spectroscopy (LC-MS).

The polymeric matrices were prepared using cellulose extracted from banana plant pseudostem (PS) or commercial cellulose (hydroxyethyl cellulose – HEC), glucose (G) and/or urea (U) and phenolic compounds extracted from banana plant leaves (L) as bioactive compounds.

The prepared matrices were characterized by Scanning Electron Microscopy (SEM), X-Ray Diffraction (XRD), Differential Scanning Calorimetry (DSC), Thermogravimetric Analysis (TGA), Fourier Transformed Infrared spectroscopy (FTIR), contact angle, swelling, mechanical properties, rheology and gas permeation studies.

The obtained results showed that the banana plant leaves present a TPC higher than banana peel, pulp and banana plant pseudostem, being the Batch-Solid Liquid with 3 days extraction and leaves dried at 40°C (BSL_3_40) allowed the highest TPC. It was also possible to extract cellulose from banana plant pseudostem. In general, the synthetized matrices were hydrophilic and just the HEC matrices exposed to 84% a_w present a dense structure. The plasticizers and water activity showed to influence the matrices flexibility, which could be controlled accordingly to the desired matrices application.

Keywords: banana plant, cellulose, leaf, polymeric structures, phenolic compounds and pseudostem.

Index

Index of Figures

Index of Tables

Lists of Abbreviations

Abbreviation	Meaning
2n	Chromosomes number presents on the genotype
Abs	Absorbance
AD	*Anno Domini*
AIDS	Acquired Immunodeficiency Syndrome
a_w	Water activity
BC	Before Christ
CAS	Registry number of chemical compounds
CID	Compound Identification
D1	Positive mode
D2	Negative mode
DPPH	2,2-diphenyl-1-picrylhydrazyl
DSC	Differential Scanning Calorimetry
FAO	Food and Agriculture Organization of the United Nations
FRAP	Ferric Reducing Antioxidant Potential
FTIR	Fourier Transform Infrared spectroscopy
FW	Formula Weight or molecular weight
G	Glucose
G’	Elastic component
G’’	Viscous component
h	Hour
HEC	Hydroxyethyl Cellulose
HIV	Human Immunodeficiency Virus
HPLC	High Pressure Liquid Chromatography
IU	International Unit

(Table continues on the next page)

Abbreviation	Meaning
L	Banana plant leaves' phenolic compounds
LC-MS	Liquid Chromatography-Mass Spectrometry
MIC	Minimum Inhibitory Concentration
min	Minutes
MS	Mass Spectroscopy
nd	Non-detected
NTS	Normalized Tensile Strength
PS	Pseudostem
rpm	Rotations per minute
SD	Standard Deviation
SEM	Scanning Electron Microscopy
TDS	Transdermal Delivery Systems
TGA	Thermogravimetric Analysis
TPC	Total Phenolic Content
U	Urea
UV/VIS	Ultraviolet/Visible
(v/v)	Volume/volume

Lists of Variables

Variable	Meaning	Unit
θ	Contact angle	°
Å	Angstron	Å
A	Area	cm^2
C	Concentration	mg/L
D	Diffusivity coefficient	m^2/s
Da	Dalton	Da
F	Force	N
l	Membrane thickness	m
MW	Molecular Weight	g/mol
P	Permeability	m^2/s
p	Pressure	bar
r	Probe radius	m
R^2	Correlation coefficient	-
S	Solubility Percentage of swelling	- %
S_c	Cross-section area	m^2
t	Time	s
T_g	Glass transition temperature	°C
T_m	Melting point temperature	°C
T_x	Crystallization temperature	°C
w	Weight	g
wt%	Weight percentage	%
v	Volume	mL or μL

Lists of Greek Letters

Letter	Meaning	Unit
α	Ideal selectivity	-
β	Geometric cell parameter	m^{-1}
γ	Tension	Pa
$\dot{\gamma}$	Shear rate	s^{-1}
η	Reaction yield Apparent viscosity	% Pa.s
λ	Wavelength	nm
σ	Tensile strength	Pa
$\sigma_{normalized}$	Normalized tensile strength	MPa/mm
ω	Frequency	Hz

1. Introduction

Since the beginning of civilization, plants have been used as a valuable source of natural products for maintaining human health, which allowed the development of traditional medicine.[1] Around 80% of individuals from developing countries use plants as medicines. However, most of these plants are not studied yet and its full chemical composition is still unknown. In the last few years, some studies have been conducted, in order to make the identification of the chemical constituents of different plants and, consequently, to achieve a better understanding of their properties, safety and efficiency.[2][3] As an example of a plant with potential health benefits, the work developed in this thesis is focused on the use of banana plant.

1.1 Banana Plant

Banana Plant Composition

Banana plant has a rhizome, the stem, which grows horizontally underground and has a pseudostem, formed by an apical meristem from which grow the spirally arranged leaves.[4] Banana plant is the largest herbaceous plant, with its pseudostem reaching a height up to 10–15 m in some wild species. It also has the largest leaf area, that can vary between 1.27–2.80 m^2/leaf, depending on the cultivars and the growing conditions.[5]

Banana flower is produced by the corm in the centre of the leaves, where the male and female flowers are placed and emerges at the top of the pseudostem. Each pseudostem only produces one flower.[4] The time between banana plant plantation and its bunch harvesting differ between 8–13 months, according to the climate zone and banana variety.[6]

Banana Plant Varieties

Banana plant belongs to the kingdom *Plantae*, division *Magnoliophyta*, class *Liliopsida*, order *Zingiberales*, family *Musaceae* and genus *Musa*.[7] The main *Musa acuminata* plant parts are shown in **Figure 1.1**.

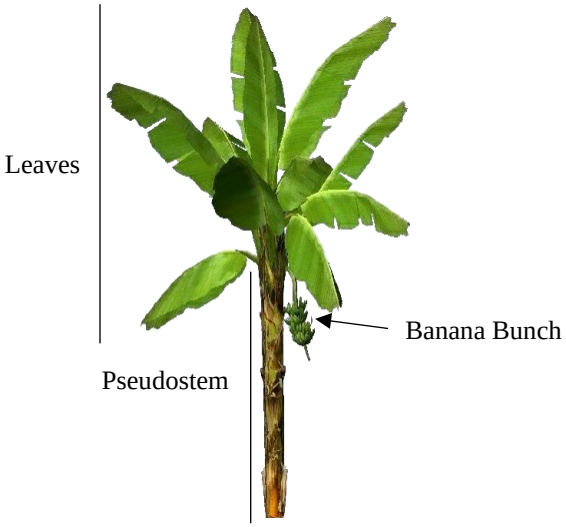

Figure 1.1: Banana plant *Musa acuminata* main plant parts.[8]

Genus *Musa* has more than 50 species, divided into three sections, accordingly to the number of chromosomes: *Musa* (2n=22), *Callimusa* (2n=20) and *Ingentimusa* (2n=28).[9] Banana plant that belong to the section *Musa*, represent the largest and most geographically widespread section and most cultivars are derived in *Musa acuminata* Colla and *Musa balbisiana* Colla species.[5] There are at least 200–300 banana clone's varieties in the world (**Figure 1.2**). However, due to the difficulty of breeding infertile plants, only a few cultivars have been introduced in the last 50 years. *Dwarf Cavendish*, *Giant Cavendish* and *Gros Michel* are some of the most important banana plantations for fresh consumption around the world.[10]

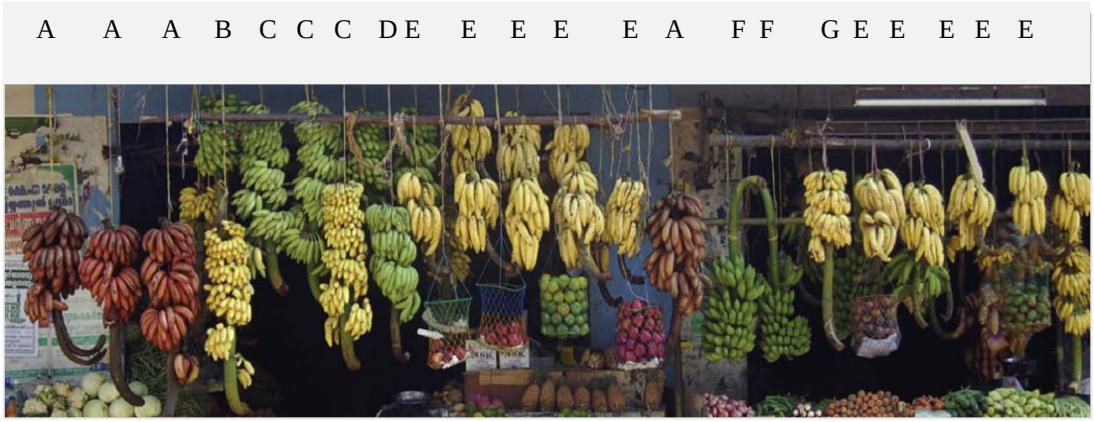

Figure 1.2: Some varieties of bananas. The letters up to the banana bunches means different varieties.[10]

Banana Word Distribution

The first record of edible bananas come from India, during 600 BC. India is considered the centre of origin for more than 300 types of bananas out of the 600 types of *Musa* germplasm. It is believed that bananas were introduced in Europe around 10 AD and then spread to the Pacific Islands and West Coast of Africa, during 200–300 BC.[10] Presently, banana is cultivated in more than 130 countries, in tropical and subtropical regions. Its world harvested area of, approximately, 10 million hectares produces, annually, 145 million tons of banana.[4] India was the major producer (29 million tons in average between 2017–2019), Ecuador the main exporter (6.4 million tons in 2017), and United States (4.8 million tons in 2018) and European Union (6.0 million tons in 2018) the major importers.[11, 12] Banana is the cheapest and most popular food all over tropical and subtropical regions of the world.[6] In 2017, the global banana production reached 114 million tonnes.[11]

Currently, *Musa acuminata* is grown worldwide, being India and China the main producers (11 million tons in 2017). **Figure 1.3** represents the banana production world distribution found in 2016.[11] Madeira and Azores islands are the only places in Portugal where banana is produced and commercialized. During 2017, the banana production at Madeira island increased 8.8%, resulting in the sale of 22 thousand tons.[13]

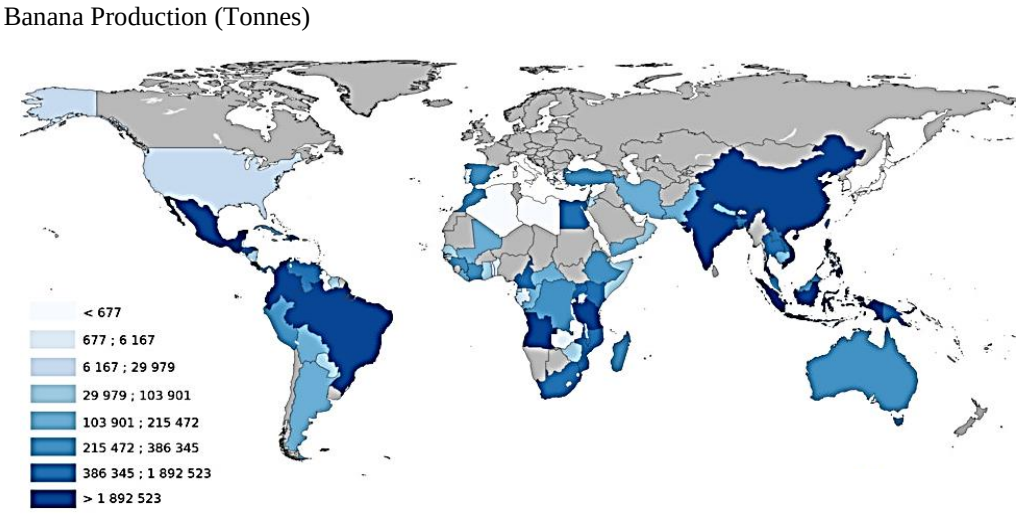

Figure 1.3: Banana world production in 2016.[14]

According to Food and Agriculture Organization of the United Nations (FAO), every year, 100 billion bananas are consumed globally, which are mainly eaten fresh.[4, 11] African countries, such as Uganda, Rwanda and Cameroon, has the highest *per capita* consumption of banana, exceeding 200 kg of banana/year and mainly in the rural areas of these countries, banana can provide up to 25% of the daily calorie intake.[11]

Even though there is a large banana production, only 12 wt% of banana plants are used, generating 220 tons of residues/banana crop's hectare, consisting mainly of lignocellulosic material. At Malaysia, these residues are discarded by farmers into rivers, lakes and on road sides, causing serious environmental problems.[15] The main residues of banana farms are leaves and pseudostems, both containing high levels of lignocellulose.[16, 17]

Banana Plant Constituent Applications

Almost all parts of banana plant have been used for centuries for many purposes, including religious, ceremonial, clothing, silage, rope, garlands, cordage, smoking material, fragrance, medicines and food.[6] In addition, different constituents are presently used, for example, as natural source of bioactive compounds, as biofertilizers, energy production from its biomass degradation, cellulose microfibrils from the rachis of banana bunches and for pulp and paper production.[6, 18, 19]

Banana is considered one of the most important sources of energy for human consumption. Its consumption contributes with an elevated intake of phytochemicals, as sterols and unsaturated fatty acid, carbohydrates, fibre, vitamins, and minerals, with a very low intake of fats, as it can be observed in **Table 8.1**, **Appendix I**.[2]

Forster *et al.* studied the same banana variety from Tenerife and Ecuador and concluded that the region of production, the cultivation method (greenhouse or outdoors) and the farming method (conventional or organic) influences the chemical composition of bananas.[3]

Musa acuminata plant have been traditionally used to manage a wild rage of diseases by tribal communities in Africa, America, Asia, India and Oceania.[20, 21] All parts of banana plant, including flower, leaf, stem and pseudostem have been used in the treatment of diseases like hypertension, allergies, infections, blood pressure control, fever and tuberculosis treatment (**Table 8.2**, **Appendix I**), due to a rich and diversified content of phytochemicals.[22] Agarwal *et al.* showed that methanolic and aqueous extracts of banana plants present wound healing activity in rats.[23] What is more, the antimicrobial activity of various extracts of different *Musa acuminata* plant parts and their active concentration is presented in **Table 8.3**, **Appendix I**.

Active Compounds Present in Banana plant

Phytochemicals, especially phenolic compounds, present on fruits and vegetables, are the major bioactive compounds known for health benefits.[24] The phytochemical analysis of different parts of *Musa acuminata*, as its leaves and pseudostem, has revealed a rich diversity of phytochemicals like tannins and phenols, that vary with the extraction method employed, as can be observed in **Table 8.4**, **Appendix I**.[22] The chemical properties and the identification of chemical compounds found in *Musa acuminata* and their pharmacological activities are presented in **Table 1.1** and **1.2**, respectively.

The diversity of phytochemical compounds present on the different constituents of banana plant provides them an interesting pharmacological activity, which triggered its phytochemical and pharmacological studies. Despite of the continuous progress on these studies, the development of an allopathic or phytomedicine from *Musa* residues requires a more detailed investigation about quality control, efficacy, safety, toxicity and ethnopharmacological research, considering that these phytochemical compounds are highly affected by genetic and environmental factors, farming practices, fruit maturity stage at harvest, harvesting time, post-harvest handling and processing, and storage conditions.[25, 26]

Free radicals are molecular fragments, whose unpaired electrons can damage our body cells through cell oxidative stress.[26, 27] Fortunately, this oxidation can be prevented or delayed throw the consumption of antioxidant species, as polyphenols, carotenoids and ascorbic acid (vitamin C).[28] Natural antioxidants, originated from the plants secondary metabolism, are the most used, due to the many health hazards, mainly toxicity, caused by the use of synthetic antioxidants.[29, 30] Natural antioxidants can have many biological effects including anti-inflammatory, antiallergenic, antibacterial and antithrombic activities.[24] Polyphenols are secondary metabolites, formed by an aromatic ring with one or more hydroxyl groups. Depending on their function and structure, polyphenols are classified as: coumarins, flavonoids, lignans, phenolic acids, stilbenes and tannis (**Figure 1.4**).

Polyphenols play an important role in the inhibition of oxidative stress and other chronic diseases, due to their antioxidant potential, which depends on the number and arrangement of the hydroxyl groups present.[31, 32]

Table 1.1: Chemical compounds identified in *Musa acuminata*.[33]

Compound	Molecular Formula	Chemical Name	Molecular Weight (g/mol)	Structure ID (Pub Chem CID)
Anigorufone	$C_{19}H_{12}O_2$	2-Hydroxy-9-phenyl-phenalen-1-one	272.30	636472
Apigenin	$C_{15}H_{10}O_5$	5,7-dihydroxy-2-(4-hydroxyphenyl)chromen-4-one	270.24	5280443
β-sitosterol	$C_{29}H_5O$	(3S,8S,9S,10R,13R,14S,17R)-17-[(2R,5R)-5-ethyl-6-methylheptan-2-yl]-10,13-dimethyl 2,3,4,7,8,9,11,12,14,15,16,17-dodecahydro-1Hcyclopenta[a]phenanthren-3-ol	414.71	222284
Campesteryl glucoside	$C_{34}H_{58}O_6$	(2R,5S)-2-[[(3S,8S,9S,10R,13R,14S,17R)-17-[(2R,5R)-5,6-dimethylheptan-2-yl]-10,13-dimethyl-2,3,4,7,8,9,11,12,14,15,16,17-dodecahydro-1Hcyclopenta[a]phenanthrene-3-yl]oxy]-6-(hydroxymethyl)oxane-3,4,5-triol	562.82	70699334
Cycloartenol	$C_{30}H_{50}O$	9beta,19-cyclo-24-lanosten-3beta-ol	426.72	92110
Delphinidin-3-rutinoside	$C_{27}H_{31}O_{16}^+$	(2R,4S,5R)-2-[[(3S,6S)-6-[5,7-dihydroxy-2-(3,4,5-trihydroxyphenyl)chromenylium-3-yl]oxy-3,4,5-trihydroxyoxan-2-yl]methoxy]-6-methyloxane-3,4,5-triol	611.52	44256887
Dopamin	$C_8H_{11}NO_2$	4-(2-aminoethyl)benzene-1,2-diol	153.18	681

(Table continues on the next page)

Table 1.1: Table continuation.

Compound	Molecular Formula	Chemical Name	Molecular Weight (g/mol)	Structure ID (Pub Chem CID)
Episesamin	$C_{20}H_{18}O_6$	5,5'-(1R,3aS,4S,6aS)-Tetrahydro-1H,3H-furo[3,4-c]furan-1,4-diylbis (1,3-benzodioxole	354.35	(ChemSpider ID) 10043748
Methoxyanigorufone	$C_{20}H_{14}O_2$	2-methoxy-9-phenyl-phenalen-1-one	286.32	10085389
Naproxen	$C_{14}H_{14}O_3$	(2S)-2-(6-methoxynaphthalen-2-yl)propanoic	230.26	156391
Phenyl-phenalenone	$C_{18}H_{10}O_4$	2-(4-hydroxyphenyl) naphthalic anhydride	290.27	10424295
Pyranone	$C_6H_8O_4$	3,5-dihydroxy-6-methyl-2,3-dihydropyran-4-one	144.12	119838
Sesamin	$C_{20}H_{18}O_6$	5-[(3S,3aR,6S,6aR)-3-(1,3-benzodioxol-5-yl)-1,3,3a,4,6,6a-hexahydrofuro[3,4-c]furan-6-yl]-1,3-benzodioxole	354.35	72307
Stigmasteryl glucoside	$C_{35}H_{58}O_6$	(2R,5S)-2-[[(3S,8S,9S,10R,13R,14S,17R)-17-[(E,2R,5S)-5-ethyl-6-methylhept-3-en-2-yl]-10,13-dimethyl-2,3,4,7,8,9,11,12,14,15,16,17-dodecahydro-1Hcyclopenta[a]phenanthrene-3-yl]oxy]-6-(hydroxymethyl)oxane-3,4,5-triol	574.83	70699355

Table 1.2: Pharmacological activity of some chemical compounds identified on *Musa acuminata*.[33]

Phytochemicals	Pharmacological Activity
2,3-dihydro-3,5-dihydroxy-6-methyl-4H-pyran-4-one	Antioxidant, anti-inflammatory and anti-proliferative activity
2-methoxy-9-phenyl-phenalen-1-one	Leishmanicidal activity
α-tocopherol	Cardiovascular diseases, cancer, inflammatory diseases, neurological disorders, cataract and age-related macular degeneration
Anigorufone	Leishmanicidal activity
Alkaloids	Pain killer
β sitosterol	Anti-mutagenic and anticancer activities
Caffeoylquinic acid (chlorogenic acid)	Antioxidant activity
Dopamine	Potent vasoconstrictor
Epi-sesamin	Antioxidant property, anticholesteremic, antihypertensive agent and antitubercular activity
Flavonoids	Antioxidant, antiallergenic, anti-inflammatory, antithrombic, antiulcerogenic, anticarcinogenic and hepatoprotective
Glycosides	Treatment of congestive heart failure and cardiac arrhythmias
Kaempferol	Anti-inflammatory
Lectin (BanLec)	Immunopotency, mitogenic activity and anticancer activity

(Table continues on the next page)

Table 1.2: Table continuation.

Phytochemicals	Pharmacological Activity
Long chain aliphatic alcohols	Decreased low-density lipoprotein cholesterol and increased high-density lipoprotein cholesterol
Octadeca-9,12,15 trienoic acid (omega-3) and Octadeca-9,12-dienoic (omega-6)	Reduced risk of chronic diseases, such as cancer, cardiovascular disease, osteoporosis and some immune disorders
Phytosterols	Reducing plasma cholesterol
Quercetin	Antivenom effects, helps in strengthening capillaries and stopping bleeding
Saponins	Treatment of epilepsy, excessive salivation, chlorosis and migraines
Sesamin	Antioxidant property, anticholesterolemic and antihypertensive agent
(S)-(+)-6-methoxy-α-methyl-2-naphthaleneacetic acid	Anti-inflammatory activity
Steryl glucosides	Lower blood cholesterol
Tannins	Antioxidant activity
Trans beta carotene	Antineoplastic, antioxidant and chemopreventive activities

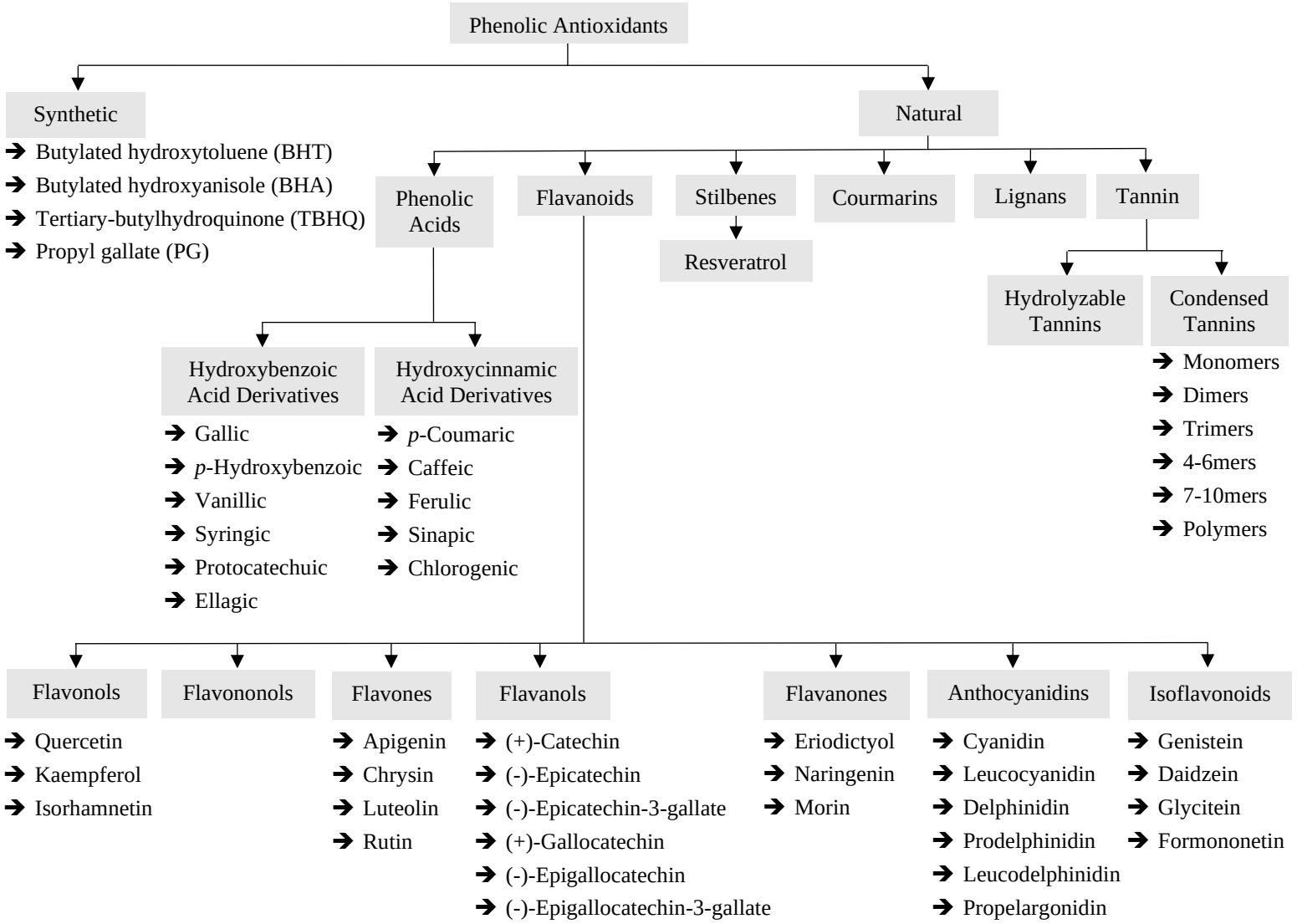

Figure 1.4: Phenolic antioxidants components.[34]

It has been reported that, banana contains a high number of phenolic compounds, mainly in the pulp. The quantity of total phenolic compounds presents on banana pulp vary between 30–60 g phenolic compounds/100 g fresh pulp, while on the banana peel vary between 0.90–3.0 g/100 g dried peel.[35, 36]

The motivation for this work was the study of banana plant leaves and pseudostem since the pulp and peel are the banana plant parts best characterized in the literature. Consequently, there is a better characterization requirement of the remaining part of the tree, mainly of the leaves and the pseudostem, which constitute the greater amount of the residues coming from the production of banana. It is therefore crucial to develop new applications for banana production residues, in order to reduce its negative environmental impact.

1.2 Banana Plant Based Polymeric Matrices

Having in mind the banana plant parts that have already been studied and the ones that required a better understanding, it would be interesting to analyse which compounds could be extracted from banana plant leaves and pseudostem. And, if it is possible, in order to explore its use for different applications, this master thesis aims the development of polymeric structures based only on banana plant extracts (in the form of films or gels).

Films Applications

Recently, much attention has been focused on bio-based films from renewable resources, like plant fibers, extracts from seeds, lipids or proteins, for packaging of commodity products, medical devices and other commercial applications.[37]

- **Biomedical Applications**

In medicine, thin films were introduced in 1970, to overtake the tables and capsules swallowing difficulties.[38, 39] These films are formed by a thin and flexible layer of polymer, with or without the presence of plasticizers.[40] The flexibility and low thickness of these films make them less obstructive as well as more appellative and easier to apply.[41, 42] The ideal thin film should have the following features: enough drug loading capacity, fast dissolution rate or long residence time at the administration site, acceptable formulation stability and should be

biocompatible, biodegradable and non-toxic.[43, 44] These films can be applied in different organs as oral cavity, eyes and skin.

Through the last 35 years the transdermal rout become an acceptable technology, offering many significant clinical benefits, over the other dosage forms.[45] The skin constitutes the biggest and most accessible organ of the body. It acts as a barrier against the environmental molecules, due to its low permeability.[46] In an average adult body, the skin occupies about $2 m^2$ surface area and receives one-third of the total blood circulation of all body.[46]

The first transdermal delivery systems (TDS) was approved in 1981, used for the relief of nausea, sickness and vomit symptoms. Since then, more than 35 TDS were developed and more than 13 molecules had been approved to be used in these systems.[45] **Table 1.3** shows the characteristics of some TDS present in the market.

Table 1.3: Characteristics of some TDS already commercialised.[45]

Active Ingredient	Molecular Weight (Da)	Trade Name	Manufacturer	Frequency of Application	Type of System
Clonidine	230	Catapres-TTS®	ALZA Corporation, Mountain View, CA, USA	Weekly	Drug-in--adhesive
Estradiol	272	Vivele®	Noven Pharmaceuticals Inc., Miami, FL, USA	Twice a week	Adhesive formulation
Nicotine	162	Nicoderm CQ®	GlaxoSmithKline Consumer Healthcare, L.P, Philadelphia, PA, USA	Daily	No available information
Testosterone	288	Androderm®	Watson Pharma, Inc. A subsidiary of Watson Pharmaceuticals, Inc., Corona, CA, USA	Androderm 5mg system or two androderm 2.5 mg systems applied nightly for 24 hours, providing a total dose of 5mg/day	Reservoir of drugs

Accordingly to Technavio, the global transdermal drug delivery market size will grow by € 1.60 billion during 2019–2023. Some factors that are expected to drive the market growth in the coming years are the advantages over parenteral and oral routes of administration and the availability of penetration enhancers used in transdermal drug delivery.[47]

The polymers used in TDS formulations should form a clear and flexible film at skin temperature.[46] Some of the most common polymers for TDS are presented in **Table 1.4**.

Table 1.4: Film forming polymers properties.[46]

Polymer	Properties
Acrylates copolymer	Tough; Breathable; Abrasion resistant films.
Chitosan	Excellent film forming ability; Opens the tight junctions of mucosal membrane, thereby enhancing the paracellular permeability and penetration of drug; Controls drug release.
Ethyl cellulose (EC)	Nontoxic; Nonirritating; Nonallergic material; Good film forming properties that form tougher films.
Hydroxypropyl cellulose	Nonionic, pH insensitive polymer; Water soluble.
Hydroxypropyl methylcellulose (HPMC)	Produce a light, non-greasy uniform film with good texture; Do not interact significantly with other ingredients; Surface active agent, therefore adsorbs water providing easy dispersion, lubricity and comfort feel in occlusive state on application to skin.
Polydimethylsiloxane (PDMS)	Water vapour permeable film; Durable film.
Polyvinyl alcohol (PVA)	Water soluble; Excellent film forming and adhesive properties; Nontoxic and biocompatible.
Polyvinyl pyrrolidine (PVP)	Solubility in water and other solvents; Adhesive and binding property; Acts as a bioavailability enhancer.

Some of the plasticizers frequently used in transdermal films are: dibutylphthalate, glycerine, polyethylene glycol and sorbitol.[46] These compounds improve the drugs solubilization and influence the drug permeation. A couple of the most widely used solvents for topical and transdermal drug delivery systems are listed in **Table 1.5**.

Table 1.5: Examples of solvents used for topical and transdermal systems.[46]

Solvent Category	Examples
Alcohols	Benzyl alcohol, butanol, ethanol, fatty alcohols and lanolin alcohols
Glycols	Polyethylene glycols and propylene glycols
Others	Ethyl acetate, isopropyl myristate and oleic acid

Just a small number of drugs are suitable for these films, once their bioavailability depends on its molecular size, pH, polarity, subcutaneous reservoir and metabolism by the skin flora as well as the patient skin hydration state and thickness.[46] The drugs applicable for this system should be highly potent, permeating rapidly on the skin and cause no skin irritation. The ideal drug properties for transdermal drug delivery are listed in **Table 1.6**.

Table 1.6: Ideal properties of drugs to be applied in drug transdermal delivery systems.[46]

Parameter	Properties
Dose	<10 mg/day
Half-life	≤ 10 h
Molecular weight (Da)	<500
Partition coefficient Log P (octanol/water)	$1-3$
Skin reaction	Non irritating and sensitizing
Oral bioavailability	Low

The other commonly used transdermal dosage forms, as creams, patches and ointments, have numerous limitations. Patches obstruct the sweat ducts leading to skin irritation, due to the prevention of water vapour loss from the skin surface, causing pain while peeling off.[48] The semisolid preparation, as creams and ointments, can be easily wiped off from the skin surface and, in case of chronic diseases, like athlete's foot, there is a need of repeated applications.[46] Therefore, the development of a dosage form that maintains the skin contact for longer time periods, implying less frequent dosing is necessary. The use of thin films prevents the permeation of water vapour from the skin surface and can cause pain at the time of peeling. Despite of this, they present a promising transdermal drug delivery alternative, due to their better cosmetic appearance, easier application and higher flexibility.[49]

- **Food Packaging Applications**

One solution to the environmental pollution problems generated by the use of non-biodegradable petroleum-based packaging materials, which are very stable in nature and have a very slow degradation, is the use of biopolymers from different natural resources, such as cellulose, agar and soy protein, as eco-friendly packaging materials.[50] These biopolymers were also studied as edible matrices and as active packaging materials.[51]

From among the various active packaging systems, bio-nanocomposite packaging materials containing antibacterial function are thought to be a promising active packaging material, improving the food shelf-life, by destroying or inhibiting the food pathogenic microorganisms, once these systems work as a physical barrier.[50] These materials can also been doped with bioactive compounds of interest combined with later controlled release at a specific target, providing a functional product with health benefits to the consumer. Some of the most used bioactive agents for food packaging are antioxidants, antimicrobials and probiotics.[52] These features are interesting for commonly spoiled foods as fruit, vegetables and meat.[53]

Studies about the use of natural polymers to create edible and biodegradable films are also growing interest.[54] Among the systems developed so far, a high focus has been given to biopolymers as cellulose, chitosan, gums, pectins and seaweed extracts. Cellulose is particularly studied due to the fact that it is highly available, renewable and is a biocompatible raw material.[52] Many efforts have been done to develop films from agriculture products and residues (**Figure 1.5**).

Figure 1.5: Edible films made from guava (left) and beetroot (right).[55]

As an example, fibres extracted from banana stems have been used as reinforcement material and to develop films. Since, as described in the section **1.1** of introduction, banana plant pseudostem is considered a residue of banana production being available in large quantities and presents good tensile properties, this is a good opportunity to give them commercial applications, adding value to this residue.[56]

2. Goals

The main goal of this master thesis was the development of polymeric matrices (in the form of films or gels) based on banana plant extracts and to study their potential for different applications, such as for biomedical and food applications.

In a first step, the phenolic compounds were extracted from the banana plant leaves and pseudostem using different extraction methods (Batch Solid-Liquid and Soxhlet) with a variety of extraction conditions: drying temperature of the leaves (20, 40, 50 and 60 °C) and time period extraction (1–5 days). After, the chemical characterization of the extracts was performed (by Hight Pressure Liquid Chromatography (HPLC) and Liquid Chromatography-Mass Spectroscopy (LC-MS)) and its Total Phenolic Content (by Folin Ciocalteau Method) and antioxidant activity (by 2,2-diphenyl-1-picrylhydrazyl Method) were quantified. Cellulose was extracted from banana plant pseudostem and quantified by HPLC.

The obtained extracts were used to prepare polymeric matrices which were characterized by the following techniques: Scanning Electron Microscopy (SEM), X-Ray Diffraction (XRD), Differential Scanning Calorimetry (DSC), Thermogravimetric Analysis (TGA), Fourier Transformed Infrared spectroscopy (FTIR), contact angle, swelling, mechanical properties, rheology and gas permeation studies.

3. Materials and Methods

3.1 Materials and Equipments

All the materials and equipments used during the experimental work of this master thesis are identified at **Tables 8.5** and **8.6**, respectively, present at **Appendix II**.

Banana plant leaves and pseudostem used were kindly provided by a Madeira island farmer. All the samples were from the same cultivation area, being exposed to the same cultivation conditions.

3.2 Phenolic Compounds Extraction

Phenolic compounds were extracted from the leaf and pseudostem of banana plant using two different methods: Batch Solid-Liquid and Soxhlet, and methanol as extraction solvent. Methanol was used since it allows the extraction of interesting phytochemicals, from the leaves and pseudostem, for the aimed applications, as can be seen at **Table 8.4**, **Appendix I**.

The samples (leaf and pseudostem) were cleaned with cold running water, dried with paper and then cut in small pieces (2×2cm) (**Figure 3.1 (A)**). After, samples were dried in a cabinet dryer (Venticell, MMM Group) for 7h, with 2.0m/s airflow, using four different temperatures: 20, 40, 50 and 60°C (**Figure 3.1 (B)**). 7h was the maximum drying time since it has been reported that after this time the loss of antioxidants compounds occurs, and 60°C was the highest temperature used since about 90% of antioxidant activity was reduced at higher temperatures.[57, 58]

Figure 3.1: Banana plant leaves after cleaned and cut **(A)** and after dried at 60°C **(B)**.

3.2.1 Batch Solid-Liquid Method

The extraction of phenolic compounds using a methanol Batch Solid-Liquid extraction method was performed accordingly to Sagrin *et al.* with slight modifications.[59] Briefly, 5 g of dried sample was blended into powder, using a crushing machine (Selecline) and 100 mL of methanol was added, during different time periods (between 1 and 5 days), at room temperature. The sample was then filtrated using a filter paper and concentrated using a rotatory evaporator (Buchi), at 40 °C and 3 rpm. After, the sample was stored at 4 °C, until further analysis.

3.2.2 Soxhlet Method

The extraction of phenolic compounds using a methanol Soxhlet extraction method was carried out by means of a procedure previously developed in the Laboratory of Membrane Processes (FCT NOVA). The experimental set-up is described in **Figure 3.2**.

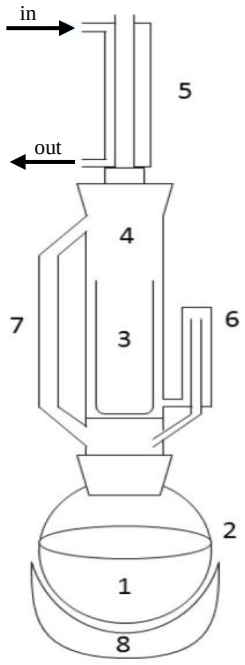

Figure 3.2: Soxhlet extraction experimental set-up, where 1 – solvent (methanol); 2 – round bottom flask; 3 – Soxhlet thimble; 4 – Soxhlet extractor; 5 – condenser with running water, being in and out the water entrance and exit, respectively; 6 – siphon; 7 – side arm and 8 – heat source.[60]

Briefly, 15.6 g of sample was blended into powder using a crushing machine and add to the Soxhlet extraction set-up. Then, 250 mL methanol was added to the extraction balloon. The extraction was performed for 7 h, followed by filtration, concentration and storage, as previously mentioned in section **3.2.1**.

3.2.3 Extracts Characterization

All the prepared samples were analysed in triplicates, except for the banana plant pseudostem. The data presented are means ± standard deviation (SD) of three determinations.

3.2.3.1 Folin Ciocalteau Method – Total Phenolic Content

The Total Phenolic Content (TPC) was determined according to Lim *et al*. method, with some adjustments.[61] Sodium carbonate solution was prepared by mixing 200 g sodium carbonate with 800 mL water, followed by 1 h sonication and filtration. Calibration curve was done by using 2 500 mg/L gallic acid samples with different dilution ratio of distilled water:gallic acid, as presented in **Figure 8.1**, **Appendix III**. The samples were prepared as described in **Table 3.1**.

Table 3.1: Samples prepared for Folin Ciocalteau method.

Dilution	$V_{extract}$ (µL)	$V_{methanol}$ (µL)
1:1	20	-
1:2	500	500
1:10	100	900

The analysed samples, containing 1.58 mL Milli-Q water, 20 µL of each dilution (presented in **Table 3.1**) and 100 µL Folin reagent, were submitted to 5 sec vortex (Reax 2000, Heidolph). After, 300 µL sodium carbonate was added and then the samples were placed in the digestor (SBH130D, Stuart) for 30 min at 40 °C. Absorbance was read in a UV/VIS spectrometer, at a wavelength of 765 nm.

This colorimetry method is based on the chemical reduction of the tungsten and molybdenum oxides present in the Folin reagent by the phenolic compounds present on the sample, generating a blue colour that exhibits a broad light absorption with a maximum at 765 nm. The light intensity's absorption at this wavelength is directly proportional to the phenolic compound's concentration.[62] The TPC was calculated using the gallic acid calibration curve equation.

3.2.3.2 DPPH Method – Antioxidant Activity

The antioxidant activity determination was carried out according to Gao *et al*. method, with some alterations.[32] 2,2-diphenyl-1-picrylhydrazyl (DPPH) stock solution was prepared with 12 mg DPPH and 100 mL methanol. The so-called working solution was prepared by the dilution of the DPPH stock solution in methanol with the relation of 1:5, for a 4 mL final volume. The samples were prepared as described in **Table 3.2**.

Table 3.2: Samples preparation for DPPH Method.

	Dilution	$V_{extract}$ (mL)	$V_{methanol}$ (mL)	$V_{working\ solution}$ (mL)
White	-	-	0.5	3.5
Extract Solution	1:1	0.5	-	3.5
	1:2	0.25	0.25	3.5
Control	1:1	0.5	3.5	-
	1:2	0.25	3.75	-

The solutions were kept for 30 min, in the dark, at room temperature, until the reaction occurred. To analyse the antioxidant activity of the banana plant leaf and pseudostem extracts, the absorbance of the samples prepared were analysed using a UV/VIS spectrometer (Evolution 201, Thermo Scientific) at the wavelength of 515 nm.[63] This wavelength corresponds to the DPPH reduced form peak absorbance. In the presence of antioxidant compounds, the DPPH's free radical is captured by the antioxidant compound present in the solution, leading to the reduction of DPPH and, consequently, the colour solution change from purple to yellow. The intensity of the yellow colour of the solution is directly proportional to the antioxidant activity of the sample and to the DPPH's inhibition percentage.[64]

DPPH inhibition percentage was calculated using **Equation 3.1**.

$$\%\ \text{DPPH Inhibition} = \frac{\text{Abs}_{\text{white}} - [(\text{Abs}_{\text{extract}} - \text{Abs}_{\text{control}}) \times \text{Dilution Factor})]}{\text{Abs}_{\text{white}}} \quad \textbf{(Eq. 3.1)}$$

where,

% DPPH Inhibition – DPPH's inhibition percentage (%)

Abs_{white} – White solution's (DPPH) absorbance, at λ=515nm

$Abs_{extract}$ – Extract solution's absorbance, at λ=515nm

$Abs_{control}$ – Control's absorbance, at λ=515nm

Dilution Factor – Dilution used in the analysed samples

3.2.3.3 Chemical Composition

3.2.3.3.1 High Pressure Liquid Chromatography (HPLC)

The chemical composition of the phenolic compounds extracted from the leaves, trough Batch Solid-Liquid and Soxhlet extraction, was first analysed by High Pressure Liquid Chromatography (HPLC), which allows the identification and quantification of the chemical compounds present in the samples, based on its retention time. These were compared with some phenolic standards: apigenin, caffeic acid, caffeine, catechin, chlorogenic acid, epicatechin, ferulic acid, gallic acid, p-coumaric acid, protocatechuic acid, quercetin, resveratrol, syringic acid, vanillin and vanillic acid.[65] All the analysis were executed by the technicians Dr. Nuno Costa and Dr. Rodrigo Duarte, from the Laboratório de Análises – FCT NOVA, LAQV-REQUIMTE.

The first chromatographic separation, where the samples were compared with all the standards, was executed on an Infinity 1100 Agilent equipment, using an analytical column Waters Novapak C18 (150mm×4μm). A gradient elution of 98%methanol:2%ethanoic acid (w/w) was performed during 60min, using the flow rate of 0.5mL/min and the injection volume of 5 μL. The column was maintained at 30°C and the wavelength was set at 280.4, 320.4 and 350.4nm.

The second separation, where the sample was compared with the apigenin standard, was performed on an Infinity 1100 Agilent equipment, using an analytical column Waters Novapak 600 C18 (250 mm × 4.6 μm). A gradient elution of 40% methanol: 20% acetonitrile: 40% water: 0.1% acetic acid (w/w) was performed during 20 min, using the flow rate of 0.6 mL/min and the injection volume of 20 μL. The column was maintained at 30 °C and the wavelength was set at 352 nm.

3.2.3.3.2 Liquid Chromatography – Mass Spectrometry (LC-MS)

To achieve a higher accuracy, Liquid Chromatography – Mass Spectrometry (LC-MS) was realized, since it allows to identify and quantify the compounds based on its molecular weight and isotope distribution, compared with the phenolic standards, listed in the section **3.2.3.3.1**.[66] All the analysis were executed by the technician Dr. Luz Fernandes, from the Laboratório de Análises – FCT NOVA, LAQV-REQUIMTE.

The analyses were achieved in a 1 200 Series LC with binary pump UV-VIS and Agilient 6 130B Single Quadrupole LS-MS equipments, using an analytical column Kromasil C18 (250 × 4.6 mm), operated with electrospray ionization. A gradient elution of eluent A: 10% MeOH: 2% CH_3CO (w/w) and eluent B: 90% MeOH: 2% CH_3CO (w/w) was performed during 60 min, using the flow rate of 0.6 mL/min and the injection volume of 20 μL. The column was maintained at 30 °C and the wavelength was set at 280.4, 320.4 and 350.4 nm.

3.3 Cellulose Extraction

Cellulose extraction was carried out following the Prado *et al*. method, with some adjustments.[67] This procedure includes four steps: fibers preparation, fibers mercerization, fibers bleaching and acid-catalysed hydrolysis method.

Fibers preparation: banana plant pseudostem was cut into small pieces (2 × 2 cm) and immersed in deionized water, at 80 °C for 1 h, under stirring, which allows to remove the non-cellulosic compounds.[67] Fibers were washed in running water, to remove soluble sugars and impurities and were dried at 100 °C for 3 h in a cabinet dryer.

Fibers mercerization: 1 g fibers were treated with 20 mL 5% NaOH, at 90 °C for 1 h, under stirring. After, samples were cooled at room temperature, filtrated and washed with deionized water, until pH = 7. After, fibers were dried, at 60 °C, until constant mass reached.

Fibers bleaching: 1g of fibers were treated with 40% [16% (v/v) H_2O_2 + 5% NaOH], at 55 °C, for 90 min, under stirring. This step allows to remove residual hemicellulose and lignin.[67] The mixture was cooled at room temperature and filtered under vacuum. The resultant fibers were washed with deionized water until pH = 5 and dried, at 60 °C, until constant mass reached.

Acid-catalysed hydrolysis method: dried pseudostem fibers were slowly added into the 60 wt% H_2SO_4 acid solution, previously cooled in an ice bath, under vigorous stirring and heated until 45 °C, during 1h. To stop the reaction, the mixture was immediately cooled in an ice bath and 500 mL deionized ice water was added. The addition of deionized water dilutes the acid solution, resulting in a turbid supernatant. The resulting solution was dialyzed against deionized water until pH = 7 was reached. This step allows to remove free acid molecules from the suspension.[67] After, the neutral solution was lyophilized (Scanvec Coolsafe) and storage in a desiccator.

Based on the cellulose sample weight before the extraction and after lyophilization, it is possible to calculate the cellulose extraction reaction yield, accordingly to the **Equation 3.2**.

$$\eta_{glucose} = \frac{w_{f\ glucose}}{w_{i\ pseudostem}} \times 100 \qquad \textbf{(Eq. 3.2)}$$

where,

$\eta_{glucose}$ – Glucose extraction reaction yield (%)

$w_{f\ glucose}$ – Glucose weight after lyophilization (g)

$w_{i\ pseudostem}$ – Pseudostem initial weight (g)

3.3.1 Extracts Characterization

To confirm the success of cellulose extraction from banana plant pseudostem, 5 mg of the extract was digested with 5 mL 5% H_2SO_4, at 100 °C, for 2 h. This digestion, described in **Figure 3.3**, allows the hydrolysis of cellulose into glucose.

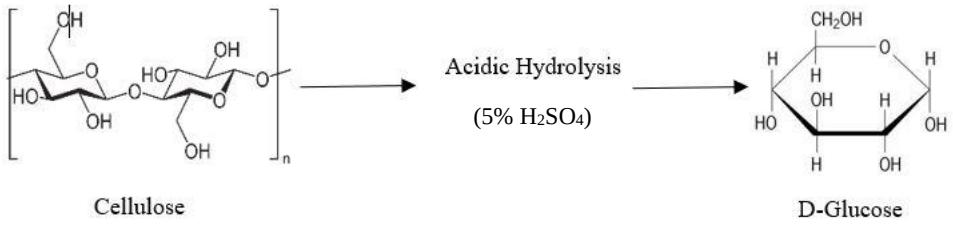

Figure 3.3: Cellulose acidic hydrolysis into D-Glucose.[68, 69]

Glucose identification and quantification was made through High Pressure Liquid Chromatography (HPLC), based on its retention time, compared with the glucose standard (purity ≥ 99.5%). The analysis was performed by the technician Dr. Nuno Costa, from the Laboratório de Análises – FCT NOVA, LAQV-REQUIMTE, using the same equipment as described in section **3.2.3.3.1** and an analytical column CarboPac PA10 (4×250 mm). A gradient elution of 18 mM NaOH was performed, using the flow rate of 1 mL/min and the injection volume of 10 µL. The column was maintained at 25 °C.

3.4 Polymeric Matrices Development and Characterization

3.4.1 Cellulose-based Polymeric Matrices

The preparation of cellulose-based polymeric matrices was carried out respecting the Boon *et al*. solvent evaporation method, with some variations.[70] Commercial hydroxyethyl cellulose (HEC) was used in order to compare the results obtained with the ones obtained with the cellulose extracted from banana plant pseudostem (PS). The plasticizers glucose (G) and urea (U) were used to improve the mechanical properties of the matrices.

Desired amount of cellulose – HEC or PS – and plasticizers – G and/or U – were weighted and added into 5 mL of deionized water, as reported in **Table 3.3**.

Table 3.3: Samples preparation for cellulose matrices.

Sample	Weight (g)		
	HEC or PS	G	U
HEC or PS	0.2	-	-
HEC or PS and G	0.2	0.1	-
HEC or PC and U	0.2	-	0.1
HEC or PS, G and U	0.2	0.075	0.025

The resultant mixture was stirred at 300 rpm and 50 °C for 60 min. After, the resulting solution was centrifuged (4-16KS, Sigma) to degas, at 10 000 rpm, for 5 min. The solution was then poured into a Teflon petri dish and left to dry in a cabinet dryer, at 60 °C for 12 h.

In order to further understand the impact of water vapour on the matrices properties, the samples were left uncovered at selected places of different water activity values, based on the pretended applications, at 30 °C, by using the salts potassium chloride (KCl), sodium chloride (NaCl) and sodium bromide (NaBr), as described in **Table 3.4**.

Table 3.4*:* Values of water activities for different salts.[71]

Salt	a_w (at 30°C) (%)
NaBr	58
NaCl	75
KCl	84

3.4.2 Polymeric Matrices Doped with Phenolic Compounds

Aiming the development of a film composed by the cellulose extracted from the banana plant pseudostem and the phenolic compounds extracted from the banana plant leaves, a protocol for the preparation of these matrices was developed accordingly to Boon *et al.* solvent evaporation method, with some variations.[70] Briefly, 0.2 g of HEC or PS were diluted in a vial containing 5 mL of distilled water and the leaf extract mass resultant from 5 mL methanol Batch Solid-Liquid extraction was diluted in a different vial with 5 mL methanol. Both solutions were heated in a 60 °C bath at 300 rpm, for 60 min. After, solutions were mixed together in the same

vial and submitted to a 4h ultrasounds bath. The resulting solution was poured into a Teflon petri dish and left to dry in a cabinet dryer for 12h at 60°C. After 12h, the resulting matrix was uncovered at selected places of different water activity values, as described in section **3.4.1**.

3.4.3 Characterization Techniques

All the prepared samples were analysed in triplicates, except the banana plant pseudostem. The data presented results are means ± standard deviation (SD) of the three determinations.

3.4.3.1 Scanning Electron Microscopy (SEM)

To evaluate the morphology of the developed matrices, cross-section and surface analysis was performed through Scanning Electron Microscopy (SEM) by the technician Dr. Isabel Nogueira, at MicroLab, Instituto Superior Técnico from Universidade de Lisboa. Small samples of the matrices (less than 1×1cm) were cryofractured by immersion in liquid nitrogen, covered with a layer of Au-Pb and placed in a SEM device (HITACHI S-2400). After preparation, the surface and cross-section of the samples were analysed with 4nm resolution, an electron beam intensity of 25kV and 2.7×10^{-5}Pa ultimate vacuum. The magnifications studied were 400, 1000 and 2000×.

3.4.3.2 X-Ray Diffraction (XRD)

To identify the crystallinity of the sample, X-Ray Diffraction (XRD) characterization was performed by the technician Dr. Nuno Costa, from the Laboratório de Análises – FCT NOVA, LAQV-REQUIMTE. The matrices analysed had the dimensions of 2×2cm and were analysed in a Rigaku Miniflex II X-Ray diffractometer, at room temperature, with a scanning range between 10–80° and using Cu X-Ray tube (30kV/15mA) as radiation source.

3.4.3.3 Differential Scanning Calorimetry (DSC)

To determine the thermal properties and phase transitions of the developed matrices (crystallization (T_x), glass transition (T_g) and melting point (T_m) temperatures), Differential Scanning Calorimetry (DSC) was executed by the technician Dr. Carla Rodrigues, from the

Laboratório de Análises – FCT NOVA, LAQV-REQUIMTE. DSC characterization was carried out using matrices squares with the dimensions of 1×1 cm, in a Setaram DSC 131 instrument, using a nitrogen atmosphere and using a heat-cool-heat cycle between -130 °C to room temperature and from room temperature to 300 °C. The results are presented as an average of 2 measurements of T_g, for each analysed matrix.

3.4.3.4 Thermogravimetric Analysis (TGA)

To evaluate the thermal stability of the prepared matrices, Thermogravimetric Analysis (TGA) was carried out by the technician Dr. Carla Rodrigues, from the Laboratório de Análises – FCT NOVA, LAQV-REQUIMTE. TGA characterization was executed by using matrices squares with the dimensions of 1×1 cm, in a TA Instrument Model TGA Q50, and analysed in a Labsys Evo program, using an argon atmosphere and a temperature increase from 25 to 475 °C, with a 10 °C/min heat range.

3.4.3.5 Fourier Transform Infrared (FTIR) Spectroscopy

To confirm the incorporation of the phenolic compounds in the matrices and to determine the interactions established between the different matrix components, Fourier Transform Infrared (FTIR) spectroscopy was carried out. A square of the samples with the dimensions of 1×1 cm was analysed in a FTIR-ATR spectrometer (Spectrum Two, Perkin-Elmer FTIR spectrometer), with a wavelength range between 400 – 4000 cm^{-1} and 10 scans acquisition.

3.4.3.6 Contact Angle

To determine the matrices hydrophobicity, the contact angle (θ) formed between the matrices surface and a drop of liquid were determined respecting a procedure previously developed in Laboratory of Membrane Processes (FCT NOVA).

The contact angle is defined by the equilibrium between the drop and three interfacial tensions: liquid-vapour (γ_{LV}), solid-liquid (γ_{SL}) and solid-vapour (γ_{SV}), as described in **Figure 3.4**.

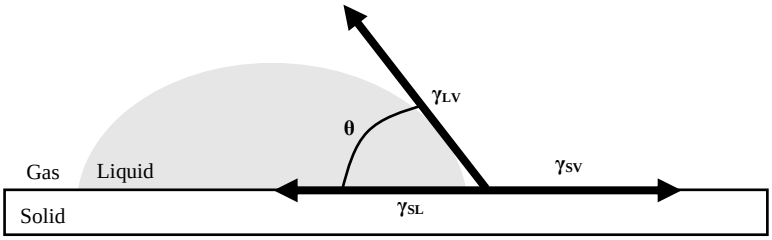

Figure 3.4: Schematic of a contact angle experiment and representation of the interfacial tensions, where θ – contact angle; γ_{LV} – liquid-vapour tension; γ_{SL} – solid-liquid tension and γ_{SV} – solid-vapour tension.[72]

The contact angle can be defined by Young's equation, an described in **Equation 3.3**.[73]

$$\cos\theta = \frac{\gamma_{SV} - \gamma_{SL}}{\gamma_{LV}} \qquad \textbf{(Eq. 3.3)}$$

where,

θ – Contact angle (degree)

γ_{SV} – Solid-vapour tension (Pa)

γ_{SL} – Solid-liquid tension (Pa)

γ_{LV} – Liquid-vapour tension (Pa)

If the obtained contact angle is superior to 90°, it means that the matrix is hydrophobic when water is used. If the opposite occurs, that is, if the contact angle is inferior to 90°, the matrix is considered hydrophilic.[73] A matrix square with the dimensions of 2×2 cm was cut and attach to the surface analyses of the goniometer (CAM100, KSV Instruments LTD).

The analysis was performed using a drop of water and/or glycerol deposited manually on the matrix surface by a small syringe. The measurements of 10 frames, with the intercalation of 1000 ms, were executed in a KSV software (CAM2008), immediately after the drop falls in the matrices surface. The results are presented as an average of 3 measurements, for each analysed matrix.

3.4.3.7 Swelling Measurements

To analyse how the developed polymeric matrices interact with water, swelling measurements were carried out respecting a procedure previously developed in Laboratory of Membrane Processes (FCT NOVA). Matrices were cut in a square of 1x1cm. The thickness (l) of the sample and its weight (w) was determined using a micrometer (Elcometer) and a digital scale (ANJ-NM/ABS-N, Kern), respectively. Samples were transferred to a vial, immersed in distilled water and then stored at 30 °C for 24 h. After 24 h, the samples dimensions, weight and thickness were remeasured.

The percentage of swelling (S) was calculated accordingly to **Equation 3.4**.[51]

$$S = \frac{w_s - w_d}{w_d} \times 100 \qquad \textbf{(Eq. 3.4)}$$

where,

S – Percentage of swelling (%)

w_s – Swollen matrix weight after 24h (g)

w_d – Dried matrix weight (g)

3.4.3.8 Mechanical Properties

The mechanical properties of the matrices were analysed through puncture tests, carried out in collaboration with Dr. Vítor Alves, Assistant Professor at Instituto Superior de Agronomia from Universidade de Lisboa.

Samples were cut in squares with the dimensions of 3×3 cm and then cut in two identical triangles, which were analysed using a texture analyser (TA XT plus, StaLe Micro Systems). The matrices were punctured through a hole with 2 mm diameter, at a constant 1 mm/sec test speed. For each matrix, three replicates were made and the mean value of the obtained Normalized Tensile Strength (NTS) was determined.

The tensile strength of each sample was calculated according to **Equation 3.5**.

$$\sigma = \frac{F}{S_c} \quad \textbf{(Eq. 3.5)}$$

where,

σ – Tensile strength (Pa)

F – Force exerted by the probe (N)

S_c – Cross sectional area (m^2)

For cross sectional area (S_c) calculation, **Equation 3.6** was used.

$$S_c = \pi \times r^2 \quad \textbf{(Eq. 3.6)}$$

where,

r – Probe radius (m)

To have a higher accuracy in the comparation of the experimental results, the tensile strength was normalized with the film thickness following **Equation 3.7**.

$$\sigma_{normalized} = \frac{\sigma}{l_{matrix}} \quad \textbf{(Eq. 3.7)}$$

where,

$\sigma_{normalized}$ – Normalized tensile strength (MPA/mm)

l_{matrix} – Matrix thickness (m)

3.4.3.9 Rheology

Some of the mixtures described in **Table 3.3**, section **3.4.1** instead of producing a film, produced a gel. To characterize the rheology of the developed gels, two properties were analysed: viscosity and viscoelasticity, carried out in collaboration with Dr. Vítor Alves, Assistant Professor at Instituto Superior de Agronomia from Universidade de Lisboa. In both experiments, the samples were directly loaded in a cone and plate geometry C35/2°Ti and a 4 cm diameter, at the respective controlled stress rheometer.

3.4.3.9.1 Viscosity

The viscosity of the gels was analysed by a rheometer RS 75 RheoStress, HAAKE, at 25 °C. Flow curve was determined using a steady-state flow ramp (a logarithmic ramp was used to impose torque – $\dot{\gamma}$) using a shear rate from 0.01 – 1000 s^{-1}. The shear rate was determined by the measurement of point by point with consecutive 60 s steps of constant shear rate. The apparent viscosity, η (Pa.s), was recorded for each point to obtain the flow curves.

3.4.3.9.2 Viscoelasticity

The viscoelastic properties of the gels were analysed by a controlled stress rheometer (Haake Mars, Thermo Scientific) equipped with a Peltier liquid temperature control unit, at 25 °C. First, to identify the ideal pressure, the samples were exposed to a stress sweep from 0.001 – 1000 Pa, using the frequency of 1 Hz. After that, to measure the frequency dependence of the storage (G' – elastic component) and loss (G'' – viscous component) of the energy by the polymer molecules, a frequency sweep from 0.01 – 100 Hz was used, using the pressure determined initially.

3.4.3.10 Pure Gas Permeation Studies

Single gas CO_2 and O_2 permeabilities, as well as CO_2/O_2 ideal selectivity were determined accordingly to L. A. Neves *et al*, using the experimental setup shown in **Figure 3.5**.[74]

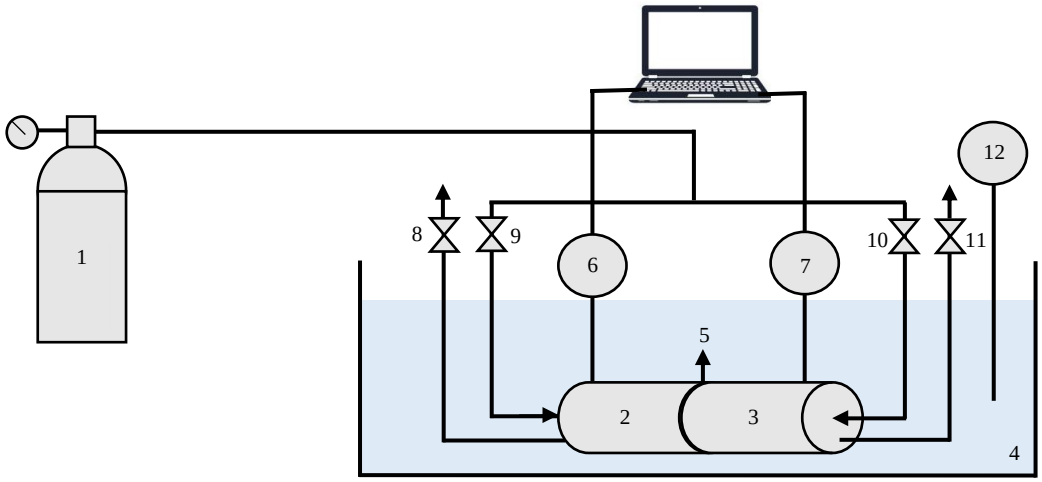

Figure 3.5: Experimental set-up for pure gas permeation experiments, where 1 – feed gas (CO_2 or O_2); 2 – feed compartment; 3 – permeate compartment; 4 – water bath; 5 – polymeric matrix; 6 and 7 – pressure indicators; 8 and 11 – exhaust valves; 9 and 10 – inlet valves and 12 – temperature controler.[75]

The utilized system was composed by a stainless-steel cell with two identical compartments: feed and permeate, which are separated by the polymeric matrix in the form of film. The cell was emerged in a water bath with a constant temperature of 30 °C, controlled by a thermostat (GmBH ED, Julabo). To guarantee that just the analysed gas was present inside the cell, a purge was made. After, the exhaust valves were closed and the experiment started by pressurizing each compartment of the cell with the analysed gas (CO_2 and O_2), until the pressure of 0.7 Bar was achieved. Reached the desired pressure, the inlet valves were closed and the pressure was left stabilizing for a few minutes. When the pressure stabilization was reached, the permeate exhaust valve were quickly opened and closed, causing a pressure variation between both cell compartments – the so-called driving force. After this, the pressure raised gradually in the permeate compartment and decreased in the feed compartment, until the equilibrium was established.

The pressure variation over time, in each compartment of the cell, was measured by pressure indicators (Druck PCDR 910, 99 166 and 991 675). The pressure monitoring and data acquisition were controlled by an inhouse developed software.

The permeability of each analysed gases through the matrices was calculated accordingly to **Equation 3.8**.[76]

$$\frac{1}{\beta} \times \ln\left(\frac{\Delta P_0}{\Delta P}\right) = P \times \frac{t}{l} \quad \textbf{(Eq. 3.8)}$$

where,

β – Experimental cell geometric parameter (m^{-1})

ΔP_0 – Pressure difference at t_0 (bar)

ΔP – Pressure difference through time (bar)

P – Matrix permeability (m^2/s)

t – Time (s)

l – Matrix thickness (m)

The graphic representation of $\frac{1}{\beta} \times \ln\left(\frac{\Delta P_0}{\Delta P}\right)$ as a function of $\frac{t}{l}$ was made, in which the slope represents the matrix gas permeability.

β is dependent of the cell geometry and was calculated from **Equation 3.9**.

$$\beta = A\left(\frac{1}{V_{feed}} + \frac{1}{V_{perm}}\right) \quad \textbf{(Eq. 3.9)}$$

where,

A – Matrix area (m^2)

V_{feed} – Feed compartment volume (m^3)

V_{perm} – Permeate compartment volume (m^3)

In this work, the experimental cell geometric parameter was determined experimentally, by using a Polydimethylsiloxane (PDMS) membrane, with a thickness of 125 µm and a known permeability to N_2 of 2.075×10^{-10} m^2/s. This calibration was executed accordingly to the same protocol previously described for matrix permeation experiments.

Therefore, with the obtained pressure values through time, the graphic representation of $\frac{1}{P} \times \ln\left(\frac{\Delta P_0}{\Delta P}\right)$ as a function of $\frac{t}{l}$ was made, in which the slope represents the β.

The ideal selectivity (α) of the matrices was calculated accordingly to the following **Equation 3.10**.

$$\alpha_{CO_2/O_2} = \frac{P_{CO_2}}{P_{O_2}} \quad \textbf{(Eq. 3.10)}$$

where,

α – Ideal selectivity

P_{CO_2} – Permeability of CO_2 (m^2/s)

P_{O_2} – Permeability of O_2 (m^2/s)

4. Results and Discussion

As previously mentioned, the main goal of this master thesis was the development of polymeric matrices based on the cellulose extracted from banana plant pseudostem and doped with phenolic compounds extracted from banana plant leaves. Aiming that, the results of the different techniques used are described below.

4.1 Phenolic Compounds Extraction

4.1.1 Extracts Characterization

To determine the Total Phenolic Content and the antioxidant activity of the chemical compounds extracted from banana plant leaves and pseudostem, Folin Ciocalteau and DPPH methods were performed, respectively. All the results presented were obtained using the dilution of 1:1, sample:Milli-Q water, since it was the dilution that allowed the most consistent results.

4.1.1.1 Folin Ciocalteau Method – Total Phenolic Content

To determine the TPC of the banana plant leaf and pseudostem extracts, the obtained absorbances of the samples prepared in section **3.2.3.1**, from both extraction methods, Batch Solid-Liquid and Soxhlet, are represented on **Figure 4.1**. The gallic acid calibration curve is presented on **Figure 8.1**, **Appendix III**.

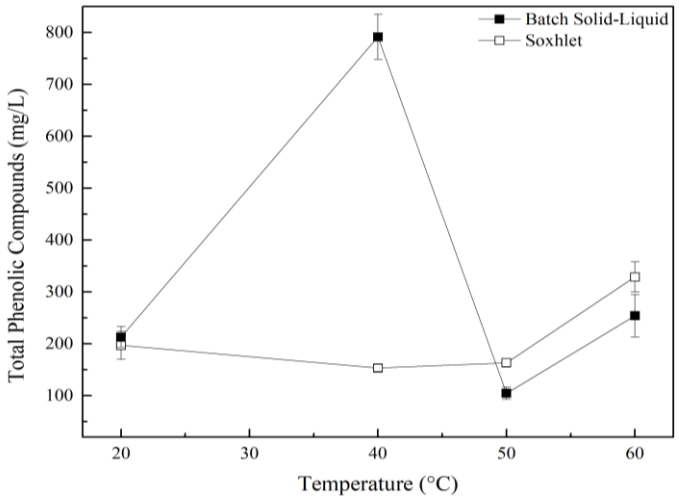

Figure 4.1: Total Phenolic Content results for Batch Solid-Liquid (■) and Soxhlet (□), 3 days leaf extraction, using four different drying temperatures: room 20, 40, 50 and 60 °C.

From the analysis of **Figure 4.1**, for all the drying temperatures the TPC in the leaves is similar in both extraction methods, except at 40°C where Batch Solid-Liquid extraction allowed the highest phenolic content ($791.74 mg/L \pm 43.75 mg/L$).

Accordingly to Dixon *et al.* and Prathapan *et al*., plants in general respond to the drying temperature by increasing their phenolic content to repair the damaged tissue and inactivating oxidative enzymes such as polyphenol oxidases, which can support a TPC increase from 20 to 40°C obtained by Batch Solid-Liquid extraction.[77, 78] The increasing temperature can lead to the binding of phenolic compounds to other leaf components or to a chemical structure alteration, resulting in a phenolic content decrease, supporting the TPC decrease for temperatures above 40°C.[79] In addition, in the experiments of Sagrin *et al.*, the highest TPC was obtained for leaves dried at room temperature ($2\,731.49 \pm 14.41 mg$), while in this work, the TPC obtained in the same conditions was $213.08 \pm 20.08 mg$.[59] The difference observed in the obtained values may be due to the fact that banana plant samples used by Sagrin *et al.* were from Malaysia and the ones used in this work are from Madeira island, Portugal, being exposed to different environmental, cultivation and farming conditions, affecting its TPC.[3]

To understand which banana plant part presents the highest antioxidant activity, banana plant pseudostem samples were dried at 40°C and exposed to a Batch Solid-Liquid extraction, evidencing an TPC of $5.71 mg/L$, which is a much lower value than the obtained with the leaves ($791.74 mg/L \pm 43.75 mg/L$). Based on these results, banana plant leaf samples were analysed using the drying temperature of 40°C but with different time periods of Batch Solid-Liquid extraction, from day 1 to 5, to study which extraction time allows a highest TPC. The obtained results are present on **Figure 4.2**.

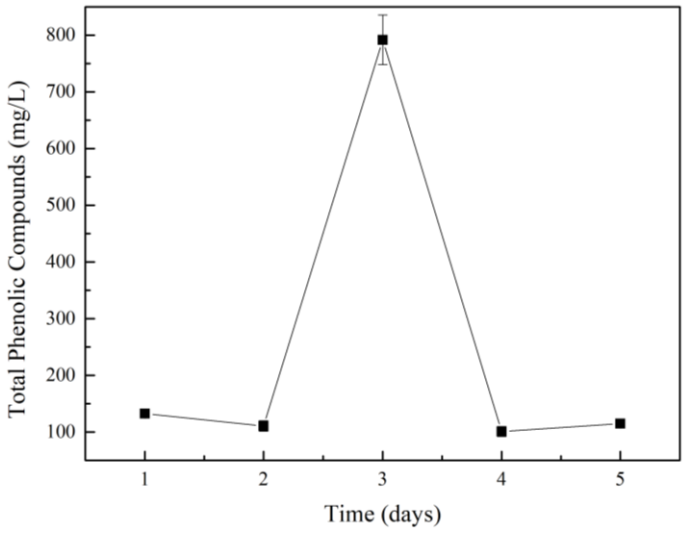

Figure 4.2: Total Phenolic Content results for Batch Solid-Liquid leaf extracts during 5 days at 40°C.

From the analysis of **Figure 4.2** results it can be concluded that the highest TPC (791.74mg/L ± 43.75mg/L) was achieved at 3 days Batch Solid-Liquid extraction. Comparing the obtained TPC results for banana plant leaves with the ones reported for banana pulp (30–60 g/100 g fresh pulp) and banana peel (0.90–3.0 g/100 g fresh peel) and the ones obtained in this work for banana plant pseudostem (5.71mg/L) it can be concluded that banana plant leaves are a better source of phenolic compounds.[80]

4.1.1.2 DPPH Method – Antioxidant Activity

To analyse the antioxidant activity of the banana plant leaf and pseudostem extracts, the obtained absorbances of the samples prepared in section **3.2.3.2** were used to calculate the DPPH Inhibition Percentage (**Equation 3.1**), from both extraction methods, Batch Solid-Liquid and Soxhlet, represented on **Figure 4.3**.

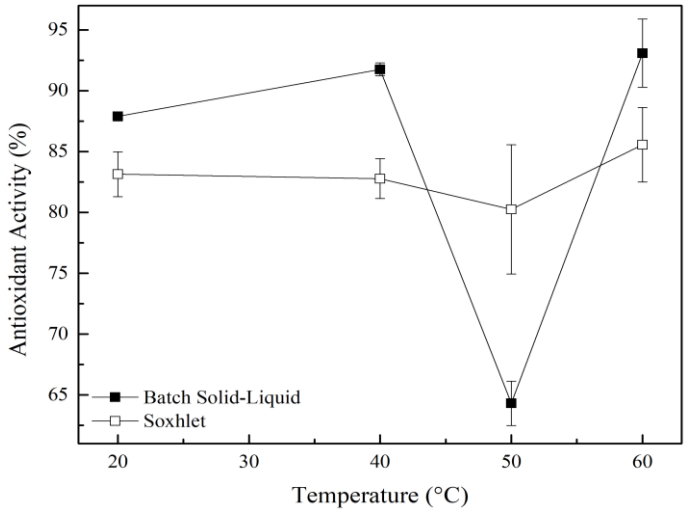

Figure 4.3: Antioxidant activity results for Batch Solid-Liquid (■) and Soxhlet (□), 3 days leaves extraction, using four different drying temperatures: 20, 40, 50 and 60 °C.

From the analysis of **Figure 4.3** it can be noticed that, for all the drying temperatures used, except 50 °C, the highest value of antioxidant activity in the leaves were obtained with the Batch Solid-Liquid extraction method. This can occur due to the high temperature used to evaporate the solvent (methanol – 65°C) in Soxhlet extraction, which can cause the degradation of the antioxidant compounds present in the leaves.[59]

Accordingly to Sagrin *et al.*, higher drying temperatures can cause significant reduction of antioxidant content and activity compared to the fresh leaves, due to the instability of natural antioxidants at high temperatures.[59] Though, as the obtained results show, some studies revealed little or no changes in the antioxidant levels after drying, owing to the presence of heat-

stable antioxidant compounds, such as tannins.[59] The drying temperature of the leaves with highest antioxidant activity in Batch Solid-Liquid and Soxhlet extractions is 60°C, corresponding to a high antioxidant percentage of, 93.09 ± 2.79 and 85.56 ± 3.07, respectively, as also reported by Mathew *et al*.[22] The highest antioxidant activity is really closed to the one achieved by using the same extraction method and the drying temperature of 40°C ($91.75\% \pm 0.53\%$), which implies lower energy costs and less leaves' compounds degradation, reason why this was the temperature used in the following analysis.

To understand which banana plant part presents the highest antioxidant activity, banana plant pseudostem samples were dried at 40°C and exposed to a Batch Solid-Liquid extraction, evidencing an antioxidant activity of $49.51\% \pm 0.38\%$, corresponding to almost half of the value obtained with the leaves. Based on these results, banana plant leaf samples were analysed using the drying temperature of 40°C but with different time periods of Batch Solid-Liquid extraction, from day 1 to 5, to study which extraction time allows the highest antioxidant activity (**Figure 4.4**).

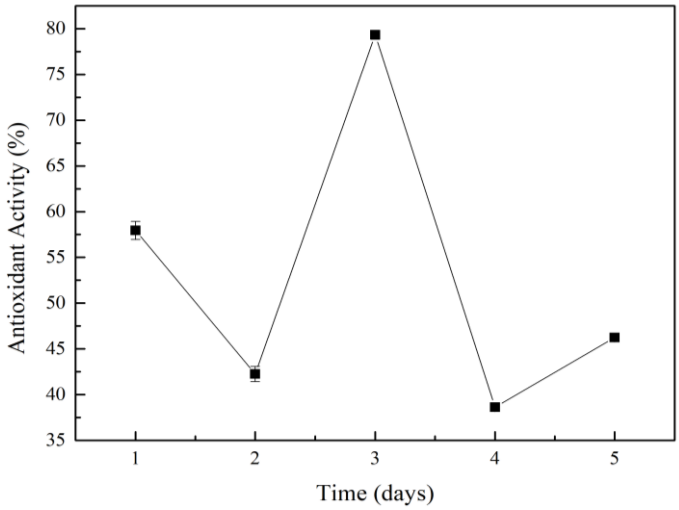

Figure 4.4: Antioxidant activity results for Batch Solid-Liquid leaf extracts during 5 days at 40°C.

From the analysis of **Figure 4.4** it can be concluded that the highest antioxidant activity percentage ($79.34\% \pm 0.5\%$) was achieved after 3 days. Comparing the obtained values for 3 days Batch Solid-Liquid extraction using the drying temperature of 40°C present on **Figures 4.3** and **4.4**, it can be noticed that the values have a small variation that can be caused by the storage and/or extraction conditions.

Once the goal of this work was the development of polymeric matrices with antioxidant capacity, the extract obtained from 3 days Batch Solid-Liquid extraction of leaves dried at 40°C (BSL_3_40) was selected for the following methods.

4.1.1.3 Chemical Composition

4.1.1.3.1 High Pressure Liquid Chromatography (HPLC) and Liquid Chromatography – Mass Spectrometry (LC-MS)

All the samples obtained from Batch Solid-Liquid and Soxhlet extraction were first analysed by HPLC, to identify and quantify its chemical compounds, based on its retention time. This was made comparing the retention time of the samples with phenolic standards, described in **Table 8.7**, **Appendix III**.[65] Since the sample that allowed the highest and TPC and antioxidant activity was BSL_3_40, three replicates of this sample were analysed (samples 1, 2 and 3).

The HPLC chromatogram obtained for sample 1 of BSL_3_40 is presented at **Figure 4.5**. The chromatograms for samples 2 and 3 are in **Figures 8.2** and **8.3**, **Appendix III**, respectively. The obtained retention times for samples 1, 2 and 3 are in **Tables 8.8**, **8.9** and **8.10**, **Appendix III**, respectively.

Based on the similarity of the obtained retention times of the studied samples and standards, a preliminary identification of the possible phenolic compounds present on the samples was made, as shown in **Table 4.1**. As a result, the identified phenolic compounds were catechin, gallic acid and resveratrol.

Accordingly to Mathew *et al.*, some phytochemicals present in *Musa acuminata* leaf, by methanol extraction, were alkaloids, steroidal lactones and tannis, which were not possible to confirm in the analysed samples due to the lack of respective standards.[22]

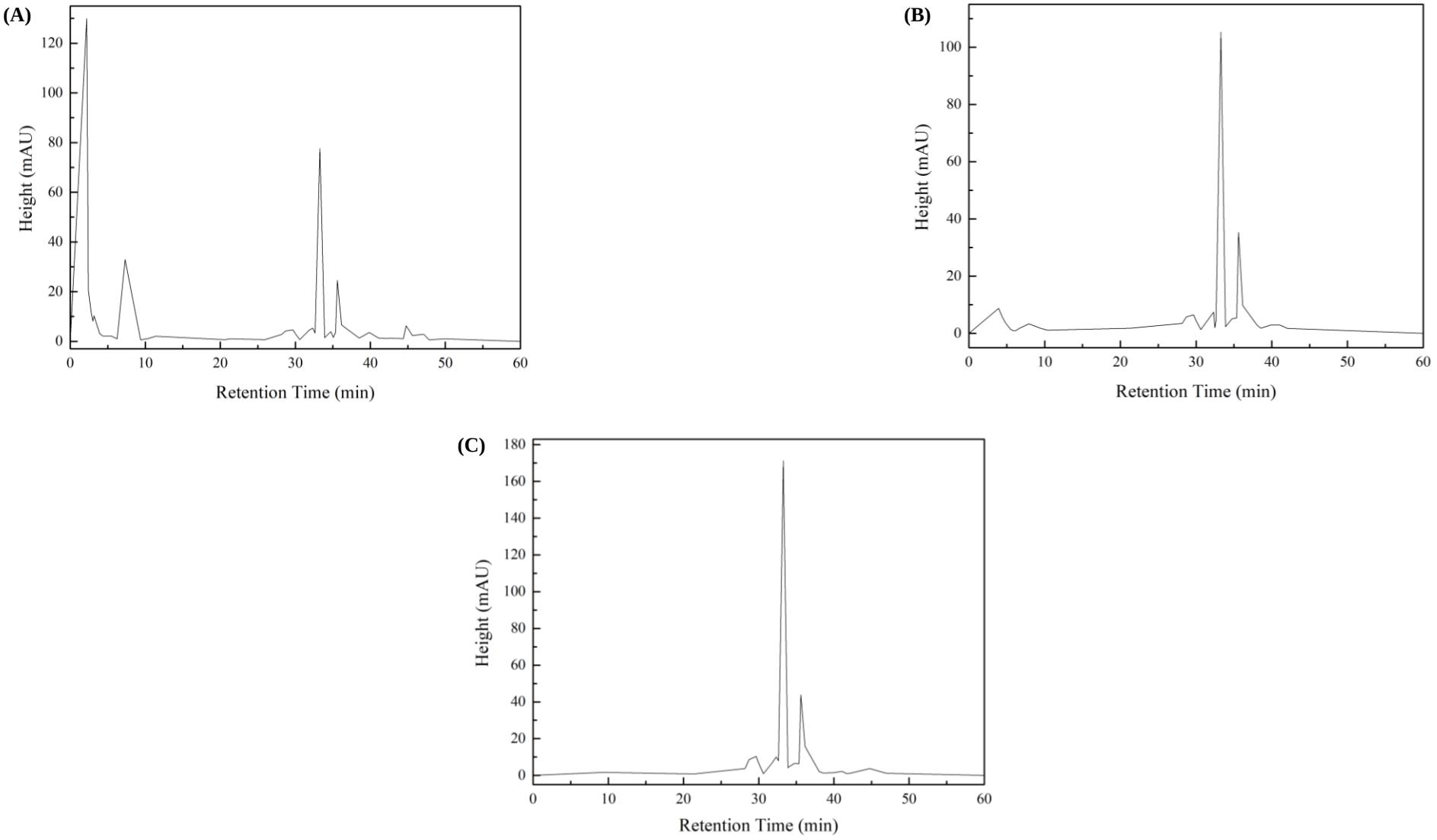

Figure 4.5: HPLC chromatogram for the sample 1 of BSL_3_40, at the drying temperature of 40°C and at the wavelength of 280.4 **(A)**, 320.4 **(B)** and 350.4 **(C)** nm.

Table 4.1: Preliminary identification of the phenolic compounds present on the analysed 3 replicates of BSL_3_40 by comparing its HPLC retention times with the standards.

Sample	Wavelength (nm)	Retention Time (min)
Catechin (Standard)	280.40 320.40 350.40	6.12 32.98 32.96
Gallic acid (Standard)	280.40 320.40 350.40	3.03 3.03 -
Resveratrol (Standard)	280.40 320.40 350.40	33.20 33.20 33.20

Sample 1	280.40 320.40 350.40	6.24 32.63 32.63	3.02 3.91 -	33.26 33.26 33.25
Sample 2	280.40 320.40 350.40	5.57 32.92 32.92	- - -	33.55 33.55 33.55
Sample 3	280.40 320.40 350.40	7.79 32.95 32.93	3.34 3.87 -	33.56 33.57 33.56

To achieve a higher accuracy in the phenolic compounds identification, a LC-MS of sample 1 was performed.[66] The obtained LC-MS diagram is accessible at **Figure 8.4**, **Appendix III**. According to the obtained results, is was noticed that the retention time range between 44–47 min had the highest UV intensity and, based on the analysed standards, an isotope distribution similar to the apigenin was identified (**Figure 4.6**).

(A)

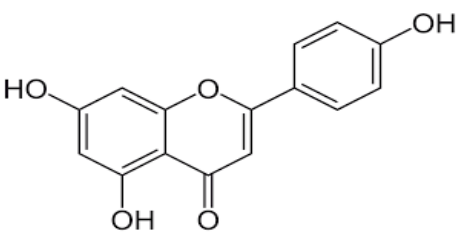

(B)

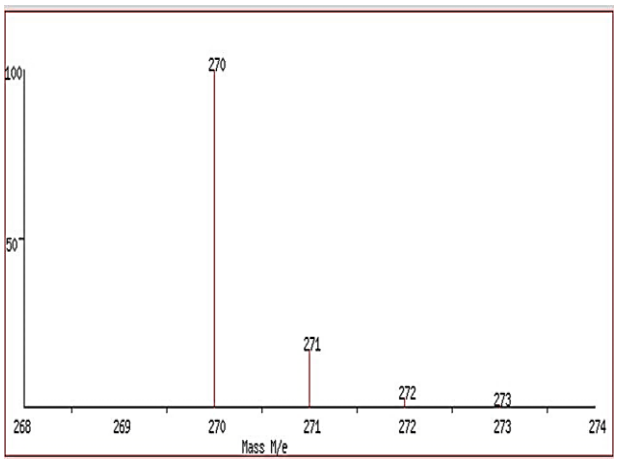

Figure 4.6: Apigenin's chemical structure **(A)** and expected isotope distribution **(B)**.[81, 82]

Thus, a HPLC analysis was done to quantify the apigenin present in sample 1. The standard apigenin characteristics and calibration curve equation are described in **Table 8.11**, **Appendix III**. The apigenin present in the sample was not quantified, due to the possible coelution with other compounds and to the proximity of its quantity to the method's detection limit. For further analysis, a search of phenolic compounds with retention times from 44 to 47 min should be done, since this is the retention time range with more UV intensity, as well as the HPLC analysis of the samples with the alkaloids, steroidal lactones and tannis standards, once they were reported to be present in *Musa acuminata* leaves.[22]

4.2 Cellulose Extraction and Characterization

Cellulose was extracted from 1 g of banana plant pseudostem, using the extraction method develop by Prado *et al.*, resulting in 0.073 g cellulose. Through **Equation 3.2**, described in section **3.3**, it was possible to calculate the cellulose extraction reaction yield of 7.3%. As reported by Sango *et al.*, long cellulose fibers extracted from banana plant pseudostem were extracted at a yield of 60%, proving that the low yield obtained by following the method used in this work, can be improved with the process optimisation or by following another method reported in the literature.[83]

To confirm the success of cellulose extraction from banana plant pseudostem, 5 mg of the extract was exposed to an acidic digestion, as described in **Figure 3.3** section **3.3.1,** that allows the hydrolysis of cellulose into glucose. Then, the glucose contained in the obtained solution was quantified by HPLC. The glucose calibration curve used is presented in **Table 8.12**, **Appendix III**. The HPLC analysis allowed the detection of 1.30 mg/L glucose, at the retention time of 10.7 min, proving that the cellulose extraction was successful.

4.3 Cellulose-based Polymeric Matrices and Polymeric Matrices Doped with Phenolic Compounds

The obtained matrices are described in **Table 4.2**. and presented in **Figure 4.7**, where L – phenolic compounds extracted from banana plant leaves.

Table 4.2: Obtained matrices structure and surface characteristics.

Matrix	Matrices Structure and Surface Characteristics		
	58% a_w	75% a_w	84% a_w
HEC	Film Homogeneous surface	Film Homogeneous surface	Film Homogeneous surface
HEC_G	Film White crystals on the surface	Film White crystals on the surface	Film Homogeneous surface
HEC_U	Film White colour	Gel Homogeneous surface	Gel Homogeneous surface
HEC_G_U	Film Homogeneous surface	Film Homogeneous surface	Film Mold on the surface
HEC+L	Film Homogeneous surface	Film Homogeneous surface	Film Mold on the surface
PS	Film Non-homogeneous surface	Film Non-homogeneous surface	Film Non-homogeneous surface
PS+L	Film Non-homogeneous surface	Film Non-homogeneous surface	Film Mold on the surface

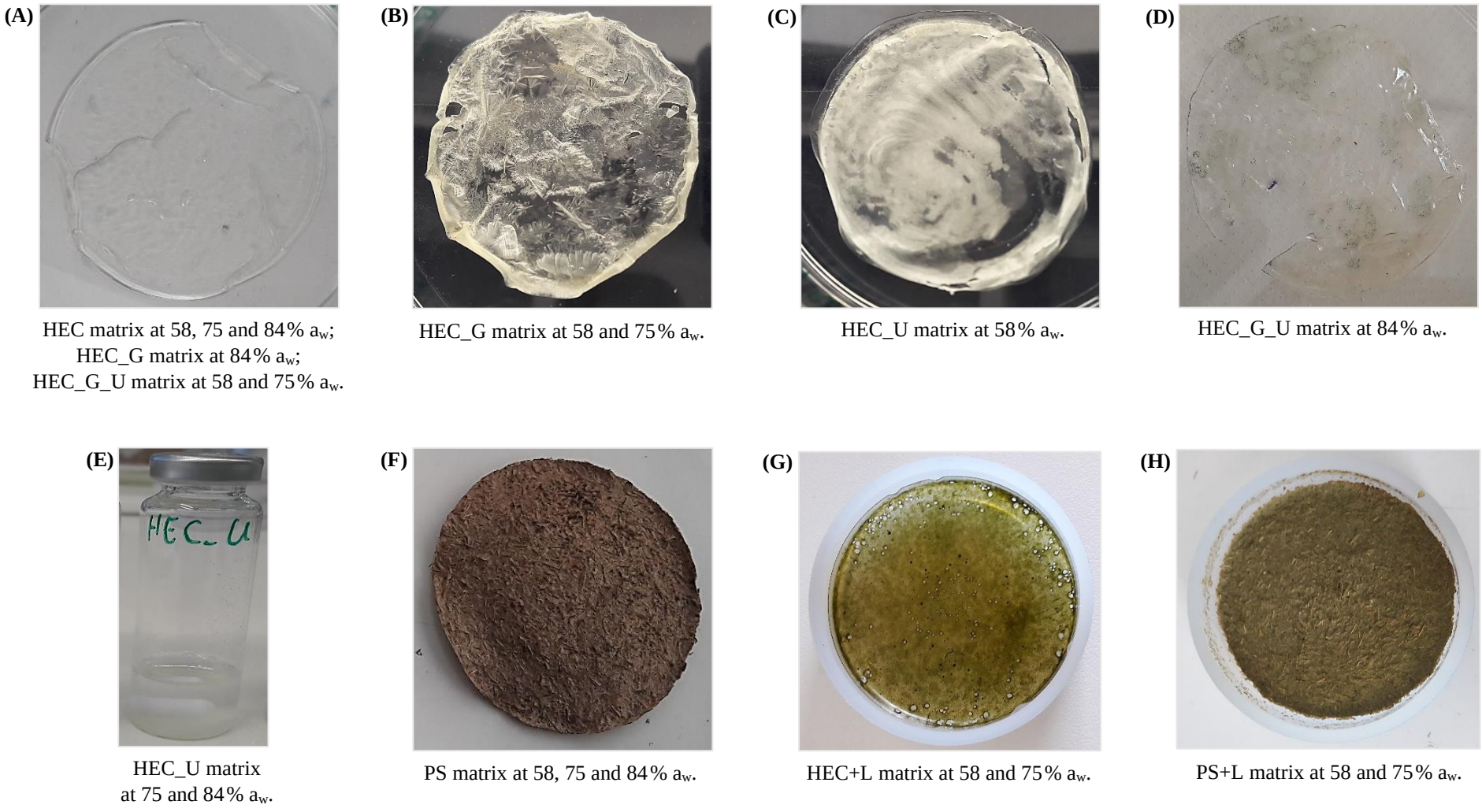

Figure 4.7: Obtained matrices.

From the analysis of the previous **Table 4.2** it can be noticed that all the mixtures produced films except the HEC_U matrix exposed to 75 and 84% a_w that resulted on a gel (**Figure 4.7 (E)**). The films of HEC_G exposed to 58 and 75% a_w presented the formation of small white crystals on their surfaces, as can be observed at **Figure 4.7 (B)**. The film obtained from HEC_U mixture and exposed to 58% aw, **Figure 4.7 (C)**, developed a white colour over time. This crystals and white colour development could be due to the bad mixture of the plasticizer in the solution, preventing the obtention of a homogeneous solution.[84]

The HEC_G_U, HEC+L and PS+L films exposed to 84% a_w developed mold on its surface, as can be seen in **Figure 4.7 (D)**, which precluded its characterization. This mold formation could be due to the presence of glucose on the HEC_G_U matrices and could had spread to the other films since they were all in the same container.[85] The mold formation could be prevented by the addition of azide.

The other HEC matrices with and without plasticizers, that did not develop crystals, white colour or mold, formed a transparent thin film, as reported by Boon *et al.* and as pretended for the aimed applications.[46][70]

All the films and gels without mold development were characterized accordingly to the techniques described in the section **3.4.3** and the obtained results were presented in the following section **4.3.1**.

4.3.1 Characterization

All the prepared films were characterized accordingly to the following methods, except the mixtures of HEC_G_U, HEC+L and PS+L exposed to 84% a_w, due to the mold formation on their surface. The obtained gels – HEC_U exposed to 75 and 84% a_w – were just characterized by Differential Scanning Calorimetry (DSC), Thermogravimetric Analysis (TGA), X-Ray Diffraction (XRD), Fourier Transform Infrared (FTIR) spectroscopy and rheology.

4.3.1.1 Scanning Electron Microscopy (SEM)

Scanning Electron Microscopy (SEM) analysis allows the observation of the membrane cross-section and surface morphology. In this technique, images of the membranes cross-section and surface were obtained, using the magnifications of 400, 1 000 and 2 000×. The analysed SEM images presented below (**Figures 4.8**, **4.9** and **4.10**), were obtained with the magnification of 1 000×, since it allows the best cross-section and surface observation.

The matrices composed of HEC when exposed to 58, 75 and 84% a_w (**Figures 4.8**, **4.9** and **4.10**); HEC_G at 84% a_w (**Figure 4.10**); HEC_G_U at 58 and 75% a_w (**Figures 4.8** and **4.9**) presents a homogeneous cross-section and surface without the formation of agglomerates, being possible to observe a dense structure without deformations, as is was reported for this type of membranes and as pretended for the aimed applications.[86] The surface images for HEC matrices at 75 and 84% a_w (**Figures 4.9** and **4.10**) present some small dirt particles.

The matrices obtained for HEC_G exposed to 58 and 75% a_w (**Figures 4.8** and **4.9**) presents crystals on their surface, and the HEC_U matrix at 58% a_w (**Figure 4.8**) presented filaments, due to the bad solution homogenization as was observed during the matrices analyses in the section **4.3**. The matrices HEC+L and HEC_G exposed 58 and 75% a_w and HEC_U matrix at 58% a_w, despite of a homogeneous dispersion of the matrice constituents, present bubbles or voids that could have been introduced in the liquid inadvertently during the mixing process. This can be optimized by centrifuging the mixture for a longer period of time.[84]

The PS films exposed to all a_w and PS+L films exposed to 58 and 75% a_w (**Figures 4.8** and **4.9**) shown a non-homogeneous dispersion of pseudostem cellulose fibers throw the matrix, resulting in a porous matrix, which could be caused by the low yield of cellulose extraction (7.3%) that prevented a better fibers packaging.

Matrix	Cross-Section	Surface
HEC	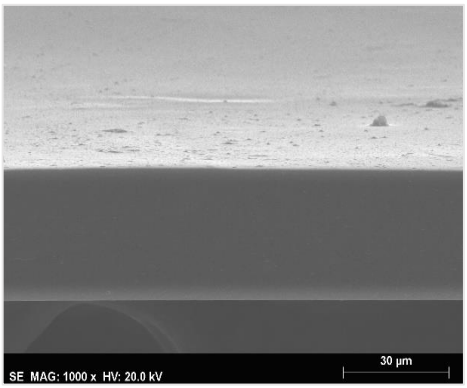	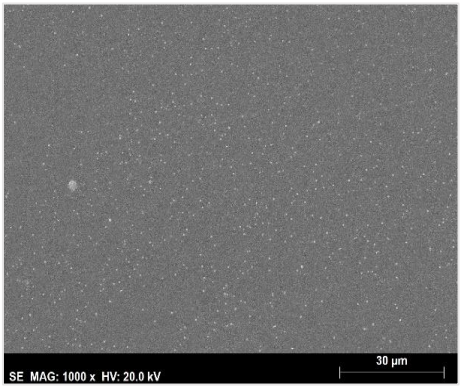
HEC_G	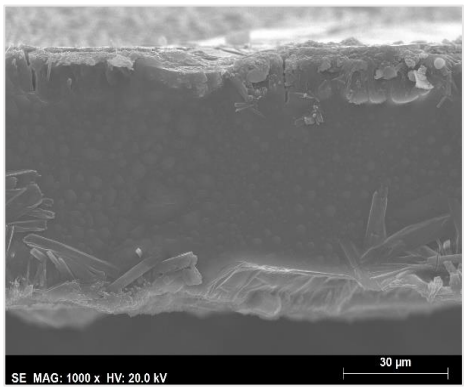	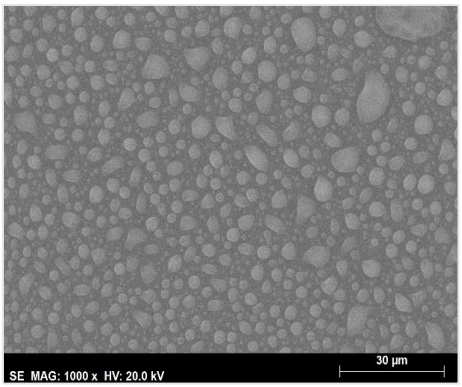
HEC_U	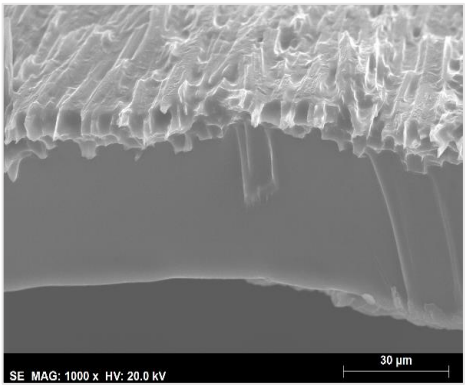	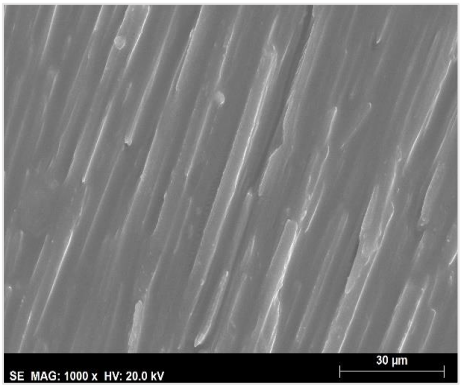
HEC_G_U	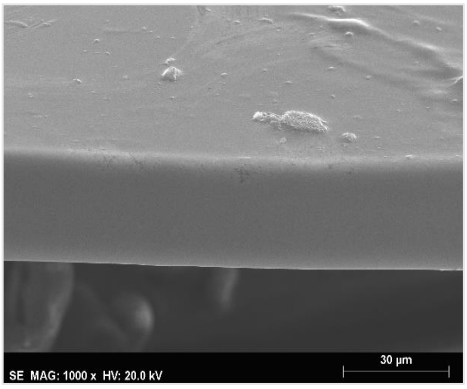	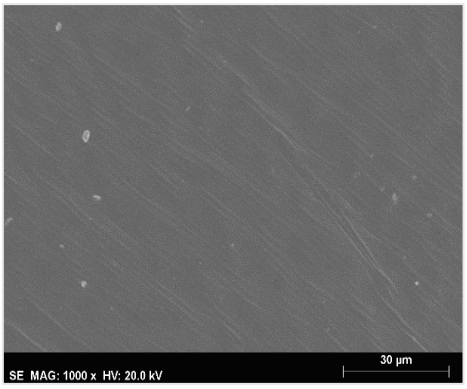

Figure 4.8: HEC and PS films results from SEM analysis exposed to 58% a_w, with 1 000× ampliation.

(Figure continues on the next page)

Matrix	Cross-Section	Surface
HEC+L	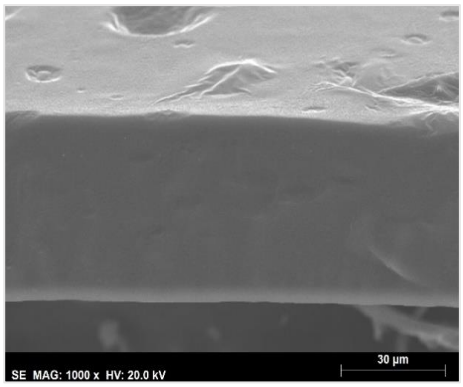	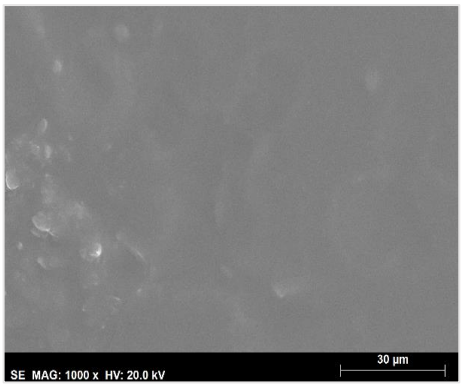
PS	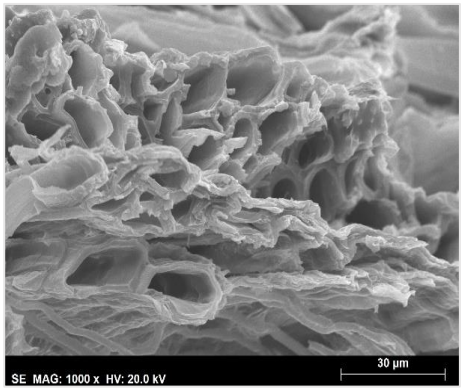	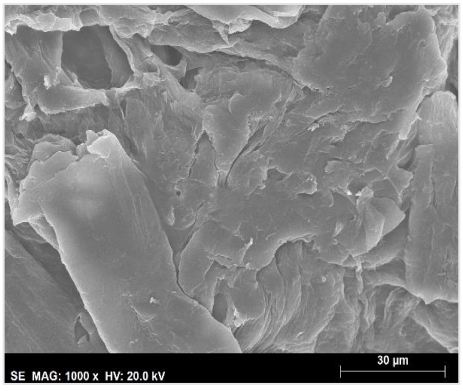
PS+L	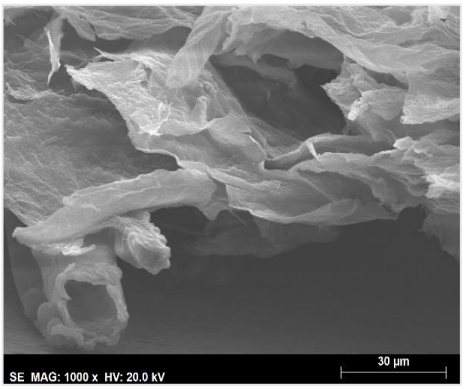	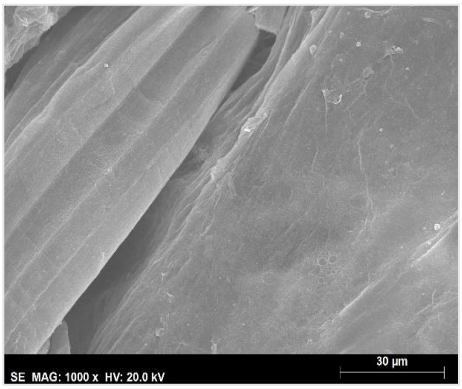

Figure 4.8: Figure continuation.

Matrix	Cross-Section	Surface
HEC	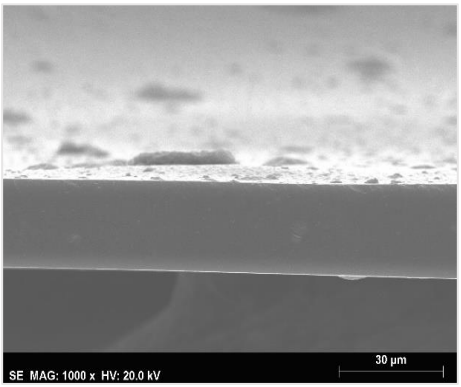	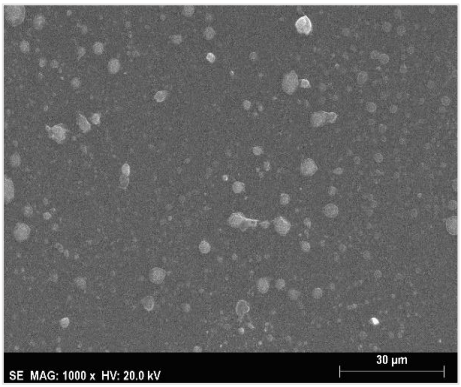
HEC_G	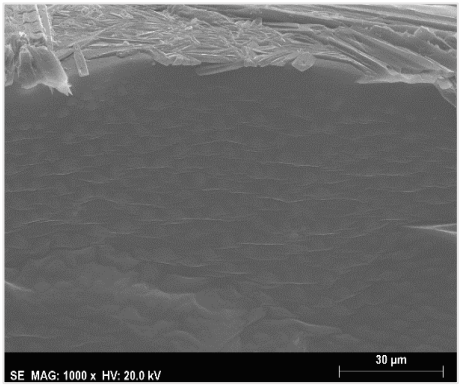	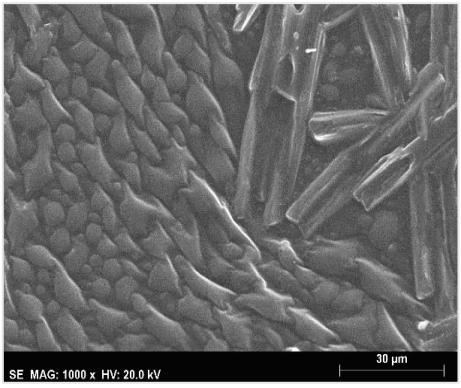
HEC_G_U	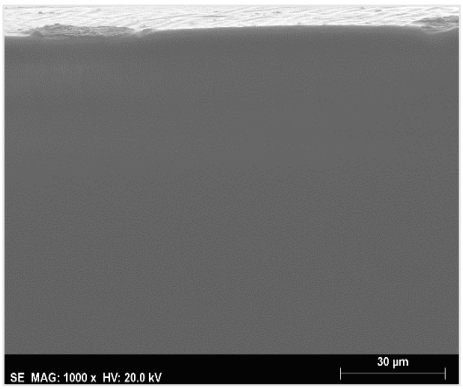	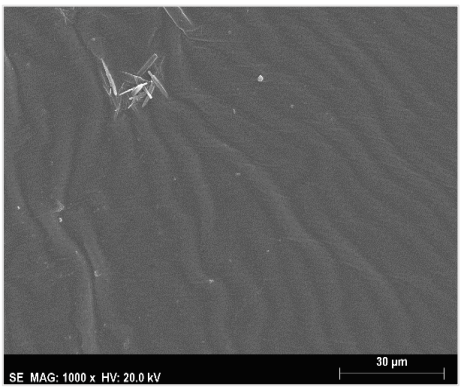
HEC+L	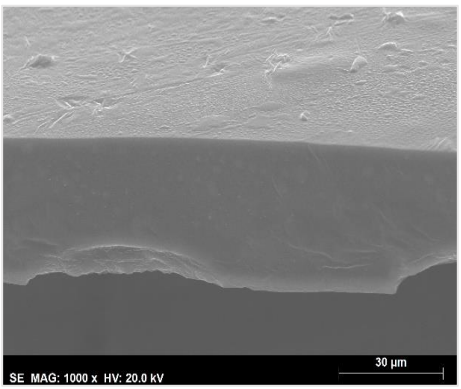	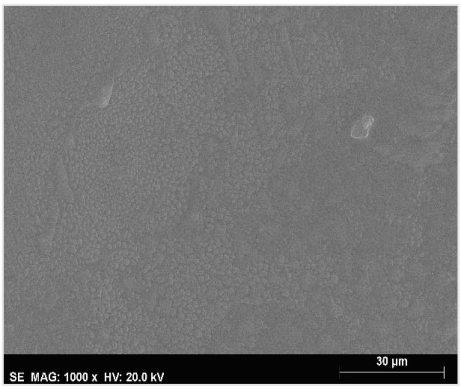

Figure 4.9: HEC and PS films results from SEM analysis exposed to 75% a_w 1 000× ampliation.

(Figure continues on the next page)

Matrix	Cross-Section	Surface
PS	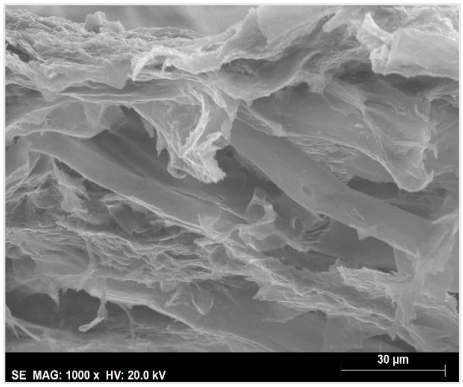	
PS+L	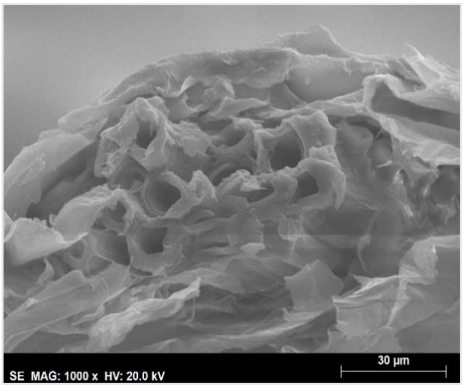	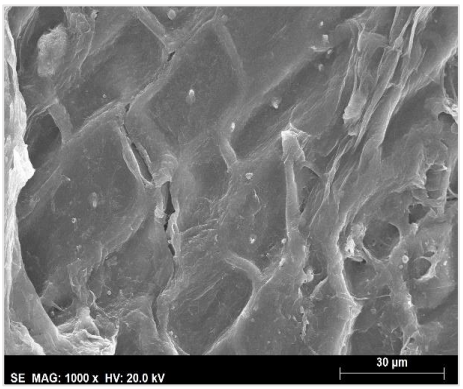

Figure 4.9: Figure continuation.

Matrix	Cross-Section	Surface
HEC	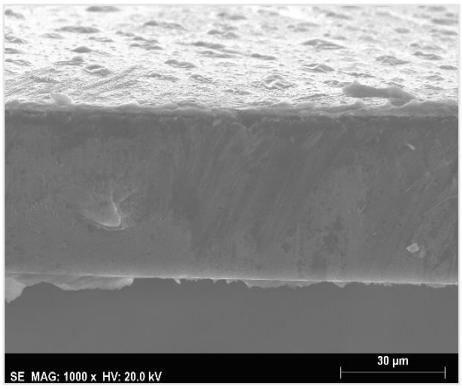	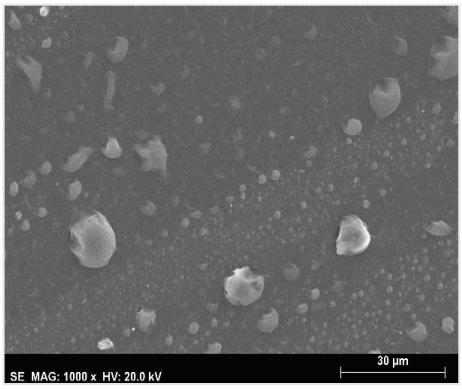
HEC_G	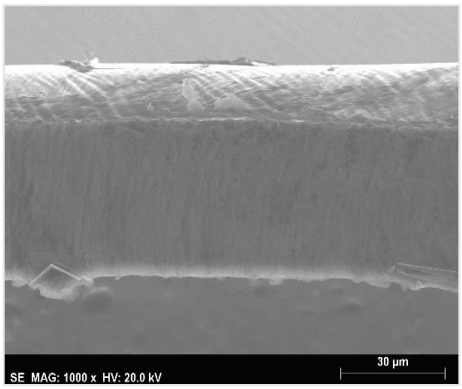	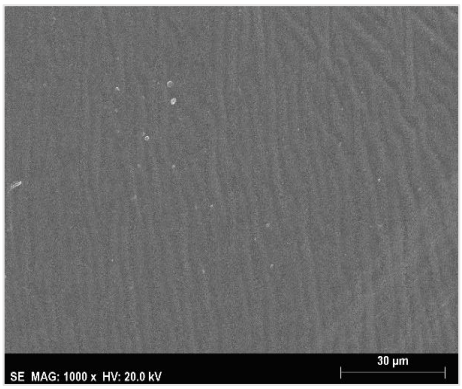
PS	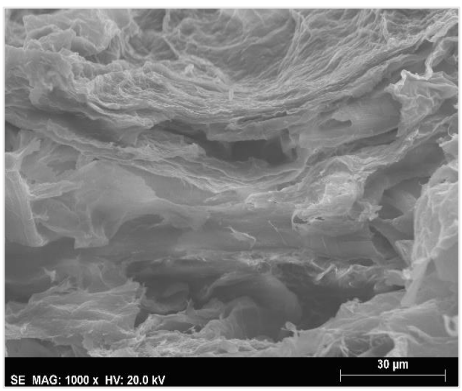	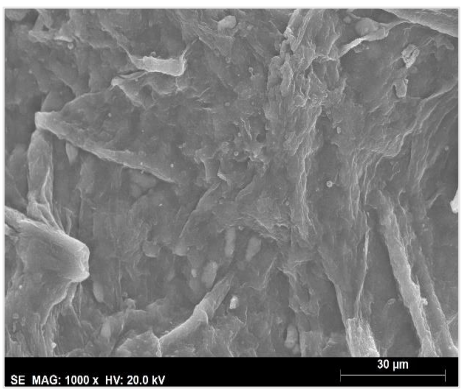

Figure 4.10: HEC and PS films results from SEM analysis exposed to 84% a_w, with 1 000× ampliation.

For the pretended applications, the matrices should be dense, in order to constitute a barrier between the environment and the skin/food. Based on these results, most matrices with HEC present a homogeneous dispersion of the matrice constituents, showing a good interaction between the polymer, plasticizers and phenolic compounds, resulting in a dense structure, being these matrices the most suitable for the aimed application.

The obtained results will be confirmed by gas permeation studies.

4.3.1.2 X-Ray Diffraction (XRD)

To study the crystallinity of the matrices, the X-Ray Diffraction (XRD) characterization was performed as described in section **3.4.3.2**. The obtained XRD results are present in **Figure 4.11**. The samples HEC_G exposed to 58% a_w, HEC_U and PS at 75% a_w and HEC_U exposed to 84% a_w were impossible to analyse by this technique, since the utilized equipment was not the best suited to analyse films or gels but rather to analyse powder samples.

The peak at around 13° belongs to the glass substrate, as reported by Boon *et al.*, which is clearly identified in HEC_G_U and PS matrices exposed to 84% a_w (**Figure 4.11 (C)**) and PS+L matrix exposed to 75% a_w (**Figure 4.11 (B)**). The other recognised peak, at around 21.3°, belongs to HEC, being present in all the characterized matrices. This peak was also observed in earlier HEC characterization reports (**Figure 8.5**, **Appendix III**).[70]

From the analysis of **Figure 8.5**, **Appendix III**, different peaks were found for urea and glucose, evidencing their highly crystalline structure. However, in the films with plasticizers these peaks were not clearly identified, as can be seen in **Figure 8.5**, **Appendix III**, and **Figure 4.11**, suggesting that there is an interaction between HEC and the plasticizers that prevent their crystallization or precipitation. The HEC chains may scatter some light but the interaction with the plasticizers will separate the HEC chains, decreasing their density, which result in the films transparency increase.[70] If the crystallization or precipitation occurred, it would have scattered the light and decrease the films transparency. This light scattering can be observed in the HEC_G matrix exposed to 75% a_w, containing crystals in their surface, as shown previously at **Figures 4.7 (B)**, section **4.3**. This crystallization was observed by XRD through the high intensity of the obtained peak around 80 000 a.u., when compared with the intensities obtain by the other transparent analysed films, as was expected by SEM analysis.

These results show that the analysed films were generally amorphous, since there were almost no peaks at XRD spectrum, as was reported in the literature, except for the matrices HEC_U exposed to 58% a_w, where crystallization of the plasticizers occurred.[70]

For the aimed applications, films should be amorphous, presenting a low rigidity.

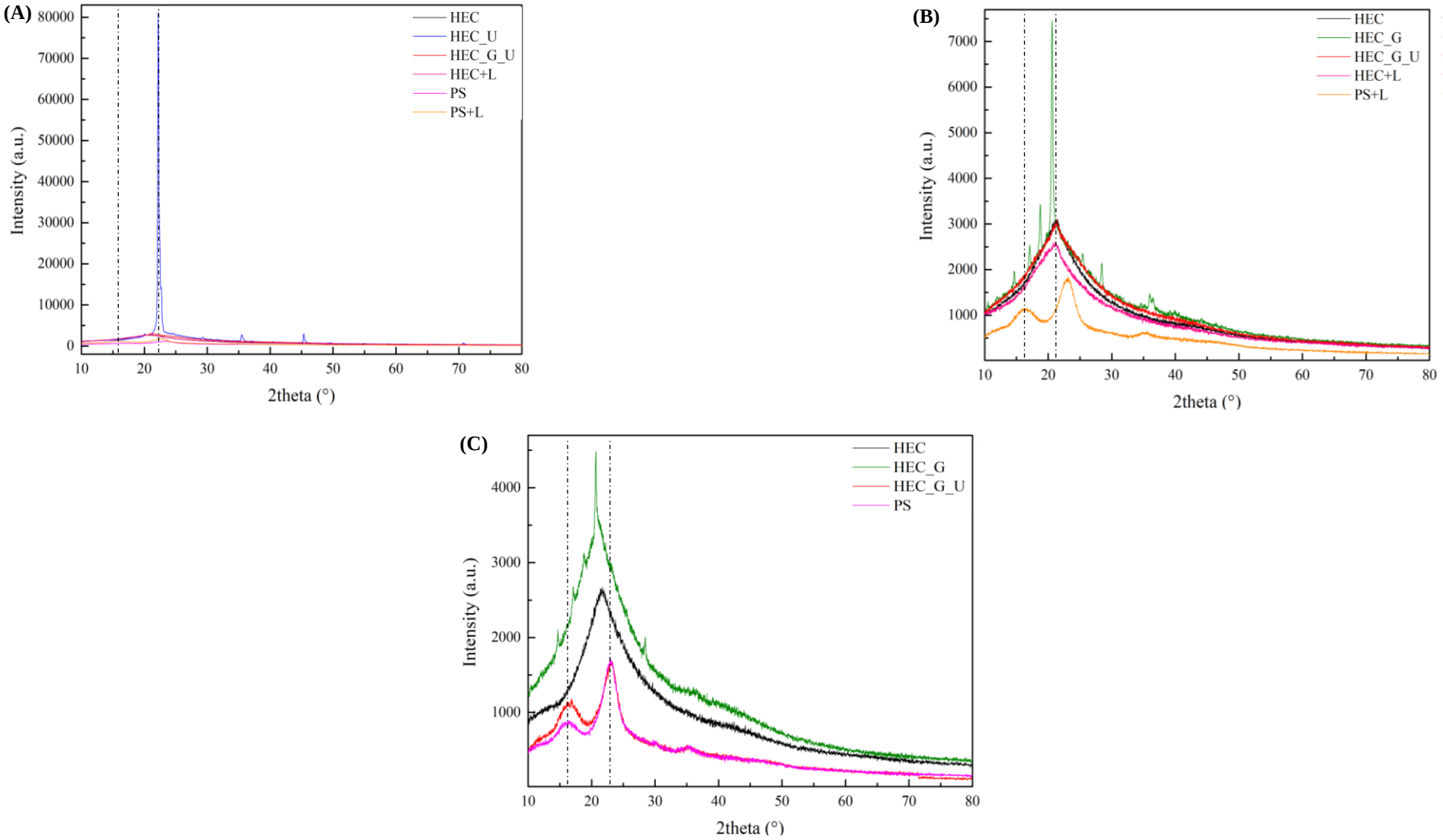

Figure 4.11: X-Ray diffraction results for HEC and PS matrices analysis exposed to 58% **(A)**, 75% **(B)** and 84% **(C)** a_w. The dashed vertical lines identify the characteristics angles of matrices constituents.

4.3.1.3 Differential Scanning Calorimetry (DSC)

To verify and monitor the thermal properties and phase transitions of the matrices constituents, DSC analysis was carried out, as described in section **3.4.3.3**. DSC results obtained for the analysed matrices are presented in **Figure 4.12** and the respective identified glass transition temperatures (T_g) at **Table 4.3**. T_g values were determined at the midpoint of the change in the slope.[70]

Table 4.3:Glass transition temperatures resultant from DSC analysis of the matrices with heat-cool-heat cycle between -130°C to room temperature.

Matrix	T_g (°C)
HEC_G_U (58% a_w)	-101.55
HEC (75% a_w)	-104.49
HEC_G_U (75% a_w)	-53.76
HEC (84% a_w)	-89.3
HEC_G (84% a_w)	-93.01

The absence of crystallization temperature (T_X) identification means that these matrices are amorphous, as concluded by XRD characterization, section **4.3.1.2**.

From the analysis of the obtains T_g values, it is possible to notice the T_g decrease with the addition of plasticizers at 84% a_w but the opposite was obtained at 75% a_w, being impossible to establish a relation between the T_g value and the presence of plasticizers.

For matrices with the same constituents, the lowest T_g values for HEC matrices were achieved at 75% a_w (-104.49°C) and for HEC_G_U matrices at 58% a_w (-101.55°C). The low T_g values are associated with the matrices flexibility, allowing to the chains a higher mobility to slide over each other's and the rearrange of the molecules when bent, to accommodate the shape change.[87] Based on this and on the obtained results, it is possible to notice that the matrices rigidity decreases with the decrease of water activity, being the matrice with more amorphous behaviour HEC when exposed to 75% a_w.

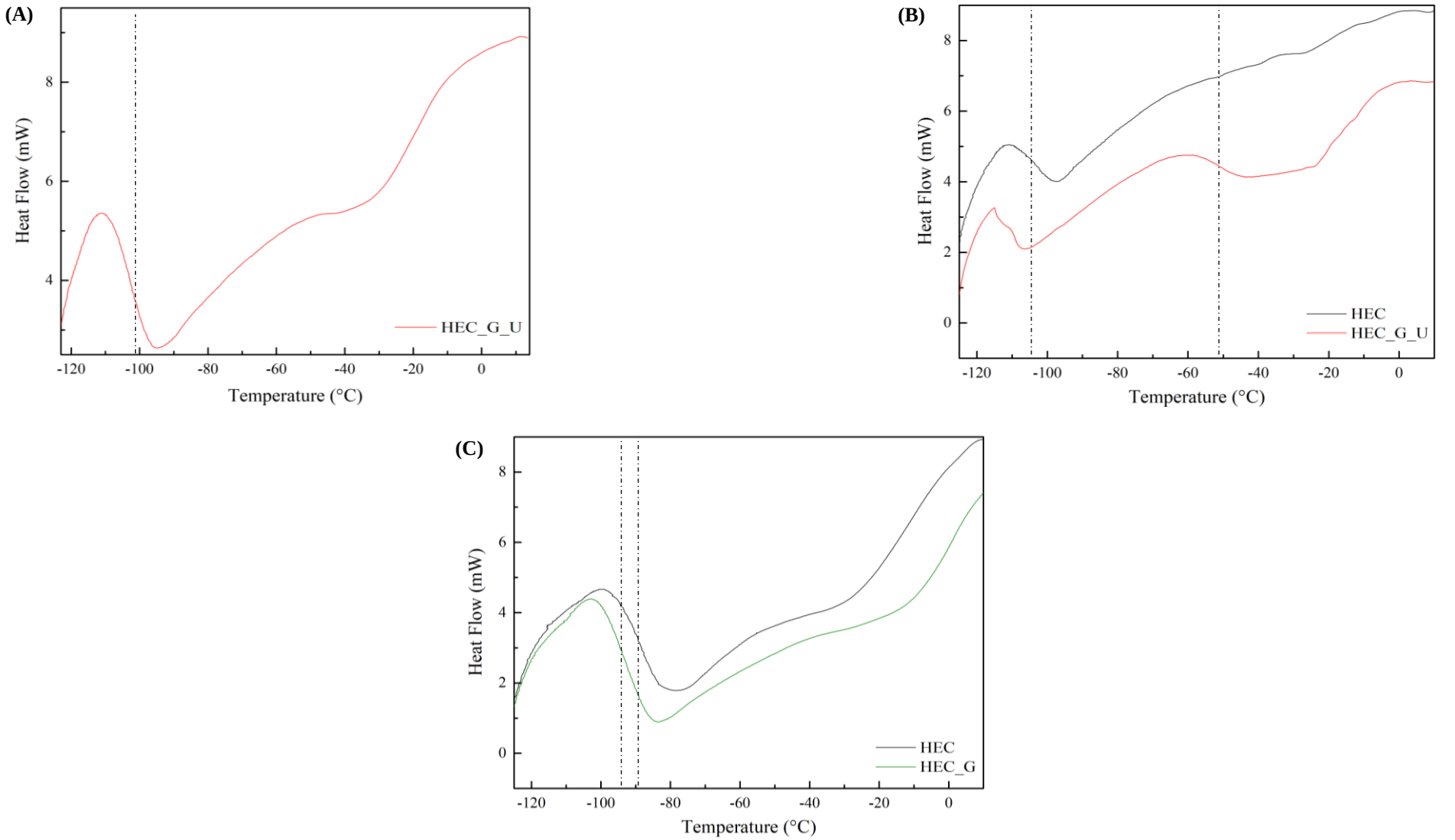

Figure 4.12: Heat flow as a function of temperature for the analysed matrices exposed to 58% **(A)**, 75% **(B)** and 84% **(C)** a_w; with heat-cool-heat cycle between -130°C to room temperature. The dashed vertical lines identifies the T_g.

4.3.1.4 Thermogravimetric Analysis (TGA)

Thermogravimetric Analysis (TGA) was executed in order to evaluate the thermal stability of the matrices constituents, based on the matrices weight loss as a function of the increasing temperature. **Figure 4.13** shows how the matrices' components were degraded at different temperature ranges and **Table 8.14**, **Appendix III** the respective weight loss. The weight loss percentage was considered as the weight loss percentage variation from the beginning up to the following horizontal portion of the graph.[70]

For all the matrices it is possible to observe a significant drop at the temperature of 100 °C, caused by the evaporation of the water absorbed in the matrix.[70] The matrices with plasticizers shown a highest water loss than the matrices without plasticizers. The highest water loss was achieved for HEC_U exposed to 84% a_w (29.75%) matrix and the matrix with lower water loss was HEC exposed to 58% a_w (1.14%), evidencing the increase of water loss with the increase of the water activity that the matrices were exposed. At 160 °C the degradation of the plasticizers, glucose and urea occurred in the matrices with this compounds, being the HEC_G exposed to 75% a_w (19.29%), HEC_U at 75% a_w (35.85%) and HEC_G_U at 84% a_w (15.95%) the matrices with highest weight loss.[70]

The final weight loss was caused by the HEC and PS cellulose degradations at around 300°C. The highest HEC weight loss occurred for PS+L when exposed to 58% a_w (69.28%) matrix and the lower for HEC_U at 84% a_w (18.06%).[70] It was not possible to identify a characteristic weight loss for the phenolic compounds present in the HEC+L and PS+L matrices.

Based on these results, the membranes containing plasticizers showed to be stable until the temperature of 160 °C and the membranes without plasticizers until 300°C, being both stable at the temperatures of the aimed applications (wound dressing: 36–40 °C and food packaging: 5–18°C).[88] These results also support the obtained results through DSC characterization, showing the high amount of water absorbed by the matrices.

For future work, a TGA analysis at constant temperature over time should be done, being the temperature determined accordingly to the possible application of the matrices.

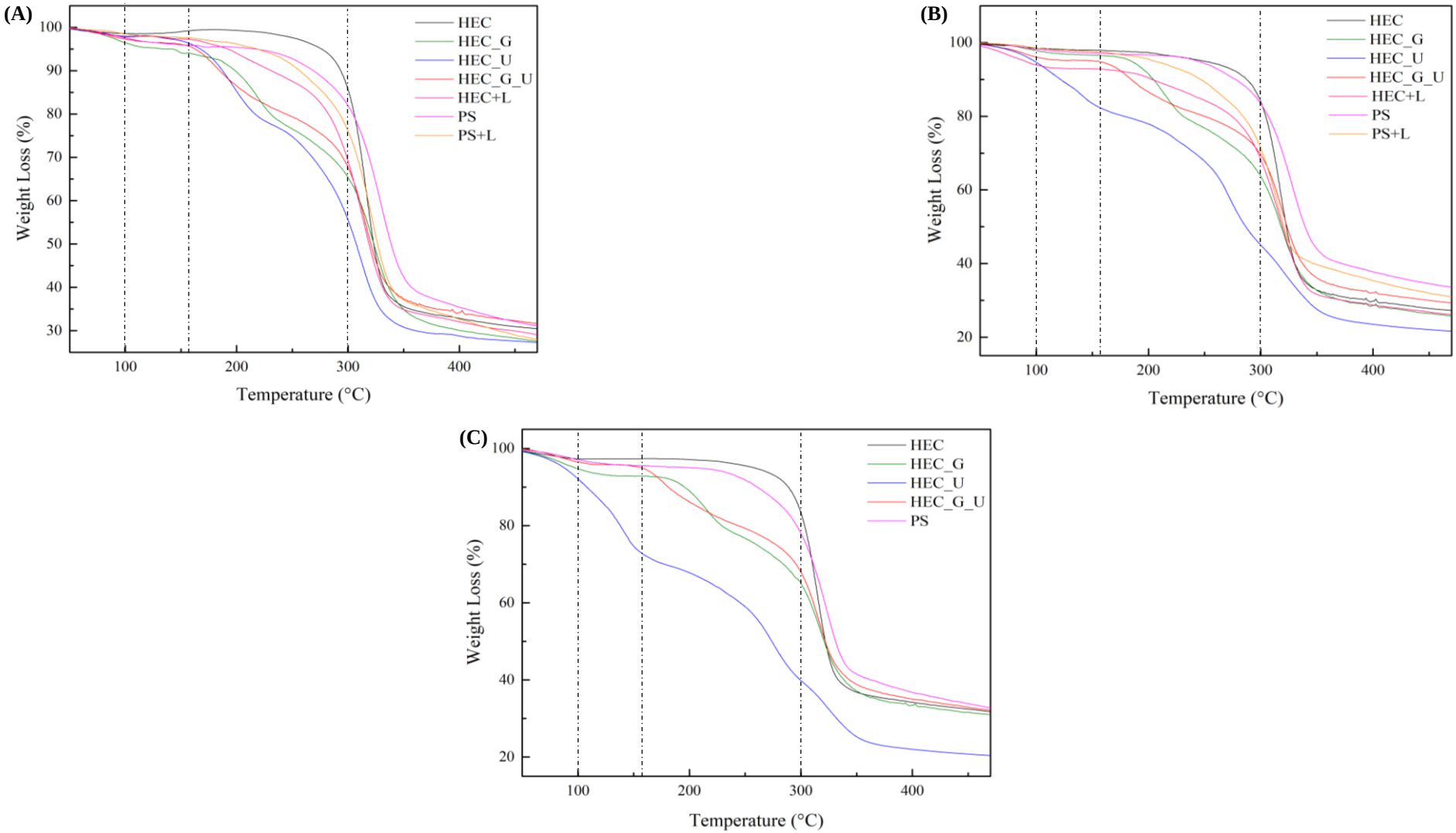

Figure 4.13: Weight loss as a function of temperature for the analysed matrices exposed to 58% **(A)**, 75% **(B)** and 84% **(C)** a_w. The dashed vertical lines identify the degradation temperatures.

4.3.1.5 Fourier Transform Infrared (FTIR) Spectroscopy

The FTIR characterization of the matrices was performed to confirm the incorporation of the phenolic compounds in the matrices and to determine possible interactions established between the different components. The results are presented in **Figure 4.14**.

The results showed that the peaks obtained for HEC, HEC_G, HEC_U and HEC_G_U matrices are quite similar, as reported in the literature, except for the matrices HEC_G exposed to 58% a_w; HEC_U at 75 and 84% a_w; and HEC_G_U exposed to 84% a_w, in which the analysis of the FTIR equipment could be not clear enough, affecting the matrices' compounds detection.[70] This similarity proves the absence of chemical reaction or chemical interaction due to the addition of plasticizers. The only difference between HEC films with and without plasticizers is the presence of two peaks instead of one for HEC films with urea, around 1 640 cm^{-1}, associated to the N-H bonds of urea presence in the matrix.[89] The glucose peaks are not identified due to the possible overlapping by the strongest HEC peaks.[70] The PS and PS+L matrices did not present any peak, showing that this technique is not appropriate to identify the interactions established between these components.

Analysing the obtained peaks, the 1 066 cm^{-1} peak characterises the primary alcohol O-H bonding, the 1 115 cm^{-1} peak the C-O-C bonding and the 1 385 cm^{-1} peak the C-H bonding. Around 1 649 cm^{-1}, the H-O-H bond shown to be broader to HEC films with plasticizers, agreeing with the TGA obtained results that indicates the highest water content in the matrices with plasticizers. The peaks around 2 362 cm^{-1} and 2 337 cm^{-1} could be associated to the atmospheric CO_2, 2 893 and 2 927 cm^{-1} were assigned to C-H symmetrical stretch and the broad peak at 3 340 cm^{-1} represents hydrogen bonding interactions with O-H stretching vibration. The obtained peak positions are consistent with earlier reports on HEC.[70]

In the future, Raman spectroscopy could be used to support the obtained results.

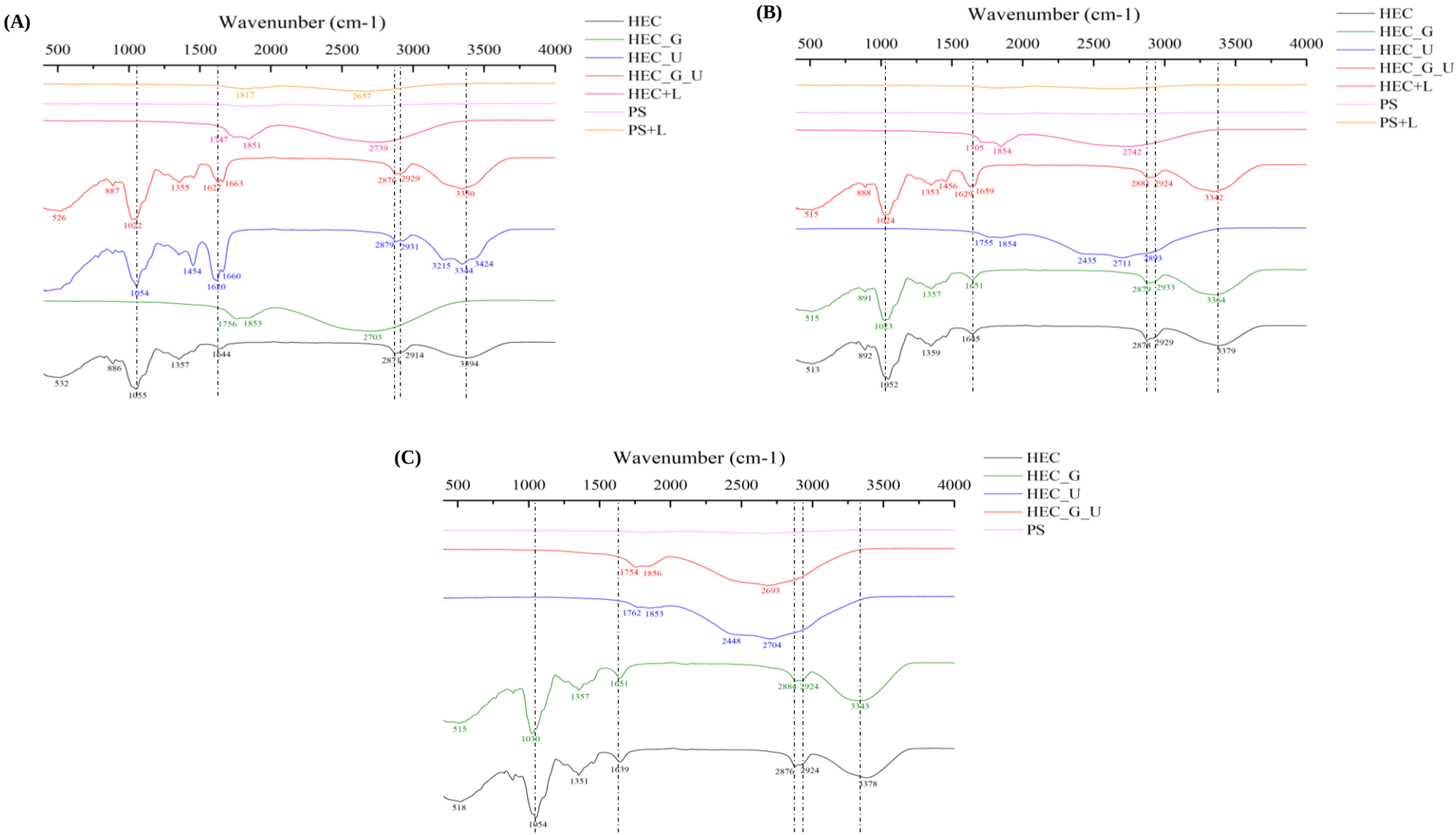

Figure 4.14: FTIR spectra for HEC and PS matrices exposed to 58% **(A)**, 75% **(B)** and 84% **(C)** a_w. The dashed vertical lines identify the analyzed peaks.

4.3.1.6 Contact Angle

The contact angle formed between the matrices surface and a drop of liquid (water or glycerol) were determined as described in the section **3.4.3.6**. The hydrophobicity of the membrane to the solvent used (water) increases with the increase of the contact angle.

The contact angles obtained with water were impossible to determine, due to the immediate absorption of the drop of water by the surface of the matrices, showing that all the analysed membranes were hydrophilic, as expected due to the strong permeability of cellulose to water.[90] In an effort to calculate the contact angles, an organic solvent was used – glycerol.[91] The obtained contact angles are present in **Figure 4.15**.

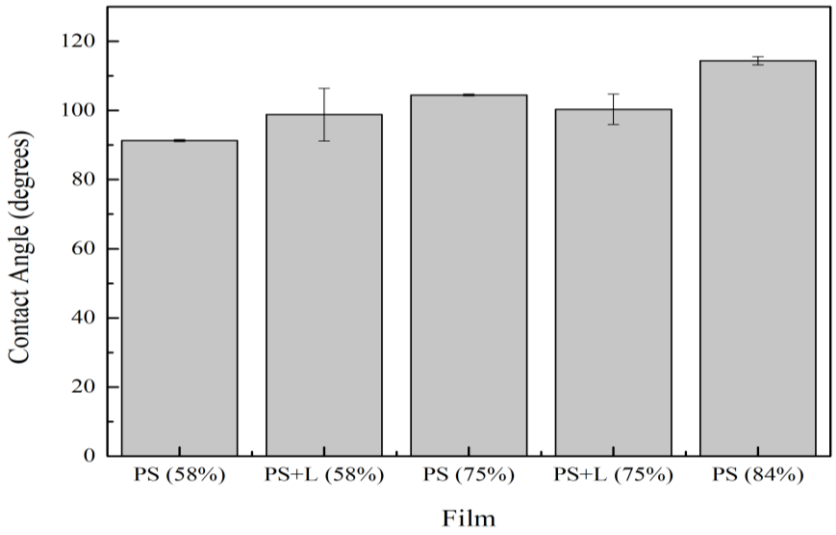

Figure 4.15: Contact angles for PS and PS+L matrices, at the water activity of 58, 75 and 84%.

As observed in **Figure 4.15**, the matrices where the angles calculation was possible were: PS when exposed to 58% ($91.31 \pm 0.33°$), 75% ($104.49 \pm 0.26°$) and 84% ($114.37 \pm 1.22°$) a_w; and PS+L when exposed to 58% ($98.8 \pm 7.63°$) and 75% ($100.36 \pm 4.41°$) a_w.

Since the utilized solvent was organic, in the opposition of when water is used, a matrix is considered hydrophilic when the contact angle is higher than 90° and hydrophobic when it is lower than 90°. Taking this into account, the most hydrophilic matrix was the one with the highest contact angle – PS at 84% a_w ($114.37 \pm 1.22°$) – and the less hydrophilic matrix was PS at 58% a_w ($91.31 \pm 0.33°$). These results prove the increase of hydrophilicity with the increase of humidity that the films were exposed. Orsuwan *et al.* reported that the contact angle obtained with water from the analysis of banana powder and glycerol films was $45.1 \pm 3.1°$, proving that this film was also hydrophilic.[50]

In the case of the films doped with phenolic compounds, there was almost no variation between the analysed water activities ($98.8 \pm 7.63°$ for 58% a_w and $100.36 \pm 4.41°$ for 75% a_w).

Regarding the aimed application, in the case of wound dressing, films should be hydrophilic, so all the obtained films can be used.[92] For food packaging, the hydrophilicity of the films depends on the food to be stored.

4.3.1.7 Swelling Measurements

The swelling percentage of the matrices immersed in distilled water for 24h were determined through **Equation 3.4**, described in the section **3.4.3.7**. The obtained results are presented in **Table 4.4**. The weight, thickness and dimensions variation are in **Table 8.13**, **Appendix III**.

Table 4.4: PS and PS doped with phenolic compounds (PS+L) matrices swelling percentage.

Matrix	Swelling Percentage (w/w %)
PS	257.14
PS+L	325.53

All the matrices containing HEC were dissolved in distilled water after some minutes of immersion, being impossible to report this swelling results, due to the solubility of the matrice compounds in water and lack of chemical cross-linking in the matrice composition.[70]

The analysed matrices with PS were insoluble in water, being possible to determine their swelling percentage. The highest swelling percentage was achieved for PS+L membrane (325.53%), showing an improvement in the water absorption capacity of PS matrices when doped with the phenolic compounds extracted from banana plant leaves.

Considering the intended applications, PS films could be used for the development of food packaging films more resistant to water.

4.3.1.8 Mechanical Properties

The tensile strength of the matrices was analysed through puncture tests. The force as a function of the time is represented at **Figure 8.6**, **Appendix III**, and the obtained thickness and tensile strength results at **Table 4.5**, determined through **Equations 3.5**–**3.7**, section **3.4.3.8**. The obtained NTS values comparation for the same matrices when exposed to different water activities is presented at **Figure 4.16**.

Usually, the elongation of the analysed material is also determined through this technique, however the initial distance of the equipment arm was not recorded, making impossible this calculation. For further analysis, this value should be registered.

Table 4.5: Puncture test results for the analysed matrices, exposed to 58, 75 and 84% a_w.

Matrix	Normalised Tensile Strength (MPa/mm)		
	58% a_w	75% a_w	84% a_w
HEC	37.10	12.47	13.44
HEC_G	12.77	6.90	4.35
HEC_U	1.84	-	-
HEC_G_U	10.51	2.09	-
HEC+L	52.62	6.52	-
PS	2.13	4.27	2.87
PS+L	1.89	1.09	-

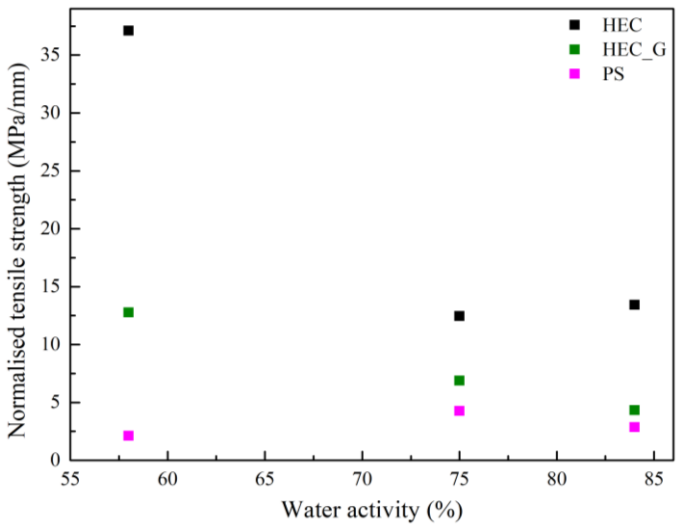

Figure 4.16: NTS values comparation for the same matrices when exposed to different water activities (58, 75 and 84%).

From the obtained results in **Table 4.5** and **Figure 4.16**, the highest values of NTS were achieved in general for HEC matrices when exposed to 58% a_w, being possible to notice the increase of the NTS as the humidity decreases, showing the increase of the force needed to break the matrice with the decrease of humidity. In general, the NTS for HEC films were at least the double than the obtained for the matrices doped or with plasticizers, proving that the addition of plasticizers reduces the necessary tensile strength applied to break them, as reported by Boon *et al*.[70] This proves that the a_w reduction and the plasticizers absence play the same role in this matrices, reducing their rigidity, as proved by DSC results. [70]

Comparing HEC and PS films, the NTS for PS films was way inferior that the applied for HEC films, evidencing the lack of robustness of these films due to the lack of packaging of their fibers, as shown in the SEM results, section **4.3.1.1**, caused by the low cellulose's extraction yield. For the aimed applications, films should present a high NTS, being the most suitable ones: HEC when exposed to 58% a_w.

4.3.1.9 Rheology

The rheology of the HEC_U gels obtained at 75 and 84% a_w was characterized by their viscosity and viscoelasticity properties, as described in section **3.4.3.9.1** and **3.4.3.9.2**, respectively. The respective obtained results are presented in the following sections, **4.3.1.9.1** and **4.3.1.9.2**.

4.3.1.9.1 Viscosity

The flow curves for the analysed gels are presented in **Figure 4.17**.

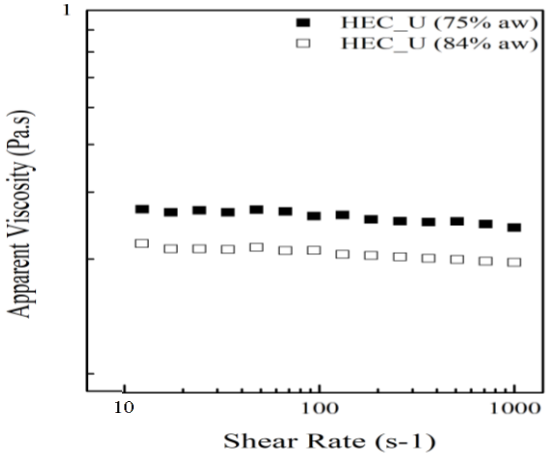

Figure 4.17: Flow curves for HEC_U gels exposed to (■) 75% a_w and (□) 84% a_w.

It is possible to identify a Newtonian behaviour of the gels, due to the low concentration of matrix constituents used.[93] The gel that had a highest viscosity was HEC_U at 75% a_w (0.30 Pa.s) which is similar to the one obtained at 84% a_w (0.24 Pa.s), not having the humidity variation of the analysed gels a great effect on this experiment.

4.3.1.9.2 Viscoelasticity

The obtained mechanical spectre for the analysed gels is in **Figure 4.18**.

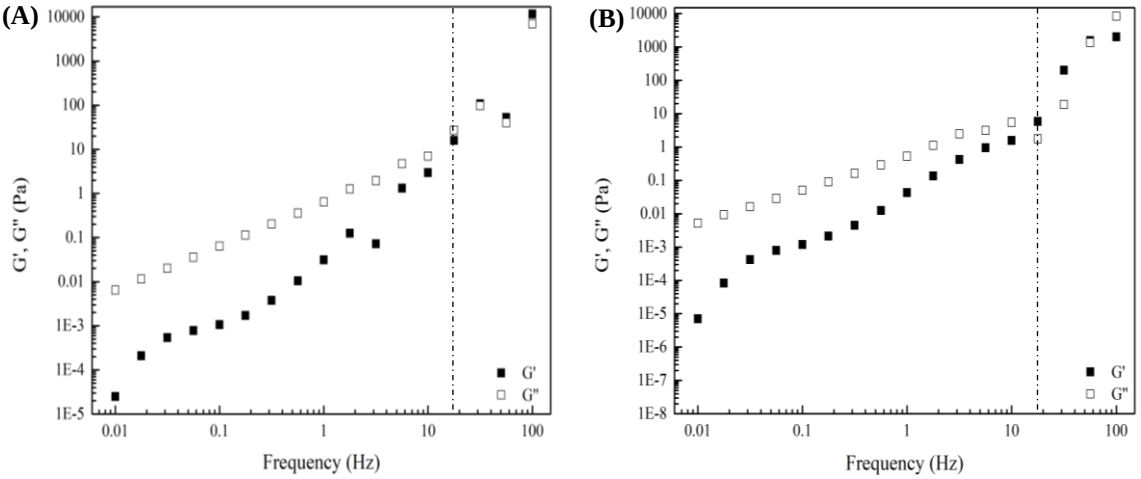

Figure 4.18: Mechanical spectra of HEC_U gels exposed to 75% **(A)** and 84% a_w **(B)**, where (■) represent the G' results and (□) the G'' results. The dashed vertical lines identify the frequency cross-over.

In both mechanical spectra, at low frequencies, the storage modulus (G') was lower than the loss modulus (G"), demonstrating a liquid-like behaviour for the polymeric gel solution. However, at the frequency around 30 Hz a cross-over was detected, being the storage modulus higher than the loss modulus, indicating the predominance of the elastic contribution.[94] These results evidence the viscous character of this samples entangled polymer chains, supporting the results obtained in the viscosity characterization, section **4.3.1.9.1**.[94]

For biomedical applications, the solution should form a gel, in order to stay at the site of application.[46] The aqueous solution with viscous comportment obtained could be optimised to form a gel by using other plasticizers. The obtention of this viscous solution for HEC_U matrices at the highest water activities is interesting for biomedical applications once the synthetized mixtures allow the obtention of films or viscous solutions, depending on the water activity which were exposed.

4.3.1.10 Pure Gas Permeation Studies

Since the aim of this work was the development of polymeric matrices for medicinal dressings or food packaging, gas permeation experiments were carried out with the pure gases CO_2 and O_2. The β result determined was 65.02 m^{-1}.

Figure 8.7, **Appendix III**, presents the pressure variation results and **Figure 8.8**, **Appendix III**, the linear fitting of the obtained results. **Table 4.6** contains the permeability and ideal selectivity results of the analysed dense films.

Table 4.6: CO_2 and O_2 permeability and ideal selectivity for HEC matrices exposed 84% a_w.

Matrix	CO_2 Permeability (m^2/s)	O_2 Permeability (m^2/s)	Ideal Selectivity (α)
HEC (84% a_w)	2×10^{-11}	4.33×10^{-12}	4.62

All the films obtained in the section **4.3** were analysed and the only ones were the gas permeation characterization was possible were the dense matrices – HEC exposed to 84% a_w. The HEC films exposed to 84% a_w present a permeability to CO_2 (2×10^{-11}) higher than the obtained to O_2 (4.33×10^{-12}), demonstrating that this membrane is more permeable to CO_2. This gas transport through nonporous membranes can be clarified by the solution-diffusion mechanism, which defends that the permeability (P) depends on the diffusivity (D) and solubility (S) coefficients of the used gas, as described in **Equation 4.1**.[95]

$$P = D\times S \qquad \textbf{(Eq. 4.1)}$$

where,

P – Permeability (m^2/s)

D – Diffusivity coefficient (m^2/s)

S – Solubility coefficient

Based on this, once the Lennard Jones molecular diameter for CO_2 (3.94Å) is higher than the obtained for O_2 (3.65 Å), the O_2 diffusivity coefficient is higher than the obtained for CO_2, being the O_2 permeability mainly controlled by its diffusion in the matrices, comparing with CO_2.[96] Despite of that, the CO_2 solubility in the membranes in higher than the obtained for O_2, explaining the higher permeability obtained for CO_2.

Based on the CO_2 and O_2 obtained permeabilities and using the **Equation 3.10**, section **3.4.3.10**, the ideal selectivity of 4.62 was determined for HEC matrix at 84% a_w. **Table 4.7** presents some CO_2 and O_2 permeabilities for the aimed applications.

Table 4.7: CO_2 and O_2 permeability for HEC matrices exposed 84% a_w, developed on this work, and for matrices reported at the literature for the aimed applications.

Reference	Application	Matrix	CO_2 Permeability (Barrer)	O_2 Permeability (Barrer)
This work	-	HEC (84% a_w)	24	5.2
Ruiz-Cardona *et al.*	Wound dressing	Bioprocess ®	2.5	0.94
Evranos *et al.*		Chitosan + Gelatin	-	1.45
Siracusa *et al.*	Food packaging	Most commercial polymers	10.4 – 18.4	2.6 – 4.3
Otoni *et al.*		Banana + Pectin	-	0.03 – 0.06

Through comparation of the obtained values of CO_2 and O_2 permeability and the ones reported at the literature, for both applications, it is possible to notice that the obtained values for the developed matrices are higher than the reported ones, which is an indication that they should be improved, for example by the addition of cross-linkers to the matrix constituents, in order to form a barrier between the environment and the skin/food.[97]

In the future, water permeability experiments should be performed, since this is an important parameter of the films for both pretended applications.[98][99]

5. Conclusions

The aim of this thesis was the development of polymeric matrices, in the form of films or gels, based on banana production residues (phenolic compounds from the leaves and cellulose from the pseudostem) to develop biomedical or food packaging solutions.

Due to the novelty of phenolic compounds extracted from banana plant leaves and pseudostem, Batch Solid-Liquid and Soxhlet extractions, with different drying temperatures of the samples and different time periods extraction, were performed. After, the Total Phenolic Content (TPC) and the antioxidant activity of the obtained extracts were determined, showing that the highest TPC and antioxidant activity was achieved by using leaves with 3 days Batch Solid-Liquid extraction and the drying temperature of 40°C, being this sample selected for the following methods. TPC results also showed that the banana leaves extract has a TPC higher than banana peel, pulp and banana plant pseudostem.

To identify and quantify the phenolic compounds present on the selected samples, High Pressure Liquid Chromatography (HPLC) and Liquid Chromatography-Mass Spectroscopy (LC-MS) was performed. The retention time range between 44–47 min had the highest UV intensity and an isotope distribution like apigenin was identified. However, the identification of the apigenin present in the sample was not possible to confirm.

The cellulose used as polymer for the matrices development was successfully extracted from banana plant pseudostem (PS), as confirmed by HPLC. Commercial hydroxyethyl cellulose (HEC) was also used, to compare the performance of PS with an already commercialised polymer.

A variety of matrices were synthetized using PS or HEC, glucose (G) and/or urea (U) as plasticizers and banana plant leaves phenolic compounds (L) as bioactive compounds, which were exposed to 3 water activities (58, 75 and 84% a_w). All the prepared matrices develop films, except for HEC_U matrix at 75 and 84% a_w that formed gels.

All the matrices without mold development were characterized by Scanning Electron Microscopy (SEM), X-Ray Diffraction (XRD), Differential Scanning Calorimetry (DSC), Thermogravimetric Analysis (TGA), Fourier Transformed Infrared spectroscopy (FTIR), contact angle, swelling, mechanical properties, rheology and gas permeation studies.

From SEM analysis, it was observed that most matrices with HEC present a homogeneous dispersion of the matrice constituents and a dense structure, as pretended for the aimed applications.

The results of contact angles measurements showed that all the analysed matrices are hydrophilic, as pretended, and the results obtained by using glycerol proves the increase of hydrophilicity with the increase of humidity that the films were exposed. The swelling analysis showed that all the matrices containing HEC were dissolved in distilled water and that the presence of phenolic compounds on PS films improves their water absorption capacity.

XRD and DSC results showed that the analysed films were generally amorphous, as intended for the aimed applications, except for the matrices HEC_U exposed to 58% a_w and HEC_G at 75% a_w, where occurred precipitation and crystallization of the plasticizers, respectively. From DSC it was also noticed that the matrices rigidity decreases with the decrease of water activity.

Through TGA characterization, the membranes containing plasticizers showed to be stable until the temperature of 160°C and the other membranes until 300°C, being stable at the temperatures of the biomedical and food packaging applications. The results obtained from FTIR spectroscopy agree with the TGA obtained results, indicating the highest water content in the matrices with plasticizers.

The mechanical properties evidenced that water and the plasticizers play the same role in the analysed matrices, showing an increase of the normalised tensile strength as the humidity decreases/ plasticizers absence. Comparing HEC and PS films, the normalised tensile strength for PS films was inferior that the applied for HEC films, evidencing the lack of packaging of their fibers, as shown by SEM results, which could be improved by the increase of the cellulose extraction yield and by the addition of other plasticizers.

From rheology tests it was possible to confirm the viscous character of the obtained gels.

The pure gas permeation assays shown that only the HEC matrices exposed to 84% a_w are dense and that its permeability for CO_2 and O_2 is higher than the reported values at the literature for the aimed applications. Though, the permeability of the developed matrices can be improved by the used of cross-linkers, in order the form films that present a barrier between the environment and the skin/food.

In conclusion, the obtained results showed that the banana plant leaves present a TPC higher than banana peel, pulp and banana plant pseudostem, proving to have a huge potential as

phenolic compounds source. The extracts from Batch-Solid Liquid 3 extraction with leaves dried at 40°C (BSL_3_40) allowed the highest TPC. The cellulose extraction method was successful, presenting a margin for improvement. In general, the synthetized matrices were hydrophilic to water and only the HEC matrices exposed to 84% water activity proved to be dense. The plasticizers and water activity showed to influence the matrices flexibility, which could be controlled accordingly to the desired matrices application.

The matrix that presented the best features for the aimed applications was HEC at 84% water activity. Nevertheless, the PS matrices showed to be very promising due to the novelty of the use of banana production residues to develop sustainable films; and since its mechanical properties can be improved using other plasticizers and its barrier properties using cross-linkers.

6. Future Perspectives

From all the results obtained during this thesis, about the development of polymeric matrices, in the form of films or gels, based on banana plan extracts for biomedical or food applications, some suggestions to improve this study and possible for future work are presented below:

1. Batch Solid-Liquid extraction to exhaustion by renewing the solvent, to improve the phenolic compounds extraction yield;
2. Search of phenolic compounds with retention times between 44–47 min, since this was the molecular weight range with more UV intensity in LC-MS analysis;
3. Optimization of cellulose losses or follow another extraction method, to improve the cellulose extraction yield;
4. Better homogenization of matrices constituents by stirring the mixture longer during the synthesis;
5. Synthesis of banana tree pseudostem matrices with plasticizers (glucose and/or urea) to improve the mechanical properties;
6. Thermogravimetric Analysis (TGA) analysis at constant temperature over time should be done, being the temperature determined accordingly to the possible application of the matrices;
7. Use of Raman technique to complement the Fourier Transformed Infrared (FTIR) spectroscopy results;
8. Elongation determination;
9. Use of cross-linker to improve the barrier properties of the matrices;
10. Biological assays to analyse the cytotoxicity of the matrices prepared.

7. References

References were constructed accordingly to IEEE style.

[1] N. K. S Hussain, F Malik, "Alternative and traditional medicines systems in Pakistan: History, regulation, trends, usefulness, challenges, prospects and limitations", A compediu., vol. 4, 2012.

[2] "Chemical composition *Musa acuminata* Colla." [Online]. Available: www.usda.gov/. [Accessed: 26-May-2019].

[3] M. P. Forster, E. Rodríguez Rodríguez, and C. Díaz Romero, "Differential characteristics in the chemical composition of bananas from tenerife (Canary Islands) and Ecuador", *J. Agric. Food Chem.*, vol. 50, no. 26, pp. 7586–7592, 2002.

[4] A. K. Thompson, "Banana (*Musa spp.*)", *Woodhead Publishing Limited*, 2011.

[5] W. M. Road and N. Lane, "Numerical taxonomy of the wild bananas (*Musa*)", *New Phytol.*, vol. 115, pp. 567–571, 1990.

[6] S. Qamar and A. Shaikh, "Trends in Food Science & Technology Therapeutic potentials and compositional changes of valuable compounds from banana- A review", *Trends Food Sci. Technol.*, vol. 79, no. June, pp. 1–9, 2018.

[7] E. E. Cheesman, "Classification of the bananas: the *genus Musa L.*", *Springer*, vol. 2, no. 2, pp. 106–117, 1947.

[8] ACCA Software, "Banana Tree" [Online]. Available: www.google.com/imgres?imgurl=https%3ª%2F%2Fcatalogue.accasoftware.com%2Fimg%2FProdotti%2F14469%2FPREVIEW%2Fbananeira.1.750x527-1_1519383559.PNG&imgrefurl=https%3A%2F%2Fcatalogue.accasoftware.com%2Fptb%2F14469%2Fbananeira.html&docid=01ipuOQ6TxTQzM&. [Accessed: 26-May-2019].

[9] C. Wong, R. Kiew, G. Argent, O. Set, S. K. Lee, and Y. Y. Gan, "Assessment of the validity of the sections in *Musa* (*Musaceae*) using AFLP", *Ann. Bot.*, vol. 90, no. 2, pp. 231–238, 2002.

[10] S. Pareek, "Nutritional and Biochemical Composition of Banana (*Musa spp.*) Cultivars", *Elsevier Inc*., no. 3, pp. 49-81, 2016.

[11] FAO - Food and Agriculture Organization of the United Nations, "Banana Facts" [Online]. Available: www.fao.org/economic/est/estcommodities/bananas/bananafacts/en/#.XOqzjaTOVhE. [Accessed: 26-May-2019].

[12] FAO - Food and Agriculture Organization of the United Nations, "Banana Market Review 2018." [Online]. Available: www.fao.org/fileadmin/templates/est/COMM_MARKETS_MONITORING/Bananas/Documents/Banana_Market_Review_Prelim_Results_2018.pdf. [Accessed: 26-May-2019].

[13] Observador, "Madeira Island Production 2017" [Online]. Available: observador.pt/2018/02/01/madeira-aumentou-producao-de-banana-e-o-mercado-nacional-absorveu-85/. [Accessed: 27-Mar-2019].

[14] Actualitix, "Banana World Production 2016" [Online]. Available: pt.actualitix.com/pais/wld/banana-paises-produtores.php. [Accessed: 26-May-2019].

[15] T. Happi Emaga, C. Robert, S. N. Ronkart, B. Wathelet, and M. Paquot, "Dietary fibre components and pectin chemical features of peels during ripening in banana and plantain varieties", *Bioresour. Technol.*, vol. 99, no. 10, pp. 4346–4354, 2008.

[16] M. Santa-Maria, A. A. Ruiz-Colorado, G. Cruz, and T. Jeoh, "Assessing the Feasibility of Biofuel Production from Lignocellulosic Banana Waste in Rural Agricultural Communities in Peru and Colombia", *Bioenergy Res.*, vol. 6, no. 3, pp. 1000–1011, 2013.

[17] J. Gabhane, S. P. M. Prince William, A. Gadhe, R. Rath, A. N. Vaidya, and S. Wate, "Pretreatment of banana agricultural waste for bio-ethanol production: Individual and interactive effects of acid and alkali pretreatments with autoclaving, microwave heating and ultrasonication", *Waste Manag.*, vol. 34, no. 2, pp. 498–503, 2014.

[18] B. S. Padam, H. S. Tin, F. Y. Chye, and M. I. Abdullah, "Banana by-products: an under-utilized renewable food biomass with great potential", *J. Food Sci. Technol.*, vol. 51, no. 12, pp. 3527–3545, 2014.

[19] P. Gañán, J. Cruz, S. Garbizu, A. Arbelaiz, and I. Mondragon, "Stem and bunch banana fibers from cultivation wastes: Effect of treatments on physico-chemical behavior", *J. Appl. Polym. Sci.*, vol. 94, no. 4, pp. 1489–1495, 2004.

[20] C. V. Passo Tsamo *et al.*, "Phenolic profiling in the pulp and peel of nine plantain cultivars (*Musa sp.*)", *Food Chem.*, vol. 167, pp. 197–204, 2015.

[21] M. I. Hossain Tuhin, M. Asaduzzaman, E. Islam, Z. Khatun, and M. Rahmatullah, "Medicinal plants used by folk medicinal herbalists in seven villages of Bhola district, Bangladesh", *Am. J. Sustain. Agric.*, vol. 7, no. 3, pp. 210–218, 2013.

[22] N. Sarah and P. Singh, "Traditional uses , phytochemistry and pharmacology of wild banana (*Musa acuminata* Colla): A review", *J. Ethnopharmacol.*, vol. 196, no. December 2016, pp. 124–140, 2017.

[23] P. K. Agarwal, A. Singh, K. Gaurav, S. Goel, H. D. Khanna, and R. K. Goel, "Evaluation of wound healing activity of extracts of plantain banana (*Musa sapientum var. paradisiaca*) in rats", *Indian J. Exp. Biol.*, vol. 47, no. 1, pp. 32–40, 2009.

[24] S. S. N. C. Cook, "Flavonoids-Chemistry, metabolism, carbdioprotective effects, and dietary sources", *Nutr. Biochem.*, vol. 7, pp. 66–76, 1996.

[25] D. B. Rodriguez-Amaya, "Quantitative analysis, in vitro assessment of bioavailability and antioxidant activity of food carotenoids: A review", *J. Food Compos. Anal.*, vol. 23, no. 7, pp. 726–740, 2010.

[26] M. Valko, D. Leibfritz, J. Moncol, M. T. D. Cronin, M. Mazur, and J. Telser, "Free radicals and antioxidants in normal physiological functions and human disease", *Int. J. Biochem. Cell Biol.*, vol. 39, no. 1, pp. 44–84, 2007.

[27] M. E. Wright *et al.*, "Intakes of fruit, vegetables, and specific botanical groups in relation to lung cancer risk in the NIH-AARP diet and health study", *Am. J. Epidemiol.*, vol. 168, no. 9, pp. 1024–1034, 2008.

[28] Y. Y. Lim, T. T. Lim, and J. J. Tee, "Antioxidant properties of several tropical fruits: A comparative study", *Food Chem.*, vol. 103, no. 3, pp. 1003–1008, 2007.

[29] Z. Rehman, "Citrus peel extract – a natural source of antioxidant", *Food Chem.*, vol. 99, pp. 450–454, 2006.

[30] R. L. Prior, H. Wang, G. Cao, and R. L. Prior, "Oxygen Radical Adsorbing Capacity of Anthocyanins Oxygen Radical Absorbing Capacity of Anthocyanins", vol. 45, pp. 304–309, 2014.

[31] C. Brennan, M. Brennan, E. Derbyshire, and B. K. Tiwari, "Effects of extrusion on the polyphenols, vitamins and antioxidant activity of foods", *Trends Food Sci. Technol.*, vol. 22, no. 10, pp. 570–575, 2011.

[32] S. Sang, K. Lapsley, W. S. Jeong, P. A. Lachance, C. T. Ho, and R. T. Rosen, "Antioxidative phenolic compounds isolated from almond skins (*Prunus amygdalus Batsch*)", *J. Agric. Food Chem.*, vol. 50, no. 8, pp. 2459–2463, 2002.

[33] B. Deepa *et al.*, "Bioresource Technology Structure , morphology and thermal characteristics of banana nano fibers obtained by steam explosion", *Bioresour. Technol.*, vol. 102, no. 2, pp. 1988–1997, 2011.

[34] F. Shahidi and P. Ambigaipalan, “Phenolics and polyphenolics in foods, beverages and spices: Antioxidant activity and health effects - A review”, *J. Funct. Foods*, vol. 18, pp. 820–897, 2015.

[35] C. Del Mar Verde Méndez, M. P. Forster, M. Á. Rodríguez-Delgado, E. M. Rodríguez-Rodríguez, and C. D. Romero, “Content of free phenolic compounds in bananas from Tenerife (Canary Islands) and Ecuador”, *Eur. Food Res. Technol.*, vol. 217, no. 4, pp. 287–290, 2003.

[36] S. Someya, Y. Yoshiki, and K. Okubo, “Antioxidant compounds from bananas (*Musa Cavendish*)”, *Food Chem.*, vol. 79, no. 3, pp. 351–354, 2002.

[37] J. Irissin-mangata and N. Gontard, “New plasticizers for wheat gluten films”, *Eur. Polym. J.*, vol. 37, pp. 1533–1541, 2001.

[38] D. Sharma, D. Kaur, S. Verma, D. Singh, M. Singh, and G. Singh, “Fast Dissolving Oral Films Technology : A Recent Trend For An Innovative Oral Drug Delivery System”, *Int. J. Drug Deliv.*, vol. 7, pp. 60–75, 2015.

[39] M. Irfan, S. Rabel, Q. Bukhtar, M. Imran, F. Jabeen, and A. Khan, “Orally disintegrating films: A modern expansion in drug delivery system”, *Saudi Pharm. J.*, vol. 24, no. 5, pp. 537–546, 2016.

[40] M. Maniruzzaman, J. S. Boateng, M. J. Snowden, and D. Douroumis, “A Review of Hot-Melt Extrusion: Process Technology to Pharmaceutical Products”, *ISRN Pharm.*, vol. 2012, 2012.

[41] V. F. Patel, F. Liu, and M. B. Brown, “Advances in oral transmucosal drug delivery”, *J. Control. Release*, vol. 153, no. 2, pp. 106–116, 2011.

[42] R. P. Dixit and S. P. Puthli, “Oral strip technology: Overview and future potential”, *J. Control. Release*, vol. 139, no. 2, pp. 94–107, 2009.

[43] E. Barbu, L. Verestiuc, G. Nevell, J. Tsibouklis, and J. Tsibouklis, “Polymeric materials for ophthalmic drug delivery: trends and perspectives”, *J. Mater. Chem.*, vol. 16, pp. 3439–3443, 2006.

[44] D. Achouri, K. Alhanout, and P. Piccerelle, “Recent advances in ocular drug delivery”, *Drug Dev. Ind. Pharm.*, pp. 1–19, 2012.

[45] T. Tanner and R. Marks, “Delivering drugs by the transdermal route: review and comment”, pp. 249–260, 2008.

[46] K. Kathe and H. Kathpalia, “Film forming systems for topical and transdermal drug delivery”, *Asian J. Pharm. Sci.*, vol. 12, no. 6, pp. 487–497, 2017.

[47] Technavio, “Factors that are expected to drive the transdermal drug delivery market growth in the coming years” [Online]. Available: www.technavio.com/. [Accessed: 30-Aug-2019].

[48] S. Dhiman, T. G. Singh, and A. K. Rehni, “Transdermal Patches: A recent approch to new drug delivery system”, *Int. J. Pharm. Pharm. Sci.*, vol. 3, pp. 26–34, 2011.

[49] R. Guo, X. Du, R. Zhang, L. Deng, A. Dong, and J. Zhang, “Bioadhesive film formed from a novel organic–inorganic hybrid gel for transdermal drug delivery system”, *Eur. J. Pharm. Biopharm.*, vol. 79, no. 3, pp. 574–583, 2011.

[50] A. Orsuwan, S. Shankar, L. Wang, R. Sothornvit, and J. Rhim, “Food Hydrocolloids Preparation of antimicrobial agar/banana powder blend fi lms reinforced with silver nanoparticles”, *Food Hydrocoll.*, vol. 60, pp. 476–485, 2016.

[51] P. Singh, S. Magalhães, L. Alves, F. Antunes, M. Miguel, and B. Medronho, “Cellulose-based edible films for probiotic entrapment”, *Food Hydrocoll.*, 2018.

[52] S. Singh, K. K. Gaikwad, and Y. S. Lee, “International Journal of Biological Macromolecules Antimicrobial and antioxidant properties of polyvinyl alcohol bio composite films containing seaweed extracted cellulose nano-crystal and basil leaves extract”, *Int. J. Biol. Macromol.*, vol. 107, pp. 1879–1887, 2018.

[53] C. C. Pola *et al.*, “Cellulose acetate active fi lms incorporated with oregano (*Origanum vulgare*) essential oil and organophilic montmorillonite clay control the growth of phytopathogenic fungi”, *Food Packag. Shelf Life*, vol. 9, pp. 69–78, 2016.

[54] A. Rajaei, M. Tabatabaei, and A. Mohsenifar, “Physical and antimicrobial properties of starch-carboxy methyl cellulose film containing rosemary essential oils encapsulated in chitosan nanogel”, *Int. J. Biol. Macromol.*, vol. 112, pp. 148–155, 2018.

[55] C. G. Otoni, R. J. Avena-bustillos, H. M. C. Azeredo, M. V Lorevice, T. H. Mchugh, and L. H. C. Mattoso, “Recent Advances on Edible Films Based on Fruits and Vegetables - A Review”, *Compr. Rev. Food Sci. Food Saf.*, pp. 1–19, 2017.

[56] D. Nataraj, S. Sakkara, M. Hn, and N. Reddy, “Industrial Crops & Products Properties and applications of citric acid crosslinked banana fibre-wheat gluten films”, *Ind. Crop. Prod.*, vol. 124, no. July, pp. 265–272, 2018.

[57] A. Wojdyło, A. Figiel, and J. Oszmiański, “Influence of Temperature and Time of Apple Drying on Phenolic Compounds”, vol. 57, no. 4, pp. 601–605, 2007.

[58] L. P. Duvivier, Hsieh and and AL Charles, “Retention of Phenolics, Carotenoids and Antioxidant Activity in the Taiwanese Sweet Potato", *African J. Food Agric. Nutr. Dev.*, vol. 10, no. 11, pp. 4413–4429, 2010.

[59] M. S. Sagrin and G. H. Chong, “Effects of drying temperature on the chemical and physical properties of *Musa acuminata* Colla (AAA Group) leaves”, *Ind. Crop. Prod.*, vol. 45, pp. 430–434, 2013.

[60] FUTURE4200, “Soxhlet extraction set-up” [Online]. Available: future4200.com/t/thoughts-on-soxhlet-extractor-for-live-resin/8770. [Accessed: 24-Jul-2019].

[61] Y. Y. Lim and J. Murtijaya, “Antioxidant properties of Phyllanthus amarus extracts as affected by different drying methods,” *LWT - Food Sci. Technol.*, vol. 40, no. 9, pp. 1664–1669, 2007.

[62] A. L. Waterhouse, "Determination of Total Phenolics", *Current Protocols in Food Analytical Chemistry*, 2002.

[63] A. P. Oliveira *et al.*, “*Ficus carica* L.: Metabolic and biological screening”, *Food Chem. Toxicol.*, vol. 47, no. 11, pp. 2841–2846, 2009.

[64] G. Cao, E. Sofic, and R. L. Prior, “Antioxidant and Prooxidant Behaviour of Flavonoids”, *Free Radic. Biol. Med.*, vol. 22, no. 5, pp. 749–760, 1997.

[65] A. Prafulla, K. Sahu, and R. N. Rao, “An Overview of Experimental Designs in HPLC Method Development and Validation”, *J. Pharm. Biomed. Anal.*, 2017.

[66] T. Kumar *et al.*, “High resolution LC-MS characterization of phenolic compounds and the evaluation of antioxidant properties of a tropical purple radish genotype”, *Arab. J. Chem.*, 2017.

[67] K. S. Prado and M. A. S. Spinacé, “International Journal of Biological Macromolecules Isolation and characterization of cellulose nanocrystals from pineapple crown waste and their potential uses”, *Int. J. Biol. Macromol.*, vol. 122, pp. 410–416, 2019.

[68] “Cellulose Chemical Structure” [Online]. Available: pt.wikipedia.org/wiki/Celulose. [Accessed: 25-Jul-2019].

[69] “D-Glucose Chemical Structure” [Online]. Available: encyclopedia2.thefreedictionary.com/D-glucose. [Accessed: 25-Jul-2019].

[70] D. Boon, K. Lim, and H. Gong, “Highly Stretchable and Transparent Films Based on Cellulose”, *Carbohydr. Polym.*, 2018.

[71] “A Physics and Chemistry”, *J. Res. Natl. boreau Stand.*, vol. 81A, 1977.

[72] C. Rawlinson, “Differential Scanning Calorimetry - Cooking with Chemicals” 2006. [Online]. Available: www.mmsconferencing.com/pdf/eyp/c.rawlinson.pdf. [Accessed: 25-Jul-2019].

[73] J. W. Drelich, “Contact angles: From past mistakes to new developments through liquid-solid adhesion measurements”, *Adv. Colloid Interface Sci.*, 2019.

[74] L. A. Neves, J. G. Crespo, and I. M. Coelhoso, “Gas permeation studies in supported ionic liquid membranes”, vol. 357, pp. 160–170, 2010.

[75] L. A. Neves, C. Afonso, I. M. Coelhoso, and J. G. Crespo, “Integrated CO_2 capture and enzymatic bioconversion in supported ionic liquid membranes”, vol. 97, pp. 34–41, 2012.

[76] E. L. Cussler, *Fundamentals of Mass Transfer*, Third edit. New York, 2009: Cambridge University Press.

[77] R. A. Dixon and N. L. Paiva, “Stress-lnduced Phenylpropanoid Metabolism”, *Plant Cell*, vol. 7, no. July, pp. 1085–1097, 1995.

[78] A. Prathapan, M. Lukhman, C. Arumughan, A. Sundaresan, and K. G. Raghu, “Effect of heat treatment on curcuminoid , colour value and total polyphenols of fresh turmeric rhizome”, *Int. J. Food Sci. Technol.*, vol. 44, no. 0, pp. 1438–1444, 2009.

[79] W. Qu, Z. Pan, and H. Ma, “Extraction modeling and activities of antioxidants from pomegranate marc”, *J. Food Eng.*, vol. 99, no. 1, pp. 16–23, 2010.

[80] P. Karuppiah and M. Mustaffa, “Antibacterial and antioxidant activities of *Musa sp.* leaf extracts against multidrug resistant clinical pathogens causing nosocomial infection”, *Asian Pac. J. Trop. Biomed.*, vol. 3, no. 9, pp. 737–742, 2013.

[81] Wikipedia, “Apigenin - Chemical Structure” [Online]. Available: www.google.com/imgres?imgurl=https%3A%2F%2Fupload.wikimedia.org%2Fwikipedia%2Fcommons%2Fthumb%2Fe%2Fe6%2FApigenin.svg%2F1200pxApigenin.svg.png&imgrefurl=https%3A%2F%2Fen.wikipedia.org%2Fwiki%2FApigenin&docid=-CTKf3LoX24e3M&tbnid=VNefvq9rIpFHkM%3A&vet=10a. [Accessed: 06-Aug-2019].

[82] Scientific Instrument Services (SIS), “Apigenin - Isotope Distribution” [Online]. Available: www.sisweb.com/mstools/isotope.htm. [Accessed: 06-Aug-2019].

[83] T. Sango *et al.*, “Step–wise multi–scale deconstruction of banana pseudo–stem (*Musa acuminata*) biomass and morpho–mechanical characterization of extracted long fibres for sustainable applications”, *Ind. Crop. Prod.*, vol. 122, no. June, pp. 657–668, 2018.

[84] S. Karki, H. Kim, S. Na, D. Shin, K. Jo, and J. Lee, “Thin films as an emerging platform for drug delivery”, *Asian J. Pharm. Sci.*, vol. 11, no. 5, pp. 559–574, 2016.

[85] E. Rico-munoz, R. A. Samson, and J. Houbraken, “Mould spoilage of foods and beverages: Using the right methodology”, *Food Microbiol.*, 2018.

[86] A. Ramos, F. C. Domingues, and A. Duarte, “Characterization and antimicrobial activity of cellulose derivatives films incorporated with a resveratrol inclusion complex”, *Food Sci. Technol.*, vol. 73, 2016.

[87] Z. H. Ping, Q. T. Nguyen, S. M. Chen, J. Q. Zhou, and Y. D. Ding, “States of water in different hydrophilic polymers - DSC and FTIR studies”, *Polymer (Guildf).*, vol. 42, pp. 8461–8467, 2001.

[88] SNS (Sistema Nacional de Saúde), “Body temperature” [Online]. Available: www.sns24.gov.pt/tema/sintomas/febre/#sec-3.

[89] S. P. Register *et al.*, “Infrared Spectroscopy Absorption Table”, 2018. [Online]. Available: www.chem.libretexts.org. [Accessed: 20-May-2019].

[90] Z. Zhou *et al.*, "Robust cellulose nanocomposite films based on covalently cross-linked network with effective resistance to water permeablity", *Carbohydr. Polym.*, 2019.

[91] A. Wolfson, C. Dlugy, and Y. Shotland, “Glycerol as a green solvent for high product yields and selectivities”, *Environ. Chem. Lett.*, vol. 5, no. 2, pp. 67–71, 2007.

[92] R. S. Ambekar and B. Kandasubramanian, “Advancements in nanofibers for wound dressing: A review”, *Eur. Polym. J.*, vol. 117, pp. 304–336, 2019.

[93] V. D. Alves *et al.*, “Rheological and morphological characterization of the culture broth during exopolysaccharide production by *Enterobacter sp*.”, *Carbohydr. Polym.*, vol. 81, pp. 758–764, 2010.

[94] M. Cruz, F. Freitas, C. A. V Torres, M. A. M. Reis, and V. D. Alves, “Influence of temperature on the rheological behavior of a new fucose-containing bacterial exopolysaccharide”, *Int. J. Biol. Macromol.*, vol. 48, no. 4, pp. 695–699, 2011.

[95] M. Mulder, "Basic principles of membrane technology", *Kluwer Academic Publishers*, 2003.

[96] M. Campestrini, P. Stringari, and P. Arpentinier, “Solid-liquid equilibrium prediction for binary mixtures of Ar , O_2, N_2, Kr, Xe and CH_4 using the LJ-SLV-EoS”, *Fluid Phase Equilib.*, vol. 379, pp. 139–147, 2014.

[97] J. Liang and R. Chen, “Impact of cross-linking mode on the physical properties of zein/PVA composite films”, *Food Packag. Shelf Life*, vol. 18, no. January, pp. 101–106, 2018.

[98] P. Ganesan, “Natural and bio polymer curative films for wound dressing medical applications”, *Wound Med.*, vol. 18, pp. 33–40, 2017.

[99] V. D. Alves, N. Costa, and I. M. Coelhoso, “Barrier properties of biodegradable composite films based on kappa-carrageenan/pectin blends and mica flakes”, *Carbohydr. Polym.*, vol. 79, no. 2, pp. 269–276, 2010.

8. Appendix

Appendix I

Table 8.1: Chemical composition of *Musa acuminata* Colla per 100 g FW.[2]

Nutrient/Content	Value
Calcium (mg)	5
Carbohydrate, by difference (g)	22.840
Energy (kcal)	89
Fatty acids, total monounsaturated (g)	0.032
Fatty acids, total polyunsaturated (g)	0.073
Fatty acids, total saturated (g)	0.112
Folate (µg)	20
Iron (mg)	0.260
Magnesium (mg)	27
Phosphorus (mg)	22
Potassium (mg)	358
Niacin (mg)	0.665
Protein (g)	1.090
Ribofravin (mg)	0.073
Sodium (mg)	1
Thiamin (mg)	0.031
Total dietary fiber (g)	2.600
Total lipid (g)	0.330
Total sugars (g)	12.230
Vitamin A (IU)	64
Vitamin B-6 (mg)	0.367

(Table continues on the next page)

Table 8.1: Table continuation.

Nutrient/Content	Value
Vitamin C (mg)	8.700
Vitamin E (mg)	0.100
Vitamin K (µg)	0.500
Water (g)	74.910
Zinc (mg)	0.150

Table 8.2: Applications of *Musa acuminata* plant parts.[22]

Place	Plant Part	Ethnomedical Uses	Mode of Application or Treatment
Bangladesh	Root	Piles	Juice prepared from crushed root is consumed
Bengal and India	Root	Anthelmintic	Used in preparation of herbal medicines and as a tonic
Brazil	Bud	Cough, asthma and bronchitis	Bud macerated in water and taken as syrup
Central America	Root	Against snake bite	Root extract is administered either orally or by external application on wound
		Prevent conception	Root juice drunk during menstruation
India	Flowers	Joint pain and better blood circulation	Boiled and eaten with salt and oil
	Flower, inner core, stem and bark fibres	Allergies, infections, bronchitis, dysentery and allergic reactions	Flower extraction in bronchitis; flower juice in allergic reactions and inner core is consumed in dysentery; stem juice of matured plant and bark fibres are used to cure allergic complains
	Leaves	Asthma and wheezing	Ash obtained by burning leaves is inhaled
	Leaves	Dressing wounds and blistered skin	Oil smeared leaves are used

(Table continues on the next page)

Table 8.2: Table continuation.

Place	Plant Part	Ethnomedical Uses	Mode of Application or Treatment
Kenya	Fruit	Blood pressure	Ripe fruit is eaten
Mexico	Stem	Tuberculosis and other respiratory diseases	Stem extract as a drink
Nigeria	Fruit	Anaemia	Ripe fruit is eaten
Philippines	Sap	Fever	Sap extraction is consumed
South Africa	Red flower bracts	Hypertension	Two handful of flower bract boiled in 1 L of water for 30 min. Quarter of a glass of the infusion is taken orally three times a day
	Root	HIV/AIDS related infection, sexually transmitted infections and sores on genital parts	A handful of chopped *Musa acuminata* roots with crushed leaves and chopped *Hypoxis hemerocallidea* corm in equal proportion is boiled in water. This concoction is consumed three times a day to cure HIV/AIDS and related infections
Western Uganda	Root	Induce labour	Root squeezed by hand or chewed after roasting

D

Table 8.3: Antimicrobial activity of *Musa acuminata* plant's leaf and pseudostem.[22]

Plant Part	Extract	Microorganism	Efficacy [a]
Leaf	96% Ethanol	*Aspergillus terreus*	C-20, D-2.7
	Acetone		C-20, D-1.7
	Petroleum ether		C-20, D-3.7
	96% Ethanol	*Penicillum solitum*	C-20, D-5.7
	Acetone		C-20, D-4.9
	Petroleum ether		C-20, D-2.9
	Ethyl acetate	*Citrobactor spp*	M-125
		Citrobactor sp	M-62
		Enterobactor aerogenes	M-31.25
		Enterobactor aerogenes	M-250
		Enterococcus feacalis	M-31.25
		Escherichia coli	M-62.50
		Proteus mirabilis	M-125
		Pseudomonas aeruginosa	M-31.25
		Pseudomonas aeruginosa	M-125
		Shigella flexneri	M-62.50
		Shigella flexner	M-250
		Staphylococcus aureus	M-62.5
		Staphylococcus aureus	M-125
		Klebsiella pneumoneae	M-125
	Hexane	*Citrobacter spp*	M-250
		Enterobacter aerogenes	M-250
		Enterococcus feacalis	M-250
		Proteus mirabilis	M-250
		Pseudomonas aeruginosa	M-250

[a] C – Active concentration (mg/mL); D – diameter inhibition zone (mm); M – MIC (μg/mL).

(Table continues on the next page)

Table 8.3: Table continuation.

Plant Part	Extract	Microorganism	Efficacy [a]
Leaf	Hexane	*Shigella flexneri*	M-250
	50% ethanol	*Streptococcus sp*	C-100, D-13
Pseudostem	50% methanol	*Staphylococcus aureus*	C-100, D-16
		Streptococccus sp	C-100, D-14

[a] C – Active concentration (mg/mL); D – diameter inhibition zone (mm); M – MIC (μg/mL).

Table 8.4: Phytochemicals identified in different parts of *Musa acuminata*.[22]

Plant Part	Extraction Solvent	Phytochemicals and Active Compounds
Bract	Water	Tannins, coumarins and total phenols
	Ethyl acetate	Flavonoids
	Methanol	Anthocyanin, delphinidin-3-rutinoside, cyanididne-3-rutinoside, petunididn-3-rutinoside, peonidin-3- rutinoside, malvidin-3-rutinoside, alkaloids, saponins, tannins, flavonoids, terpenoids, coumarins, cycloglycosides, total phenols and steroids
Corm	Ethanol	Sterols, flavonoids, glycosides, terpenoids, tannins and quinones
Flower	Methanol	Glycosides, tannins, saponins, phenols, steroids and flavonoids
Fruit cell wall	Chloroform: methanol	Hydroxycinnamic acid 1 & 2, ferulic acid, procyanidins and phenolics
Leaf	Acetone	Phenolics and tannic acid
	Ethanol	Phenolics and tannic acid
	Methanol	Alkaloids, steroidal lactones and tannins
	Petroleum ether	Phenolics and tannic acid

(Table continues on the next page)

Table 8.4: Table continuation.

Plant Part	Extraction Solvent	Phytochemicals and Active Compounds
Peel	Acetone: water	Phenolics, anthocyanins, dopamine and catecholamines
	Ethanol	Glycosides, tannins, saponins, phenols, steroids and flavonoids
	Hexane	Saponins, carotenoids, phenolics, flavonoids and tannins
	Methanol, oil	Glycosides, tannins, saponins, flavonoids, alkaloids, steroids, terpenoids, triterpenes, phenols, palmitic, oleic and linoleic acids and their methyl esters, 2,3-dihydro-3,5- dihydroxy-6-ethyl-4H-pyran-4-one, 5-(hydroxymethyl)-2-furancarboxyaldehyde, methyl hexadeconoate, methyl- 9,12-octadienoate, methyl 1-9-octadeconoate, 9,12- ocatadecanoic acid, 13- octadecanoic acid, octadecanoic acid, 2-methyl-5-(1-methylethyl) phenol, pentadecanoic acid, cis-9-hexadecenal, cis-9-hexadecenoic acid, benzoic acid, pyrogallol, sesamin and epi-sesamin
Petioles, leaf blades, floral stalk, leaf sheaths and rachis	Dichloromethane	Steryl glycosides (campesteryl, stigmasteryl, sitosteryl)
Pseudostem	Water	Alkaloids, flavonoid, phenol, protein, saponin, steroid, tannin and terpenoid
	Ethanol	Cardiac glycosides, flavonoid, phenol, protein, steroid and terpenoid
	Methanol	Alkaloids, cardiac glycosides, flavonoid, phenol, protein, saponin, steroid, tannin and terpenoid

(Table continues on the next page)

Table 8.4: Table continuation.

Plant Part	Extraction Solvent	Phytochemicals and Active Compounds
Rhizome	Acetone	(+) Catechin hydrate, vanillic acid, caffeic acid, epicatechin and ellagic acid
Ripe Fruit	Dichloromethane	Fatty acids, octadeca-9,12,15 trienoic acid, octadeca-9,12-dienoic acid, long chain aliphatic alcohols, sterols (campesterol, stigmasterol, β sitosterol) and cycloartenol and α tocopherol
	Ethanol	Alkaloids, saponins, tannins, terpenes, flavonoids, anthroquinones, cardiac glycosides, carbohydrates, glycosides, proteins and phenols
	Methanol	Saponins, triterpenes, tannins, (+) catechin, gallocatechin, (−) epicatechin, procyanidins and phenolics
Root	Methanol	2-hydroxy-9-phenylphenalen-1-one (anigorufone)
Sap	Ethanol	Hydrocinnamic acid, caffeoylquinic acid, flavonoids (apigenin, myricetin, kaempferol, quercetin), dopamine and N-acetylserotonin
Seeds	Acetone	Leucoanthyocyanidn
Unripe fruit	Methanol	(+) catechin, gallocatechin, (-) epicatechin, procyanidins and phenolics

J

Appendix II

Table 8.5: Reagents used during the experimental work.

Material	Chemical Formula	Characteristics	Purity (%)	Supplier
2,2-difenil-1-picrilhidrazilo (DPPH)	$C_{18}H_{12}N_5O_6$	CAS: 1898-66-4 Lot: Q28D038	95.0	Alfa Aesar
Apigenin	$C_{15}H_{10}O_5$	CAS: 520-36-5	≥98.0	TCI
Banana plant leaf	-	*Musa acuminata* Colla	-	Farmer from Madeira island
Banana plant pseudostem	-	*Musa acuminata* Colla	-	Farmer from Madeira island
Caffeic acid	$C_9H_8O_4$	CAS: 331-39-5	≥98.0	Sigma-Aldrich
Caffeine	$C_8H_{10}N_4O_2$	CAS: 58-08-2	-	Sigma-Aldrich
Carbon dioxide	CO_2	-	≥99.9	PRAXAIR
Catechin	$C_{15}H_{14}O_6$	CAS: 225937-10-0	≥96.0	Sigma-Aldrich
Chlorogenic acid	$C_{16}H_{18}O_9$	CAS: 327-97-9	≥95.0	Sigma-Aldrich
D-(+) glucose	$C_6H_{12}O_6$	CAS: 50-99-7 Lot: LRAB8922	-	Sigma-Aldrich
Epicatechin	$C_{15}H_{14}O_6$	CAS: 490-46-0	≥90.0	Sigma-Aldrich

(Table continues on the next page)

Table 8.5: Table continuation.

Reagent	Chemical Formula	Characteristics	Purity (%)	Supplier
Ferulic acid	$C_{10}H_{10}O_4$	CAS: 537-96-4 Lot: 10172285	99.0	Alfa Aesar
Folin reagent	-	CAS: 251567.1609 Lot: 0000495390	-	AppliChem Panreac
Gallic acid	$C_7H_6O_5$	CAS: 27645 Lot: SZB61290	99.0	Sigma-Aldrich
Hydroxyethyl cellulose (HEC)	$C_{36}H_{70}O_{19}$	CAS: 9004-62-0 Lot: MKCD2790	≥85.0	Aldrich
Hydrogen peroxide	H_2O_2	Lot: AX1705076	-	Alifar
Methanol	CH_3OH	Cat: 34860-2.5L-R Lot: SZBG106DV	≥99.9	Sigma-Aldrich
Oxygen	O_2	-	≥99.9	PRAXAIR
p-Coumaric acid	$C_9H_8O_3$	CAS: 501-98-4	≥98.0	Sigma-Aldrich
Potassium chloride	KCl	Cat: P9333-500G Lot: BCBZ4557	≥99.0	Sigma-Aldrich
Protocatechuic acid	$C_7H_6O_4$	CAS: 99-50-3	99.8	HWI
Quercetin	$C_{15}H_{10}O_7$	CAS: 117-39-5 Lot: SLBK4625V	≥95.0	Sigma-Aldrich

(Table continues on the next page)

Table 8.5: Table continuation.

Reagent	Chemical Formula	Characteristics	Purity (%)	Supplier
Resveratrol	$C_{14}H_{12}O_3$	CAS: 501-36-0	≥99.0	Sigma - Aldrich
Sodium bromide	NaBr	CAS: 141646.1211 Lot: 0000672010	≥98.5	ITW Reagents
Sodium carbonate	Na_2CO_3	CAS: 131648.1211 Lot: 0000750117	≥99.0	AppliChem Panreac
Sodium chloride	NaCl	CAS: 131659.1211 Lot: 0001070064	≥99.5	ITW Reagents
Sodium hydroxide	NaOH	CAS: 1310-73-02 Lot: 180317	-	Eka
Syringic acid	$C_9H_{10}O_5$	CAS: 530-57-4 Lot: BCBM9739V	≥95.0	Sigma - Aldrich
Sulfuric acid	H_2SO_4	Cat: 30743-2.5L Lot: I2570	95.0 – 97.0	Honeywell, fluka
Urea	CH_4N_2O	CAS: 57-13-6 Lot: s5795810 846	≥99.0	Merck
Vanillic acid	$C_8H_8O_4$	-	-	-
Vanillin	$C_8H_8O_3$	CAS: 121-33-5	99.0	Sigma - Aldrich

M

Table 8.6: Equipments used during the experimental work.

Equipment	Brand
Cabinet dryer	Venticell, MMM Group
Centrifuge	4-16KS, Sigma
Crushing machine	Selecline
Differential Sanning Colorimeter (DSC)	DSC 131, Setaram
Digestor	SBH130D, Stuart
Digital scale	ANJ-NM/ABS-N, Kern
Fourier Transform Infrared (FTIR-ATR) Spectrometer	Spectrum Two, Perkin-Elmer
Goniometer	CAM100, KSV Instruments LTD
Heating and stirring plate	Arex, Velp Scientic
High Pressure Liquid Chromatography (HPLC)	Infinity 1100, Agilent
Liquid Chromatography - Mass Spectrometry (LC-MS)	1200 Series, Agilent
Lyophilizator	Scanvec, Coolsafe
Micrometer	Elcometer
pH electrode	Thermo Scientific
Pressure transducers	Druck PCDR 910, 99166 and 991675
Rheometer (viscoelasticity)	Haake Mars, Thermo Scientific
Rheometer (viscosity)	RS 75 RheoStress, HAAKE
Rotatory evaporator	Buchi
Sonicator	Bandelin
Scanning Electron Microscopy (SEM)	HITACHI S-2400
Textute analyser	TA XT plus, StaLe Micro Systems
Thermogravimetric Analyser (TGA)	EVO, Setaram Labsys
Thermostatic water bath	GmBH ED, Julabo
UV/VIS spectrometer	Evolution 201, Thermo Scientific
Vortex	Reax 2000, Heidolph
X-Ray Diffractometer (XRD)	MiniFlex II, Rigaku

N

Appendix III

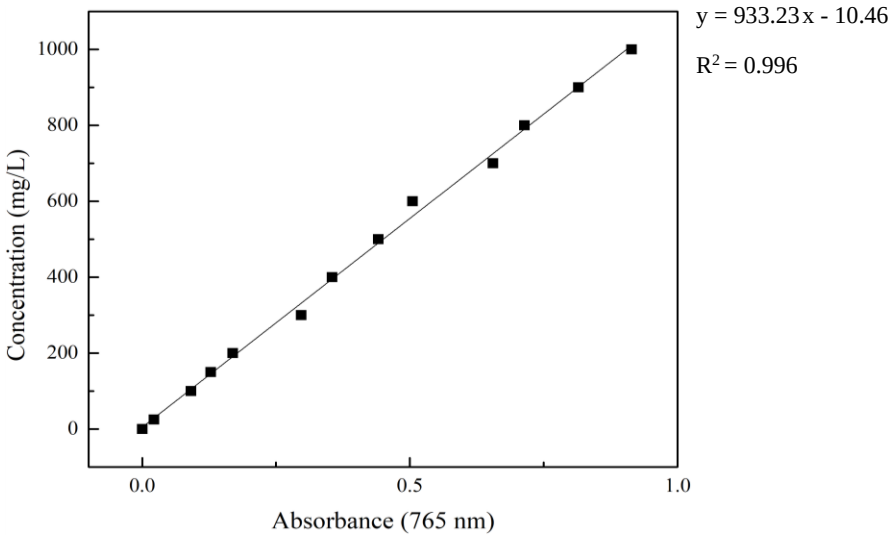

Figure 8.1: Folin Ciocalteau method calibration curve (black linear fit) made with gallic acid solutions with different dilution ratios of distilled water:gallic acid (■).

Table 8.7: Phenolic standards chemical formula, molecular weight, retention time and calibration curves linear range, regression equation and correlation coefficient for HPLC fingerprint.

Standard	Chemical Formula	Molecular Weight (g/mol)	Wavelength (nm)	Retention Time (min)	Linear Range (mg/L)	Regression Equation	Correlation Coefficient (R^2)
Apigenin	$C_{15}H_{10}O_5$	270.10	280.40 320.40 350.40	40.68 40.68 40.68	nd*	nd	nd
Caffeic acid	$C_9H_8O_4$	180.10	280.40 320.40 350.40	9.81 9.81 9.81	6.78−135.60	y = 17.20x + 7.93	0.99
Caffeine	$C_8H_{10}N_4O_2$	194.10	280.40 320.40 350.40	13.54 - -	5.65−113.00	y = 13.74x + 21.33	0.99
Chlorogenic acid	$C_{16}H_{18}0_9$	354.31	280.40 320.40 350.40	8.36 8.36 8.36	4.73−94.60	y = 8.02x + 5.05	0.99
Catechin	$C_{15}H_{14}O_6$	290.10	280.40 320.40 350.40	6.12 32.98 32.96	5.29−105.80	y = 3.46x + 2.48	0.99
Epicatechin	$C_{15}H_{14}O_6$	290.10	280.40 320.40 350.40	13.23 - 36.18; 36.19	0.99−99.20	y = 3.88x + 7.37	0.99

nd* - Limited solubility. Inaccurate result.

(Table continues on the next page)

P

Table 8.7: Table continuation.

Standard	Chemical Formula	Molecular Weight (g/mol)	Wavelength (nm)	Retention Time (min)	Linear Range (mg/L)	Regression Equation	Correlation Coefficient (R^2)
Ferulic acid	$C_{10}H_{10}O_4$	194.10	280.40 320.40 350.40	22.22 22.22 22.22	4.67−93.40	y = 16.59 x + 8.32	0.99
Gallic acid	$C_7H_6O_5$	170.10	280.40 320.40 350.40	3.03 3.03 -	5.39−107.80	y = 15.24 x - 19.47	0.99
p-Coumaric acid	$C_9H_8O_3$	164.10	280.40 320.40 350.40	17.34 17.34 17.34	5.10−102.00	y = 25.99 x + 14.85	0.99
Protocatechuic acid	C_7H_604	693.10	280.40 320.40 350.40	4.35 4.35 -	6.97−139.30	y = 5.30 x - 1.95	0.99
Quercetin	$C_{15}H_{10}O_7$	302.10	280.40 320.40 350.40	37.85 37.85 37.85	1.28−25.76	y = 13.54 x - 18.91	0.99
Resveratrol	$C_{14}H_{12}O_3$	228.10	280.40 320.40 350.40	33.20 33.20 33.20	5.39−107.80	y = 14.04 x + 6.66	0.99
Syringic acid	$C_9H_{10}O_5$	198.10	280.40 320.40 350.40	12.06 12.04 -	1.00−100.60	y = 15.92 x + 27.22	0.99

(Table continues on the next page)

Table 8.7: Table continuation.

Standard	Chemical Formula	Molecular Weight (g/mol)	Wavelength (nm)	Retention Time (min)	Linear Range (mg/L)	Regression Equation	Correlation Coefficient (R^2)
Vanillic acid	$C_8H_8O_4$	168.10	280.40 320.40 350.40	9.04 9.06 -	1.02−102.40	y = 9.36x + 19.76	0.99
Vanillin	$C_8H_8O_3$	152.10	280.40 320.40 350.40	12.12 12.12 12.12	5.23−104.64	y = 22.86x - 0.53	0.99

R

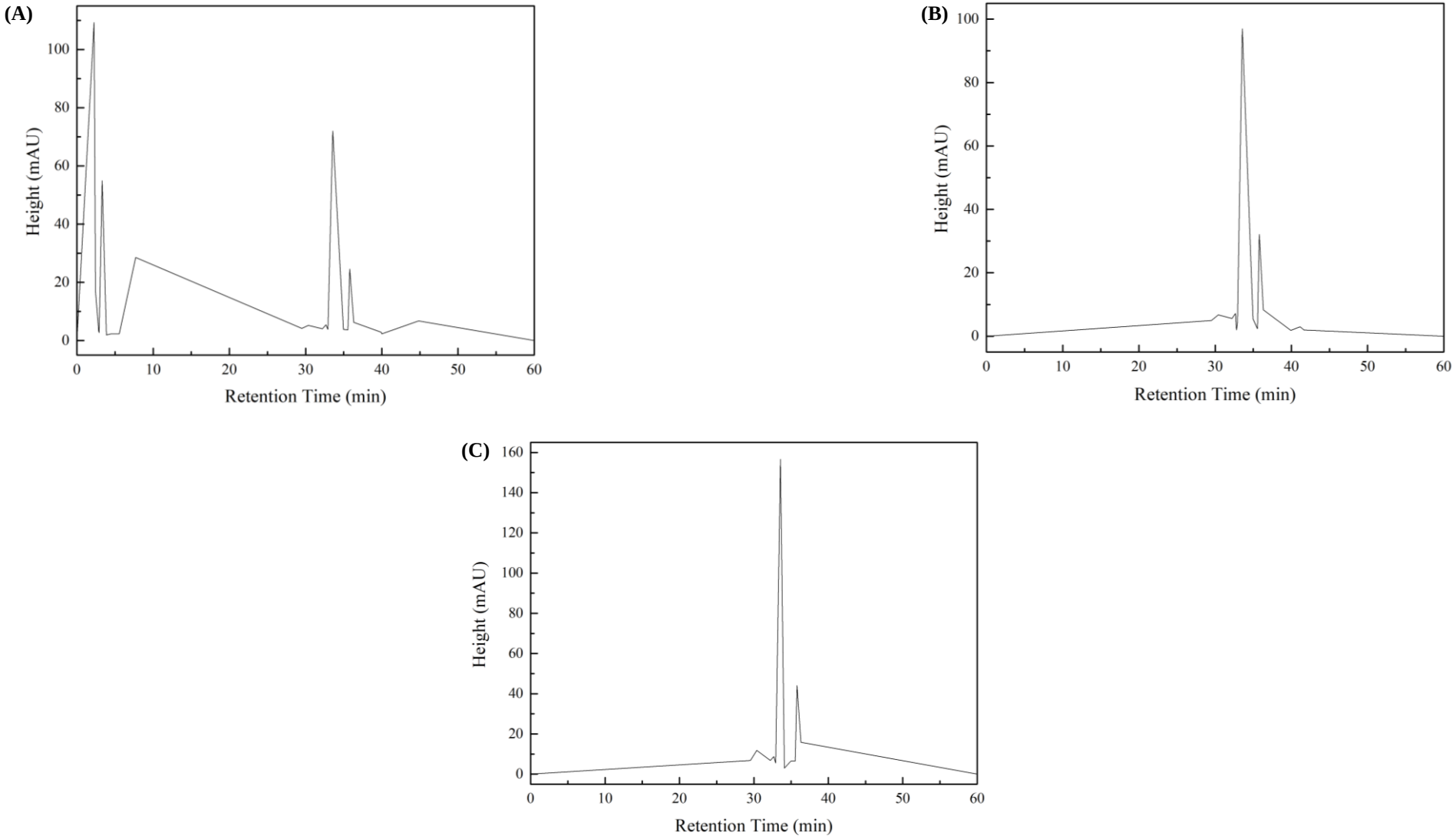

Figure 8.2: HPLC chromatogram for the sample 2 of BSL_3_40 and at the wavelength of 280.4 **(A)**, 320.4 **(B)** and 350.4 **(C)** nm.

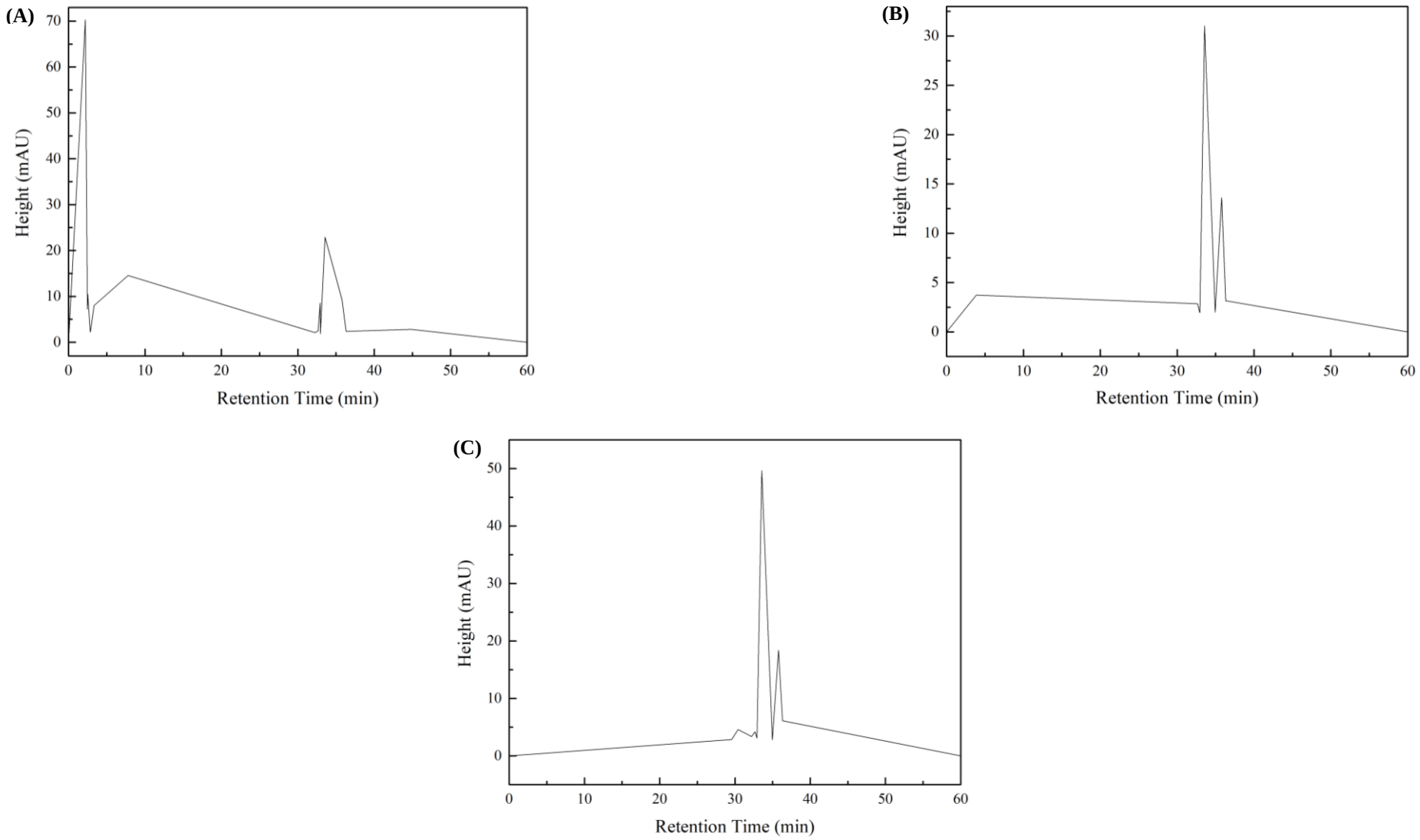

Figure 8.3: HPLC chromatogram for the sample 3 of BSL_3_40 and at the wavelength of 280.4 **(A)**, 320.4 **(B)** and 350.4 **(C)** nm.

T

Table 8.8: HPLC retention times and respective height for the sample 1 of BSL_3_40.

λ=280.4nm		λ=320.4nm		λ=350.4nm	
Retention Time (min)	Height (mAU)	Retention Time (min)	Height (mAU)	Retention Time (min)	Height (mAU)
0.00	0.00	0.00	0.00	0.00	0.00
2.19	129.96	3.91	8.78	9.38	1.62
2.41	20.60	4.38	5.77	21.35	0.75
2.78	11.69	4.78	3.86	28.17	3.72
3.01	8.15	5.49	1.47	28.70	8.59
3.02	8.17	5.80	1.01	29.66	10.39
3.17	10.32	6.20	1.02	29.96	7.03
3.18	10.22	6.64	1.75	30.62	0.91
3.91	3.11	7.93	3.35	31.81	7.01
4.38	2.10	9.43	1.81	32.32	10.03
5.49	2.12	10.39	1.13	32.63	7.95
6.24	1.01	11.41	1.22	33.25	171.21
7.30	32.97	21.33	1.82	33.87	4.18
9.36	0.60	28.16	3.51	33.88	4.23
10.33	1.10	28.70	5.75	34.73	6.56
11.40	2.04	29.66	6.47	35.36	6.50
19.96	0.77	29.99	4.50	35.59	43.88
20.61	0.67	30.61	1.36	36.15	15.81
21.35	1.01	31.81	5.66	38.04	2.14
25.95	0.71	32.31	7.47	38.53	1.35
28.14	2.79	32.48	1.93	39.87	1.45
28.71	4.18	32.63	4.54	41.08	2.26
29.68	4.61	33.26	105.28	41.68	1.02
29.96	3.25	33.89	2.29	42.08	1.14
30.59	0.69	34.72	5.09	44.76	3.78
31.81	4.47	35.36	5.44	46.92	1.26
32.32	5.32	35.59	35.38	47.40	1.11
32.63	3.30	36.15	9.74	60.00	0.00
33.26	77.58	38.03	2.95	-	-
33.91	1.41	38.53	1.80	-	-
34.72	3.88	39.86	2.92	-	-
35.06	1.55	41.08	2.94	-	-
35.36	3.64	41.10	2.84	-	-
35.59	24.52	42.07	1.73	-	-

(Table continues on the next page)

Table 8.8: Table continuation.

λ=280.4nm		λ=320.4nm		λ=350.4nm	
Retention Time (min)	Height (mAU)	Retention Time (min)	Height (mAU)	Retention Time (min)	Height (mAU)
36.15	6.57	60.00	0.00	-	-
38.04	2.39	-	-	-	-
38.52	1.34	-	-	-	-
39.86	3.58	-	-	-	-
41.10	1.34	-	-	-	-
42.12	1.16	-	-	-	-
42.67	1.24	-	-	-	-
44.39	1.10	-	-	-	-
44.77	6.29	-	-	-	-
45.62	2.32	-	-	-	-
45.64	2.36	-	-	-	-
45.65	2.40	-	-	-	-
47.13	2.86	-	-	-	-
47.82	0.65	-	-	-	-
49.90	1.03	-	-	-	-
51.5	0.82	-	-	-	-
60.00	0.00	-	-	-	-

Table 8.9: HPLC retention times and respective height for the sample 2 of BSL_3_40.

λ=280.4nm		λ=320.4nm		λ=350.4nm	
Retention Time (min)	Height (mAU)	Retention Time (min)	Height (mAU)	Retention Time (min)	Height (mAU)
0.00	0.00	0.00	0.00	0.00	0.00
2.24	109.28	29.51	4.97	29.52	6.83
2.44	16.97	30.40	6.73	30.37	11.80
2.85	3.00	32.21	5.58	32.20	6.85
2.86	3.05	32.65	7.19	32.66	8.77
2.88	3.01	32.80	1.94	32.92	5.54
2.89	2.97	32.92	4.39	33.55	156.63
2.90	2.90	33.55	96.95	34.10	2.95
2.92	2.75	34.95	5.43	34.96	6.52
3.31	54.94	35.55	2.35	35.54	6.50
3.87	1.92	35.78	32.08	35.78	44.08
3.88	1.94	36.32	8.31	36.33	15.88
4.48	2.30	39.89	1.89	60.00	0.00
4.51	2.32	39.91	1.84	-	-
5.54	2.31	41.14	2.97	-	-
5.57	2.36	41.68	1.88	-	-
7.72	28.52	41.70	1.95	-	-
29.50	4.18	41.71	1.97	-	-
30.36	5.26	60.00	0.00	-	-
32.20	4.07	-	-	-	-
32.21	4.03	-	-	-	-
32.66	5.43	-	-	-	-
32.93	3.80	-	-	-	-
33.55	72.01	-	-	-	-
34.95	3.86	-	-	-	-
34.96	3.82	-	-	-	-
35.55	3.68	-	-	-	-
35.78	24.58	-	-	-	-
36.32	6.24	-	-	-	-
39.92	2.86	-	-	-	-
40.00	2.30	-	-	-	-
44.82	6.77	-	-	-	-
60.00	0.00	-	-	-	-

Table 8.10: HPLC retention times and respective height for the sample 3 of BSL_3_40.

λ=280.4nm		λ=320.4nm		λ=350.4nm	
Retention Time (min)	Height (mAU)	Retention Time (min)	Height (mAU)	Retention Time (min)	Height (mAU)
0.00	0.00	0.00	0.00	0.00	0.00
2.20	70.31	3.87	3.72	29.56	2.85
2.45	7.23	32.21	2.86	30.40	4.58
2.51	10.46	32.67	2.85	32.21	3.37
2.83	2.23	32.92	1.97	32.66	4.22
2.86	2.27	32.93	2.01	32.93	3.10
3.34	8.01	32.95	1.93	33.56	49.65
7.79	14.56	33.57	31.03	34.96	2.78
32.22	2.12	34.95	1.98	35.78	18.42
32.66	2.44	35.78	13.62	36.32	6.12
32.91	8.56	36.32	3.11	60.00	0.00
32.94	1.84	36.34	3.15	-	-
33.56	22.92	60.00	0.00	-	-
35.78	9.22	-	-	-	-
36.32	2.37	-	-	-	-
44.84	2.79	-	-	-	-
60.00	0.00	-	-	-	-

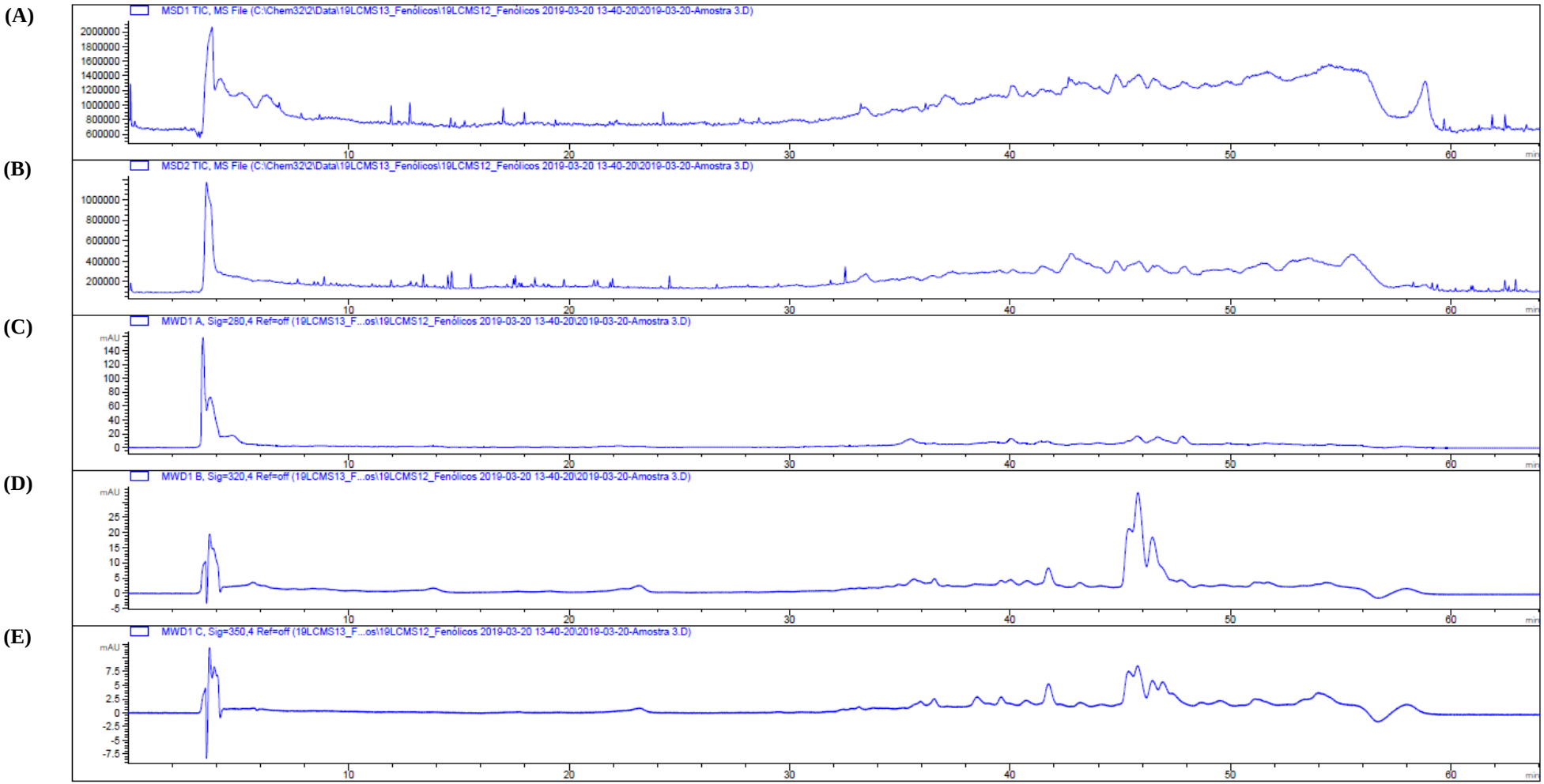

Figure 8.4: LC-MS diagrams for the analysis of the sample 1 of BSL_3_40, where **(A) (B)** – total ions chromatograms (MS) in the positive mode (D1) and negative mode (D2), respectively; **(C) (D) (E)** – UV chromatograms (MW), at the wavelength of 280.4, 320.4 and 350.4nm, respectively, in the positive mode.

Y

Table 8.11: Apigenin standards chemical formula, molecular weight, retention time and calibration curve linear range, regression equation and correlation coefficient for HPLC fingerprint.

Standard	Chemical Formula	Molecular Weight (g/mol)	Wavelength (nm)	Retention Time (min)	Linear Range (μg/L)	Regression Equation
Apigenin	$C_{15}H_{10}O_5$	270.10	352	12.27	10−160	0.19 x - 0.24

Table 8.12: Glucose standard concentration, retention time, height and glucose detected, utilized for glucose calibration fingerprint by HPLC.

Glucose Standard Concentration (mg/L)	Retention Time (min)	Height (nC)	Glucose Amount Detected (mg/L)
5.17	10.06	28.42	4.98
10.34	10.84	51.72	10.35
20.65	11.03	97.72	20.99
41.28	11.06	108.45	41.14
62.04	11.06	239.31	56.70
82.72	11.07	289.42	72.94
103.40	10.96	315.44	85.38

Table 8.13: Swelling analysis results for PS and PS doped with phenolic compounds (PS+L) matrices.

Matrix	Dimension Media (cm)		Thickness Media (cm)		Weight Media (g)	
	Before	After	Before	After	Before	After
PS	1×1	1×1	0.017	0.013	0.014	0.05
PS+L	1×1	1×1	0.012	0.0071	0.0094	0.04

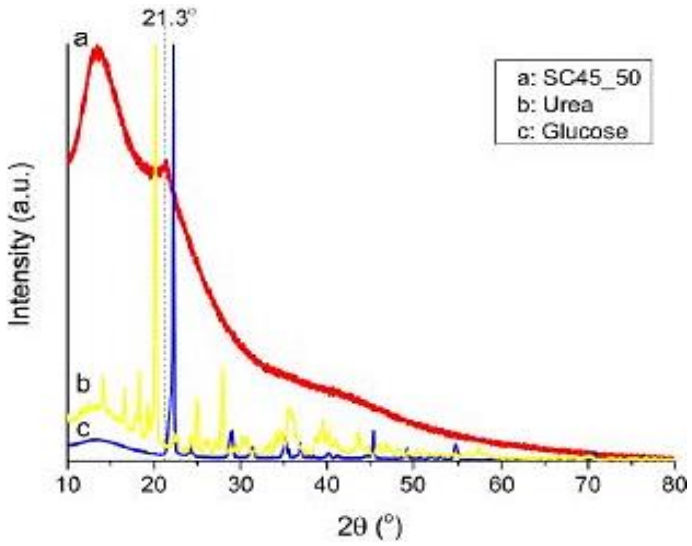

Figure 8.5: XRD results for HEC_G_U film at 50% a_w **(a)**, urea **(b)** and glucose **(c)**.[70]

Table 8.14: Weight loss and respective temperature range, resultant from TGA analysis of the matrices exposed to 58%, 75% and 84% a_w.

Matrix 58% a_w	Total Weight Loss (%)	Temperature Range (°C)	Matrix 75% a_w	Total Weight Loss (%)	Temperature Range (°C)	Matrix 84% a_w	Total Weight Loss (%)	Temperature Range (°C)
HEC	1.14 70.06	49.72–115.95 176.26–466.04	HEC	71.69	46.37–443.42	HEC	2.09 675.490	46.90–132.06 172.42–464.33
HEC_G	5.19 22.81 71.21	33.36–127.69 157.76–250.97 251.21–454.66	HEC_G	3.1 22.39 73.84	47.73–144.95 144.04–246.52 246.02–461.91	HEC_G	6.97 22.55 68.65	34.13–144.72 144.34–245.56 245.71–463.05
HEC_U	1.5 21.51 72	50.87–111.57 111.38–228.43 227.75–454.07	HEC_U	20.19 56.04 78.4	30.35–180.57 178.78–303.05 302.68–460.76	HEC_U	29.75 60.26 78.34	31.54–176.85 185.45–303.97 303.97–452.77
HEC_G_U	3.34 18.68 68.15	46.88–123.81 124.01–233.5 233.41–464.66	HEC_G_U	4.38 17.96 69.95	48.53–123.02 122.36–233.89 233.47–458.27	HEC_G_U	4.47 20.42 68.04	33.02–133.73 133.59–247.72 247.89–469.08
HEC+L	2.72 70.9	32.16–126.29 126.39–456.38	HEC+L	7.22 73.47	32.55–139.54 140.19–455.15	-	- -	- -
PS	4.03 68.17	35.29–164.38 192.6–463.86	PS	3.45 66.32	33.05–180.96 181.42–462.35	PS	4.32 66.93	47.88–176.97 176.97–472.71
PS+L	2.09 71.37	47.35–152.38 152.64–463.66	PS+L	2.41 68.85	49.67–151.13 150.08–466.91	-	- -	- -

BB

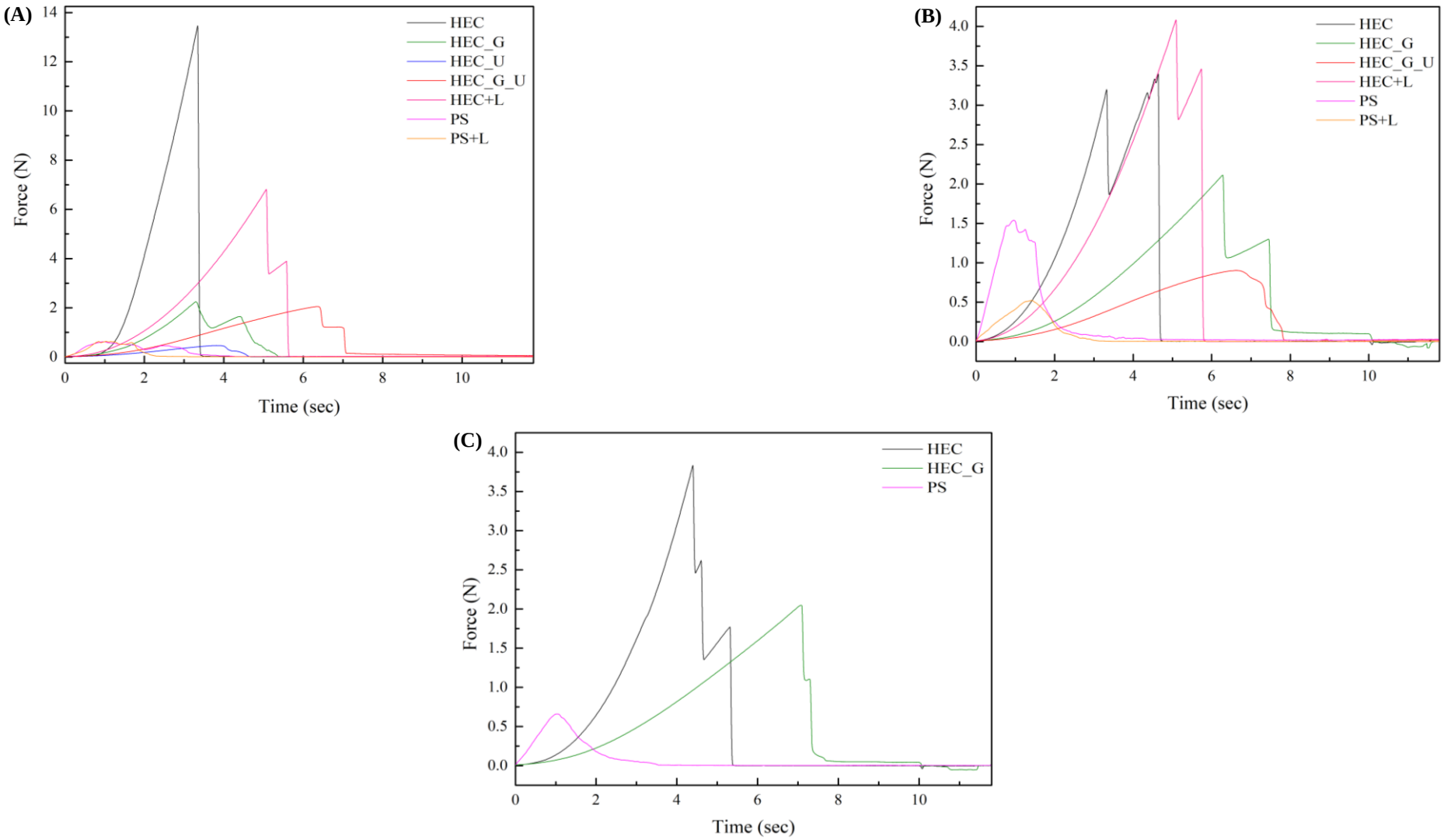

Figure 8.6: Puncture test media results for HEC and PS matrices analysis exposed to 58 **(A)**, 75 **(B)** and 84% **(C)** a_w.

CC

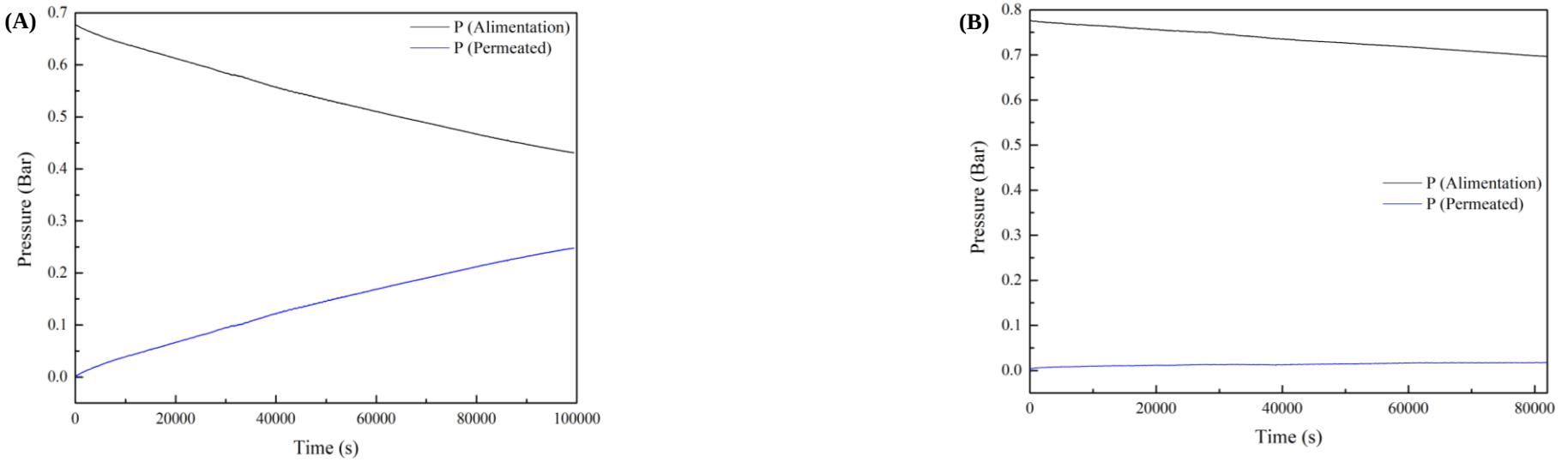

Figure 8.7: Pressure variation as a function of time for HEC matrices exposed to 84% a_w **(A) (B)**; by using CO_2 **(A)** and O_2 **(B)**.

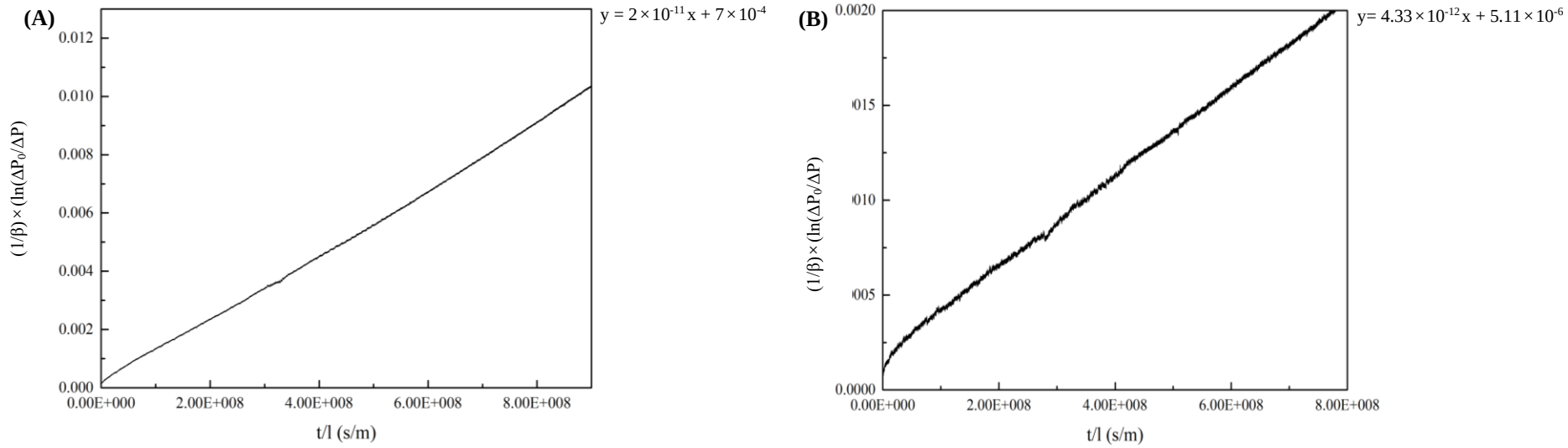

Figure 8.8: Linear fitting for HEC matrices exposed to 84% a_w **(A) (B)**, for gas permeability calculation; by using CO_2 **(A)** and O_2 **(B)**.

DD